Study on Surface-Medicated Transfer of Small Interfering RNA into Mammalian Cells toward Large-Scale Analysis of Gene Functions(Dissertation_全文)

AUTHOR(S):

Fujimoto, Hiroyuki

Study on Surface-Mediated Transfer of Small Interfering RNA into Mammalian Cells toward Large-Scale Analysis of Gene Functions

Hiroyuki Fujimoto

2008

CONTENTS

ABBREVIATIONS

bp	Base pair
cDNA	Complementary DNA
DNA	Deoxyribonucleic acid
d-siRNA	Dicer-digested siRNA
DsRed	*Discosoma sp.* red fluorescent protein
dsRNA	Double-stranded RNA
EGFP	Enhanced green fluorescent protein
FBS	Fetal bovine serum
GFP	Green fluorescent protein
HEK	Human embryonic kidney
IR-RAS	Infrared reflection absorption spectroscopy
LBL	Layer-by-layer
LDR	Lipid-DNA-siRNA complex
MEM	Minimal essential medium
mRNA	Messenger RNA
Mw	Molecular weight
PBS	Phosphate buffered saline
PCR	Polymerase chain reaction
PEI	Poly(ethyleneimine)
RNAi	RNA interference
SAM	Self-assembled monolayer
SD	Standard deviation
siRNA	Small interfering RNA
SPR	Surface plasmon resonance
ssRNA	Single-stranded RNA
TE	Tris-EDTA
Tris	Tris(hydroxymethyl)aminomethane
U	Unit
UV	Ultraviolet

GENERAL INTRODUCTION

Genetic information is essential for the development, physiology, and reproduction of any organisms. This information is accumulated in genes and succeeded from cell to cell and from generation to generation. Genes encode the information that defines the feature of species. In the discipline of biology, genes have been the matter of upmost concerns, and identification of genes has been believed to provide deeper insights into living systems. In this sense, the sequencing of the human genome, completed by the International Consortiumin 2003 (1, 2), can be considered as a scientific milestone.

After the success of the human genome project, interests in biological science has been sifted to post-genomic problems. Currently, biologists have a possibility to identify any genes that are responsible for the biological complexity in several model organisms. Accordingly, increasing studies have been focused on the annotation of human genes as well as recently-discovered noncoding RNA such as microRNA (3). In addition, growing attention has been paid to the elucidation of relationship between genes, which is believed to provide the basis for understanding gene regulation mechanisms and protein–protein interaction networks, and hence the dynamic behaviors of living systems.

High-throughput analytical systems have been developed as a tool for conducting

large-scale parallel experiments for genes in a genome-wide. One of the most successful example is the DNA microarray (4) that allows us to massively profiling gene expression. In this technique, a number of probe nucleotides are displayed in an array format on a small plate, and the abundance of complementary nucleotides in a sample solution is analyzed by hybridization. The microarray format has become the leading technology that enables fast, easy, and parallel detection of thousands of addressable elements and side-by-side measurements. Importantly, the massiveness of data obtained by the DNA microarray makes large contrast to the data obtained by the conventional reverse transcriptase-polymerase chain reaction.

Alternatively, protein microarrays (5, 6) and peptide microarrays (7, 8) have been developed as new means to perform parallel characterization of protein–protein, protein–nucleic acid, and peptide–substrate interactions. These arrays are used for the parallel detection of small molecules (9), proteins (5, 6), antibodies (10), and drugs (11) in a variety of biological samples. As in the DNA microarrays, the protein and peptide microarrays also provide significant information on protein networks.

In spite of invaluable usefulness of these technologies, DNA, protein, and peptide microarrays could only be used in principle to analyze binding between biomolecules. In order to study the function of genes and proteins, we absolutely need new analytical

platforms that permit studies at a cellular level. One of the versatile methods is the transfection technique in which protein-coding genes or small interfering RNA (siRNA) is introduced into living cells to overexpress or knockdown target genes, generating cells that gain or lose the function of specific genes. By analyzing the alteration of phenotypes caused in cells, one can identify the functions of the target genes.

Recently it was discovered that a target gene can be silenced easily and specifically using RNA interference (RNAi) (12). When introduced into cytoplasm, double-stranded RNA (dsRNA) triggers the post-transcriptional degradation of messenger RNA (mRNA) with homologous sequence to suppress its translation. Especially in mammalian cells, 21–27 nt dsRNA, so-called small interfering RNA (siRNA), is used for avoiding nonspecific suppression effects (13). This technique enabled the silencing of specific genes at a cellular level, providing much simpler means for the loss-of-function study compared with the conventional knockout animal technique.

For high-throughput approach to characterize gene products, Ziauddin and Sabatini developed a microarray-driven gene expression system for functional analysis of many gene products in parallel (14). This transfection cell microarray is prepared by microspotting multiple plasmid vectors together with a transfection enhancer onto a glass-based slide in an array format. When seeded directly onto the array, cells uptake

the spotted plasmids to express protein products in the cells. Consequently, an array of clusters of cells expressing the genes encoded by the respective cDNAs is obtained.

Transfection cell microarrays developed so far have employed chemical, biological, or physical means to enhance gene transfer, such as cationic lipids (14), atelocollagen (15), cationic polymers (16), electric pulse (17), magnetic force (18), and virus (19). Instead of plasmid, microarrays were also fabricated with siRNA (20, 21). siRNA-loaded cell microarrays have potential to provide an efficient platform for carrying out high-throughput loss-of-function studies. In the functional analysis on these microarrays, specific functions of genes may be analyzed using reporter assays or immunological methods.

There are a number of advantages in transfected cell microarrays as compared to functional assays performed on mammalian cells in a microwell plate format. The array approach requires less number of cells per gene tested. In addition, much less amount of DNA or RNA as well as transfection reagents is needed in the microarray-based assay than the assays performed in a microwell plate. The cost of a single assay should be reduced as much as possible in the case of high-throughput analysis. It seems that the microarray technologies provide cost-effective tools.

The main subject of this thesis is the development of transfection cell microarrays

that allow efficient transfer of multiple siRNAs into living cells. The results of these investigations are described in Chapter 1 through Chapter 5. The motivation of this study mainly came from three issues associated with current siRNA-loaded microarray platforms. First issue is the site-specificity of siRNA loading on a chip, which is important for the quantitative assays on siRNA microarrays. To address this issue, micropatterned surface prepared by a photo-assisted process was used in Chapter 1. The second issue is related to the difficulty in preparing a large set of siRNAs for high-throughput functional analysis. In Chapter 2, attempts were made to utilize siRNA library generated by endoribunuclease digestion of long double-stranded RNA (dsRNA). The third issue is concerned with transfection efficiency of siRNA in the microarray-based analysis. The reasonably-high transfection efficiency is crucial for reliable functional studies. To address this issue, Chapters 3–5 are involved in electric pulse-triggered transfection for transferring siRNA into cells on a microarray with high efficiency.

A key requirement for the fabrication of transfected cell array includes well-designed substrates for the site-restricted loading of siRNA and silencing of exogenous or endogenous genes. In addition, successful transfection from siRNA-loaded surfaces requires that the affinity of siRNAs for the substrate surface is

sufficient to support the loading yet not so excessive as to limit cellular internalization. Chapter 1 describes the fabrication of transfected cell arrays through micropatterning of self-assembled monolayer (SAM) of alkanethiols formed on a gold substrate and the subsequent site-specific loading of the siRNA-lipid-plasmid DNA complexes by alternate electrostatic adsorption. This chapter is focused on the surface microarchitecture for the efficient site-specific transfection of siRNA. SAMs provide well-defined surfaces for studying biomolecular interactions at surfaces (22, 23) and have been often employed for patterning biomolecules (24, 25). Therefore, in Chapter 1, the hydrophilic SAM surface with carboxylic acid was prepared as a small spot on the hydrophobic surface with methyl-terminated SAM. The surface was examined for the ability of binding and introducing siRNA-lipid complex into directly cultured cells. The efficiency of siRNA transfer was evaluated using a model system in which siRNA-lipid-plasmid complexes spotted on microspots were transfected into HEK293 cells seeded directly on the microarray. It is demonstrated that the alternate electrostatic adsorption of siRNA-lipid-DNA complex and DNA is an effective method for loading the complex onto the surface. The micropatterned SAM could be used for the highly site-specific loading and transfer of the siRNA complex.

Furthermore, new methodology was needed to extend the utility of siRNA

transfection microarrays. As described above, one of the problem is that the preparation of a large number of synthetic siRNAs is not practical. Because the efficiency of the gene silencing is greatly dependent on target sequences within mRNA, optimal targets are selected in advance experimentally or using empirically customized algorithms (26, 27). However, target optimaizatin is time-consuming and not viable in principle for mRNA with unknown sequences. These problems make it difficult to perform knockdown studies for the large set of DNA transcripts. To address this problem, microarrays were prepared using endoribonuclease-digested dsRNA (d-siRNA) in Chapter 2. The preparation of siRNA involves the transcription of cDNA to generate dsRNA followed by digestion with endoribonuclease, dicer (28, 29, 30). Because the digestion products include dsRNA (21–25 nt dsRNA) with various sequences of target genes, the optimization of target sequence is not necessary. Thus, the d-siRNA has great advantage for large-scale loss-of-function studies. In Chapter 2, a patterned SAM was also used as in Chapter 1. It is demonstrated that the d-siRNA-loaded microarray can be suitably used to silence specific gene.

In Chapter 3, a microarray for the electroporation of siRNA was fabricated with a gold electrode. The strategy is based on the expectation that application of a short electric pulse enhances the release of siRNAs from the electrode and thus the cellular

uptake of the released siRNAs. In this method, a gold electrode bearing SAM was used to load siRNA onto the entire surface or micropatterned surface through polyelectrolyte complex formation. Cells were adhered to the electrode and then transfected with loaded siRNA by applying an electric pulse. Because siRNAs were ionically adsorbed to the surface, it is expected that the release of siRNA is largely prevented during cell culture periods before electric pulsing and that siRNA is protected against nuclease-mediated degradation. These effects are likely to provide the possibility of transferring siRNAs into cells at a preferred moment after cell seeding. Chapter 2 demonstrates that endogenous gene was effectively suppressed using the method.

The electroporation microarrays are developed in Chapter 3 for the high-throughput gene transfer into mammalian cells. However, further improvement of electroporation efficiency will improve the reliability and reproducibility of knockdown studies on siRNA microarrays. Based on the hypothesis that the amount of loaded-siRNA is important factor to achieve effective knockdown efficiency. In Chapter 4, the layer-by-layer (LBL) assembly technique (31) was used to increase the amount of loaded-siRNA on an electrode. In this chapter, the LBL technique was employed to construct a multilayer consisting of cationic polymer, poly(ethyleneimine) and anionic polymer, siRNA on the surface of a gold electrode. The results obtained in this chapter

emphasize the usefulness of the LBL assembly process for fabricating siRNA-loaded microarrays for highly-efficient knockdown experiments.

As demonstrated in Chapters 3 and 4, the electroporation microarray is a useful tool for the high-throughput analysis of gene functions. However, transfection efficiency is greatly impaired by the storage of microarrays due to water evaporation from arrayed nucleotides. To address this desiccation problem, the effects of various moisture retention agents such as saccharides and sugar alcohols added to plasmid DNA or siRNA were examined in Chapter 5. After storage of these microarrays at different temperature for various time periods, transfection efficiency was evaluated using human embryonic kidney cells. In the case of plasmid DNA-loaded microarrays, the addition of saccharides served to retain transfection efficiency at a reasonably high level after storage at –20˚C. On the other hand, the addition of saccharides and sugar alcohols had insignificant results on the siRNA-loaded microarray after storage of a microarray.

In summary, this thesis describes the result of methodological studies for the fabrication of siRNA microarrays. The technologies developed in this thesis accelerate cell-based functional analysis for a large set of genes.

References

(1) International Human Genome Sequencing Consortium. (2001) Initial sequencing and analysis of the human genome. *Nature* **409** 860–921.

(2) Venter JC, Adams MD, Myers EW, Li PW, Mural RJ, Sutton GG, Smith HO, Yandell M, Evans CA, Holt RA *et al*. (2001) The sequence of the human genome. *Science* **291** 1304–1351.

(3) He L, Hannon GJ. (2004) MicroRNAs: small RNAs with a big role in gene regulation. *Nat. Rev. Genet.* **5** 522–531.

(4) Schena M, Shalon D, Davis RW, Brown PO. (1995) Quantitative monitoring of gene expression patterns with a complementary DNA microarray. *Science* **270** 467–470.

(5) Ge H. (2000) UPA, a universal protein array system for quantitative detection of protein-protein, protein-DNA, protein-RNA and protein-ligand interactions. *Nucleic Acids Res.* **28** e3.

(6) MacBeath G., Schreiber SL. (2000) Printing proteins as microarrays for high-throughput function determination. *Science* 289 1760–1763.

(7) Fodor SP., Read JL., Pirrung MC., Styer L., Lu AT., Solas D. (1991) Light-directed, spacially addressable parallel chemical synthesis. *Science* **251** 767–773.

(8) Houseman BT., Huh JH., Kron SJ., Mrksich M. (2002) Peptide chips for the

quantitative evaluation of protein kinase activity. *Nat. Biotechnol.* **20** 270–274.

(9) MacBeath G., Koehler AN., Schreiber SL. (1999) Printing small molecules as microarrays and detecting protein-ligand interaction *en masse*. *J. Am. Chem. Soc.* **121** 7967–7968.

(10) Lueking A., Horn M., Eickhoff H., Bussow K., Lehrach H., Walter G. (1999) Protein microarrays for gene expression and antibody screening. *Anal. Biochem.* **270** 103–111.

(11) Fang Y., Frutos, AG., Lahiri J. (2002) Membrane protein microarrays. *J. Am. Chem. Soc.* **124** 2394–2395.

(12) Fire A., Xu S., Montgomery MK., Kostas SA., Driver SE., Mello CC. (1998) Potent and specific genetic interference by double-stranded RNA in *Caenorhabditis elegans*. *Nature* **391** 806–811.

(13) Elbashir SM., Harborth J., Lendeckel W., Yalcin A., Weber K., Tuschl T. (2001) Duplexes of 21-nucleotide RNAs mediate RNA interference in cultured mammalian cells. *Nature* **411** 494–498.

(14) Ziauddin J., Sabatini DM. (2001) Microarrays of cells expressing defined cDNAs. *Nature* **411** 107–110.

(15) Honma K., Ochiya T., Nagahara S., Sano A., Yamamoto H., Hirai K., Aso Y.,

Terada M. (2001) Atelocollagen-based gene transfer in cells allows high-throughput screening of gene functions. *Biochem. Biophys. Res. Commun.* **289** 1075–1081.

(16) Chang FH, Lee CH., Chen MT., Kuo CC., Chiang YL., Hang CY., Roffler S. (2004) Surfection: a new platform for transfected cell microarrays. *Nucleic Acids Res.* **32** e33.

(17) Yamauchi F., Kato K., Iwata H. (2004) Spatially and temporally controlled gene transfer by electroporation into adherent cells on plasmid DNA-loaded electrodes. *Nucleic. Acids. Res.* **32** e187.

(18) Isalan M, Santori MI, Gonzalez C, Serrano L. (2005) Localized transfection on arrays of magnetic beads coated with PCR products. *Nat. Methods* **2** 113–118.

(19) Bailey SN., Ali SM., Carpenter AE., Higgins CO., Sabatini DM. (2006) Microarrays of lentiviruses for gene function screens in immobilized and primary cells. *Nat. Methods* **3** 117–122.

(20) Kumar R, Conklin DS, Mittal V. (2003) High-throughput selection of effective RNAi probes for gene silencing. *Genome Res.* **13** 2333–2340.

(21) Mousses S, Caplen NJ, Cornelison R, Weaver D, Basik M, Hautaniemi S, Elkahloun AG, Lotufo RA, Choudary A, Dougherty ER, Suh E, Kallioniemi O. (2003) RNAi microarray analysis in cultured mammalian cells. *Genome Res.* **13** 2341–2347.

(22) Mrksich M, Whitesides GM. (1996) Using self-assembled monolayers to understand the interactions of man-made surfaces with proteins and cells. *Annu. Rev. Biophys. Biomol. Struct.* **25** 55–78.

(23) Lopez GP, Biebuyck HA, Harter R, Kumar A, Whitesides GM. (1993) Fabrication and imaging of two-dimensional patterns of proteins adsorbed on self-assembled monolayers by scanning electron microscopy. *J. Am. Chem. Soc.* **115** 10774–10781.

(24) Milan M, Dike LE, Tien J, Ingber DE, Whitesides GM. (1997) Using microcontact printing to pattern the attachment of mammalian cells to self-assembled monolayers of alkanethiolates on transparent films of gold and silver. *Exp. Cell Res.* **235** 305–313.

(25) Kumar A, Biebuyck HA, Whitesides GM. (1994) Patterning self-assembled monolayers: applications in materials science. *Langmuir* **10** 1498–1511.

(26) Reynolds A., Leake D., Boese Q., Scaringe S., Marshall WS., Khvorova A. (2004) Rational siRNA design for RNA interference. *Nat. Biotechnol.* **22** 326–330.

(27) Pei Y., Tuschl T. (2006) On the art of identifying effective and specific siRNAs. *Nat. Methods* **3** 670–676.

(28) Yang D., Buchholz F., Huang Z., Goga A., Chen CY., Brodsky FM., Bishop

J.M. (2002) Short RNA duplexes produced by hydrolysis with *Escherichia coli* RNase III mediate effective RNA interference in mammalian cells. *Proc. Natl. Acad. Sci. U.S.A.* **99** 9942–9947.

(29) Myers JW., Jones JT., Meyer T., Ferrell JE. (2003) Recombinant Dicer efficiently converts large dsRNAs into siRNAs suitable for gene silencing. *Nat. Biotechnol.* **21** 324–328.

(30) Buchholz F., Kittler R., Slabicki M., Theis M. (2006) Enzymatically prepared RNAi libraries. *Nat. Methods* **3** 696–700.

(31) Decher G. (1997) Fuzzy nanoassemblies: Toward layered polymeric multicomposites. *Science* **277** 1232–1237.

Chapter 1

Fabrication of cell-based arrays using micropatterned alkanethiol monolayers for the parallel silencing of specific genes by small interfering RNA

INTRODUCTION

Small interfering RNA (siRNA) has recently been recognized as a powerful tool for analyzing gene functions in mammalian cells (1). When introduced into cytoplasm, double-stranded RNA of ~21 nucleotides triggers RNA interference (RNAi) by which specific genes having homologous sequences are transiently silenced to yield mutants. The abnormal phenotypes caused by RNAi provide the biological readouts from which one can infer the functions of particular genes. Recently, deep insights have been gained into the cellular mechanism involved in siRNA-triggered gene silencing (2, 3), while advances in siRNA technology opened a new opportunity to study gene functions in a genome-wide (4–7).

The genome-wide RNAi screens require several methodological arrangements: A library of siRNA clones must be implemented to cover the huge number of genes. Efficient cell reporting systems are further needed to monitor phenotypic alterations on living cells. In addition, it is practically important especially for high-throughput screens to develop

efficient and flexible platforms that permit parallel introduction of siRNA clones into living cells. Because the number of genes has reached few tens of thousands, this is not straightforward by conventional microplate formats. To solve this problem, a number of groups have developed the cell-based arrays that allow parallel introduction of multiple siRNAs into cultured mammalian cells (8–11).

The idea of cell-based arrays for large-scale genetic screens was derived from the pioneering study by Ziauddin and Sabatini (12). In that study, expression constructs for defined cDNAs were printed together with cationic lipid and gelatin onto a glass slide in an array format. It was shown that, when cultured directly on the slide, cells were successfully transfected with released DNA to express individual cDNAs within the defined areas. This technology was immediately extended to the parallel transfection of siRNA into living cells (8–11, 13). In most cases, siRNA arrays were fabricated in a similar way to the plasmid DNA array as mentioned above, but simply replacing DNA with siRNA.

Although early studies (8–11, 13) succeeded in demonstrating the feasibility of the cell-based arrays for RNAi screens, further improvements are considered necessary to obtain quantitative and accurate data for finding out specific phenotypes from a large data set. First of all, it is obvious that low transfection efficiency would make experimental data difficult to interpret. Other important factors include deviation of transfection efficiency between different siRNAs on separate spots on a single array. Such deviation would make it difficult to distinguish small difference in phenotypic readouts, such as fluorescent intensity in an assay combined with a reporter system using mutants with green fluorescent protein (GFP). In addition, the efficiency of gene silencing at the different regions within a

single spot is also a matter of utmost concern in quantitative analysis. Because the extent of gene silencing is expressed as a reduction rate of protein expression in total transfected cells, siRNA should be introduced to the cells on precisely restricted regions and, at the same time, homogenously to the entire cells over the spot.

The aim of this chapter is to fabricate cell-based siRNA arrays using surface chemical processes including the micropatterning of a self-assembled monolayer (SAM) (14–16) and the layer-by-layer (LBL) assembly (17) of siRNA and cationic lipid. In previous study, cell-based arrays for the efficient overexpression of defined cDNAs were successfully fabricated using the LBL process on the micropatterned SAM (18). It was demonstrated that these processes provide an effective way to reproducibly introduce plasmid DNA into cells at the restricted regions on the array. This chapter is therefore the extension of an outstanding method for the array-based loss-of-function assays using siRNA. In this chapter, photo-assisted micropatterning of SAM was employed to create an array of small anionic dots on a glass substrate. The array was then utilized as a platform for loading siRNA with cationic lipid and plasmid DNA by the LBL process to obtain siRNA arrays. The feasibility of this siRNA array was examined for the sequence- and site-specific gene silencing. Furthermore, the effects of siRNA loading and culture period after transfection were studied to optimize cell-based assays on the siRNA arrays. It is shown that the method used in this chapter provides the siRNA arrays with spatial specificity in gene silencing, which will serve to obtain a quantitative data set from the cell-based screens on siRNA arrays.

EXPERIMENTAL

Preparation of patterned SAM

A glass plate (22 × 26 × 0.5 mm^3, Matsunami Glass Industries, Ltd., Osaka, Japan) was immersed in piranha solution (7:3, vol/vol 96% H_2SO_4/30% H_2O_2) for 5 min at room temperature to remove impurities and then washed with 2-propanol and MilliQ water. Thin layers of chromium (thickness: 1 nm) and gold (thickness: 49 nm) were sequentially deposited onto the purified glass plate in a continuous process with a vacuum evaporator (V−KS200, Osaka Vacuum Instruments, Osaka, Japan) operated at a pressure of 3–4 × 10^{-4} Pa. Immediately after deposition, the plate was immersed in 1 mM 1-hexadecanethiol (Tokyo Kasei Kogyo Co., Tokyo, Japan) solution in ethanol at room temperature for 24 h to allow the formation of a methyl terminated SAM (CH_3−SAM) on gold. The plate was washed with ethanol and water to remove unreacted alkanethiols, and dried under a stream of dried N_2 gas.

For micropattterning, the glass plate having a CH_3−SAM was radiated by ultraviolet light through a photomask (15). The photomask was made of a quartz plate deposited with a thick chromium layer having 5 × 5 circular holes with a diameter of 1 mm. The SAM surface was overlaied with the photomask and irradiated with ultraviolet light through the photomask from an ultra-high-pressure mercury lamp (500 W, Optical Modulex SX−UI500HQ, Ushio Inc., Osaka, Japan). After 2 h irradiation, the plate was washed with ethanol and water to remove photo-cleaved alkanethiols and immediately immersed in a 1 mM solution of 11-mercapto-1-undecanoic acid (Aldrich Chemical Co., Milwaukee, WI,

USA) or 1 mM solution of 11-amino-1-undecanethiol (Dojindo laboratories, Kumamoto, Japan) to allow the formation of a carboxylic terminated SAM (COOH–SAM) or an amine-terminated SAM (NH_2–SAM) in ethanol. The plate was kept in the solution for 2 h at room temperature to allow the formation of a carboxylic acid terminated SAM (COOH–SAM) within the UV-radiated spots. Finally the plate was washed with ethanol and water to remove unreacted alkanethiols and dried under a stream of N_2 gas.

siRNA and plasmid DNA

Synthetic siRNAs of 21 or 22 nucleotides were purchased from Qiagen, Hilden, Germany, and Dharmacon, Inc., Colorado, USA: Specific siRNA for enhanced GFP (EGFP–siRNA): sense, 5'-GCAAGCUGACCCUGAAGUUCAU-3'; antisense, 5'-GAACUUCAGGGUCAGCUUGCCG-3' (Qiagen). For *Discosoma sp.* red fluorescent protein (DsRed–siRNA): sense, 5'-AGUUCCAGUACGGCUCCAAUU-3'; antisense, 5'-UUGGAGCCGUACUGGAACUUU-3' (Dharmacon). Nonspecific siRNA (control–siRNA): sense, 5'-UUCUCCGAACGUGUCACGUdTdT-3'; antisense, 5'-ACGUGACACGUUCGGAGAAdTdT-3' (Qiagen). EGFP–siRNA conjugated with rhodamine at the 3'-end (EGFP–siRNA–Rho): sense, 5'-GCAAGCUGACCCUG AAGUUCAU-3'; antisense, 5'-GAACUUCAGGGUCAGCUUGCCG-3' (Qiagen).

Plasmids used were pEGFP-C1 and pDsRed2-C1 (Clontech Laboratories, Palo Alto, CA, USA), which encoded, respectively, EGFP and DsRed, under the control of the immediate early promoter of human cytomegalovirus. These plasmids are referred to as pEGFP and pDsRed, respectively. These plasmids were amplified in *Escherichia coli*

DH5α and purified using a Plasmid Maxiprep Kit (Qiagen). A rhodamine labeled plasmid, pGeneGrip^{TM} Rhodamine/GFP, was purchased from Gene Therapy Systems, California, USA, and used as received.

Loading of siRNA and plasmid DNA

The outline of array preparation is shown in Scheme 1. Opti–MEM (Gibco Life Technologies, Grand Island, NY, USA), containing siRNA (0–20 μg/mL) and plasmid DNA (10 μg/ml), and lipofectAMINE2000 (30 μg/mL; Invitrogen Corp., Carlsbad, CA, USA) was prepared and kept at room temperature for 20 min to form an electrolyte complex between the anionic nucleic acids (siRNA and plasmid DNA) and the cationic lipid. This lipid-DNA-RNA complex is referred to as LDR complex hereafter. The solution (approximately 200 nL) of LDR complex was manually pipetted to COOH-terminated dots on the patterned SAM and kept for 5 min to adsorb the complex to the dot surface. After aspiration of the LDR complex solutions, 200 nL of a plasmid DNA solution (10 μg/mL) in Opti–MEM was then pipetted to the LDR-adsorbed dots and kept for 5 min to adsorb DNA to the dots. These procedures were repeated to form a multilayer consisting of LDR-DNA-LDR-DNA-LDR. Finally, the entire surface of the array was washed with PBS and immediately used for further experiments without drying.

To determine the amount of plasmid DNA and siRNA loaded to the dots, either the rhodamine-conjugate of plasmid DNA (pGeneGrip^{TM} Rhodamine/GFP) or siRNA (EGFP–siRNA–Rho) was loaded to the patterned SAM together with unlabeled siRNA or plasmid DNA, respectively, in the same manner as described above. The dots were

observed with a fluorescence stereomicroscope (MZ FLIII, Leica, Switzerland) equipped with a cooled-CCD camera (ORCA–ER; Hamamatsu Photonics K.K., Shizuoka, Japan). A fluorescence intensity was measured for the entire area within a single dot using an AQUA-Lite digital imaging software (Hamamatsu Photonics). The fluorescence intensity was converted to the amount of DNA or siRNA using a calibration curve obtained by depositing the rhodamine-labeled DNA and siRNA of known amount to a dot. The data was expressed as mean ± standard deviation for n = 5.

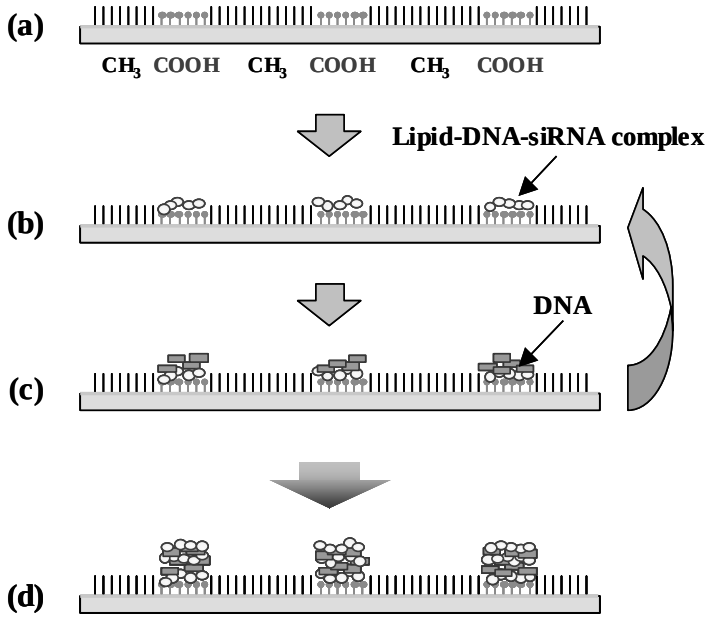

Scheme 1. Loading of siRNA by LBL assembly to individual dots on the micropatterned SAM. (a) Micropatterned alkanethiol SAM. (b) Adsorption of LDR complex. (c) Adsorption of plasmid DNA. The procedures (b) and (c) were repeated to obtain a siRNA-loaded array (d).

Gene silencing on siRNA array

Human embryonic kidney cell, HEK293, was obtained from Health Science Research Resources Bank, Tokyo, Japan, and grown in minimal essential medium (MEM; Gibco) containing 10% fetal bovine serum (FBS), 100 U/ml penicillin, and 0.1 mg/ml streptomycin at 37 °C under 5% CO_2. The cells were harvested by trypsin treatment and suspended in antibiotics-free MEM with or without 10% FBS. The siRNA-loaded array was placed in a 35-mm Petri dish, and the cells were seeded onto the array at a density of 6.7×10^4 cells/cm^2. The cells were incubated at 37 °C under 5% CO_2 to allow cell adhesion and cotransfection of plasmid DNA and siRNA. Then the medium was replaced with a fresh MEM containing 10% FBS and antibiotics 6 h (for cells seeded without FBS) or 24 h (for cells seeded with FBS) after cell seeding. During culture, cells were observed with an epifluorescence microscope (Olympus, Tokyo, Japan). The fluorescence intensity of EGFP or DsRed was measured 48 h after cell seeding for the entire area of a dot using a fluorescence stereomicroscope (MZ FLIII, Leica). The efficiency of gene silencing (suppression efficiency) was determined according to the following equation.

$$\text{Suppression efficiency (\%)} = [1 - (I_{\text{specific}} / I_{\text{control}})] \times 100$$

where I_{specific} is the fluorescent intensity of EGFP measured for the dot on which plasmid DNA and the specific siRNA were cotransfected, and I_{control} is that for the dot on which either of the plasmids were cotransfected with control–siRNA. All the data presented in this chapter were the average of three independent experiments.

RESULTS

Preparation of siRNA array

The photoassisted patterning of CH_3–SAM and the subsequent formation of COOH–SAM within the radiated areas gave rise to the patterned SAM which possessed hydrophilic dots (COOH–SAM) surrounded by the hydrophobic regions (CH_3–SAM). Thanks to the difference in hydrophilicity, a liquid droplet pipetted was readily positioned to the hydrophilic dot. This feature served to confine siRNA to the dots, and eventually to produce well-formatted siRNA arrays.

A previous study revealed that the complex consisting of plasmid DNA and excess cationic lipid (lipofectAMINE2000) was attracted by the negatively charged surface of COOH–SAM through electrostatic interactions (18). From an analogy to the previous observation, it is plausible that the LDR complex employed in this chapter adsorbed ionically to the COOH–SAM surface. Similarly, alternate adsorption of LDR complex (cationic assembler) and free plasmid DNA (anionic assembler) is expected to produce a multilayer comprising siRNA, plasmid DNA, and cationic lipid. The amount of adsorbed siRNA and plasmid DNA reached, respectively, 38 ± 11 ng/cm^2 and 150 ± 67 ng/cm^2, when determined for a multilayer formed using 1 mg/mL siRNA solution after 5 adsorption procedures, i.e. a multilayer with LDR-DNA-LDR-DNA-LDR.

Sequence specific gene silencing on siRNA array

Figure 1 shows the representative results of sequence-specific gene silencing on the siRNA-loaded array. When seeded in the presence of FBS, adhesion of HEK293 cells were restricted to the dots (Figure 1 b–d), probably due to preferential adsorption of abundant

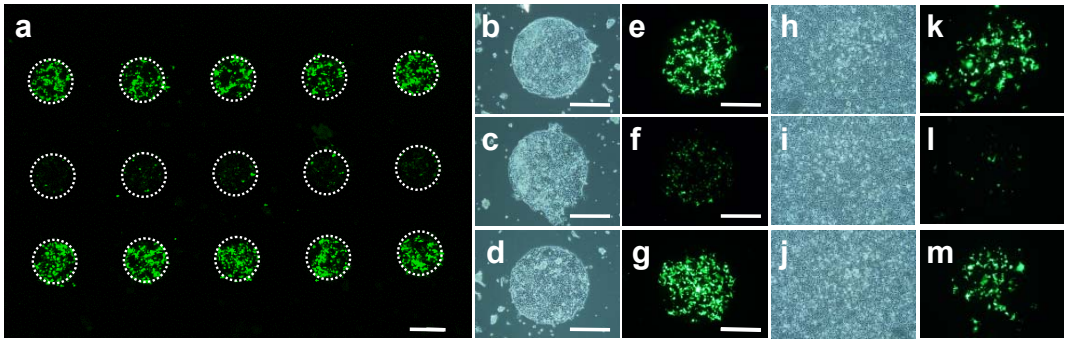

Figure 1. Gene silencing on the siRNA array. (a) Fluorescent image of the array on which HEK293 cells were seeded in the presence of FBS. The images were recorded 48 h after cell seeding. The position of dots is indicated in the image with dotted circles. (b–m) Higher magnification images of selected dots. Cells were seeded in (b–g) the presence and (h–m) the absence of FBS. Phase-contrast (b–d, h–j) and the corresponding fluorescent (e–g, k–m) images are shown for three cases: (top) pEGFP alone, (middle) pEGFP + EGFP–siRNA, (bottom) pEGFP + control–siRNA. Bar = (a) 1 mm, (c–m) 500 μm.

serum proteins such as albumin and globulin onto hydrophobic regions between dots (19–22), which might suppress cell adhesion to these areas. The cell adhesion within dots may be promoted by the cationic nature of the uppermost surface, because the LBL process was always ended with the LDR complex. The typical number of cells was approximately 2500 cells per dot under the conditions employed here. EGFP expression was observed on the dots loaded with the EGFP-coding plasmid but lacking siRNA (5 dots on the upper line

in Fig. 1a) with a similar extent between the spots. Cells on the dots with both plasmid and control–siRNA (5 dots on the bottom line in Fig. 1a) also expressed EGFP, indicating the insignificant effect of nonspecific siRNA on protein synthesis. In contrast, a lower level of EGFP expression was observed on the dots with EGFP-coding plasmid and EGFP–siRNA (5 dots on the middle line in Fig. 1 a), indicating the suppression of EGFP synthesis. The fluorescence intensity was determined to be 0.19 ± 0.09 (EGFP–siRNA), 2.30 ± 0.31 (control–siRNA), and 2.36 ± 0.86 (no siRNA). The observed small deviations denote the reproducibility of transfection. These results suggested that both plasmid and siRNA were transferred from the array into the cells to reproducibly silence EGFP synthesis in sequence- and region-specific manners.

Similar to the case in which cells were seeded in the presence of FBS, sequence- and region-specific gene silencing was observed in the absence of FBS (Fig. 1 h–m). In the absence of FBS, however, cells adhered and grew on the entire surface of the array.

In order to gain deeper insights into the interactions operated in the LBL process, an amine-terminated SAM (NH_2–SAM) having a positively charged surface was used instead of a COOH–SAM. When the LDR complex (lipid/pEGFP/control–siRNA) was adsorbed as the first assembler to obtain five-layered LDR-DNA composites, EGFP was expressed in HEK293 cells to a lower extent compared to the case with COOH–SAM (Fig. 2), indicating that the combination of the COOH–SAM having an anionic surface and the LDR complex plays an important role in efficient transfection. This finding supports the hypothesis that the LDR complex bares cationic charges and that electrostatic interactions are predominant

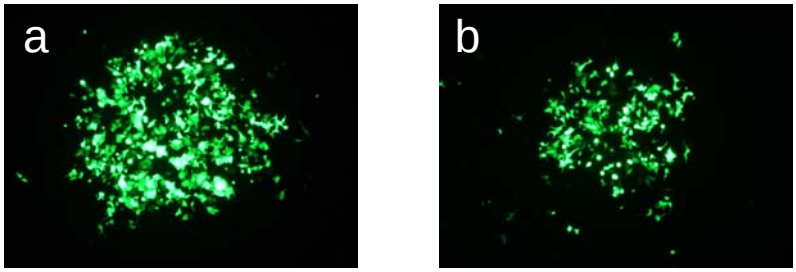

Figure 2. Fluorescence microphotographs of HEK293 cells transfected on the siRNA arrays. The LDR complex and plasmid DNA were assembled on the dots with (a) COOH–SAM and (b) NH_2–SAM. Note that EGFP expressed much efficiently on COOH–SAM than on NH_2–SAM.

forces operated in the LBL assembly process. It seems that the cationic NH_2–SAM surface attracts inefficiently the LDR complex with the same sign of charges.

To clarify the mechanism by which the array functions, two different plasmids, pEGFP and pDsRed, were used respectively as a component of the LDR complex and anionic assembler, or vice versa. GFP–siRNA and control–siRNA were used as a RNA component in the LDR complex. As shown in Figure 3, the plasmid contained in the LDR complex was efficiently expressed in the cells (Fig. 3 a and f), but that used as an anionic assembler was not (Fig. 3 b and e). The expression of GFP was efficiently suppressed by the GFP–siRNA incorporated to the LDR complex (Fig. 3 c and d). The DsRed expression was not influenced by GFP–siRNA, as expected (Fig. 3 g and h). These results demonstrate that plasmid contained in the LDR complex is transfected more efficiently than that used as an anionic assembler.

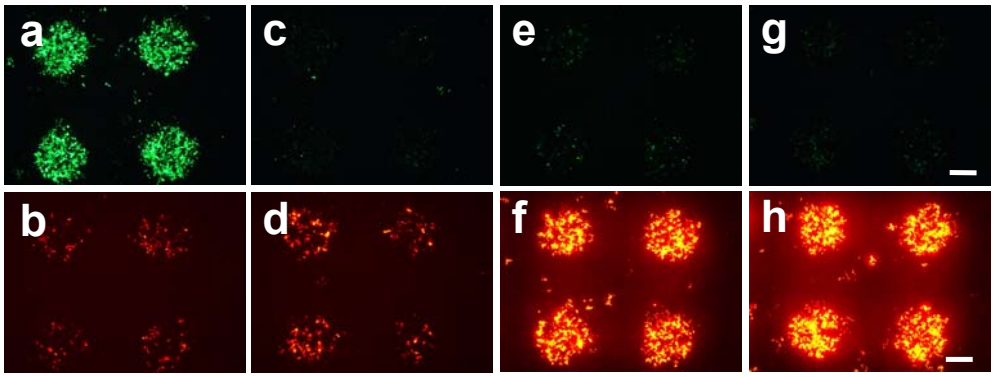

Figure 3. Fluorescent images of HEK293 cells transfected on siRNA arrays prepared from different compositions of siRNAs and plasmid DNAs. Plasmid DNA: (a–d) LDR; pEGFP, D; pDsRed, (e–h) LDR; pDsRed, D; pEGFP. siRNA: (a, b, e, f) control–siRNA, (c, d, g, h) GFP–siRNA. Bar = 500 μm.

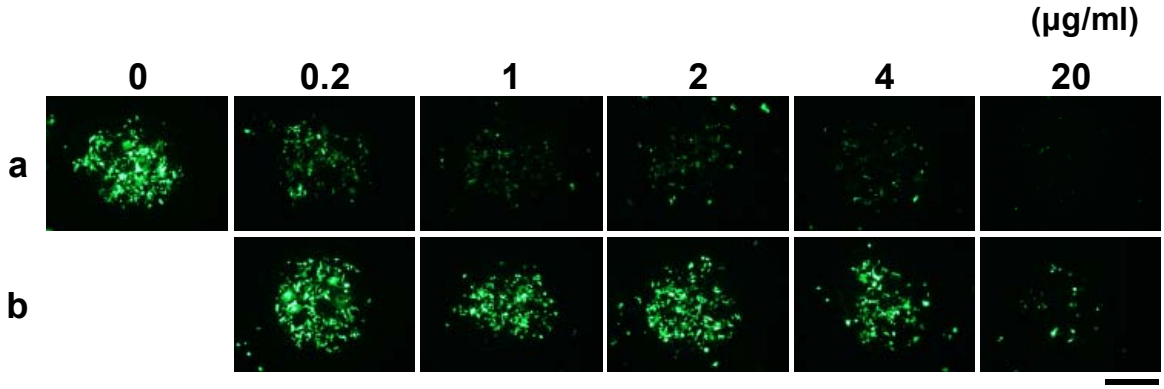

Figure 4. Fluorescent images showing the effect of siRNA loading on the silencing of EGFP expression. EGFP–siRNA (a) and control–siRNA (b) were co-transfected with pEGFP. The concentration of siRNA used in the preparation of LDR complex is indicated above the corresponding photographs. Bar = 500 μm.

Attempts were further made to examine the feasibility of the SAM array for silencing endogenous targets. The LBL assembly was conducted using the complex consisting of GFP–siRNA and the lipid as cationic assembler and GFP–siRNA as anionic assembler. HEK293 cells stably transformed with GFP gene were plated to the array. It was found that the expression of GFP was efficiently reduced in a sequence-specific manner (data not shown).

Effect of siRNA loading

Figure 4 shows the effect of siRNA loading on the suppression of EGFP expression. The LDL complex was prepared using different concentrations of siRNA together with the fixed concentration of plasmid DNA and cationic lipid. As is seen from the series of fluorescent images, silencing by specific siRNA (Fig. 4a) was evident at a siRNA concentration of 0.2 μg/mL with a suppression efficiency of 76%. The highest suppression efficiency (= 90%) was achieved at a siRNA concentration of more than 1.0 μg/mL. When a siRNA solution of relatively high concentration (> 4 μg/mL, Fig. 4 b) was used, EGFP expression was impaired in the cells transfected with both EGFP-specific and control siRNAs. This is partly because of nonspecific inhibition of protein synthesis by highly concentrated exogeneous RNA (23). Another factor that affects EGFP expression may be altered charge balance in the LDR complex, which would affect introduction of plasmid DNA into cells. These results suggest that the most efficient, sequence-specific gene silencing can be achieved with 1.0–2.0 μg/mL siRNA under the experimental conditions employed here, while nonspecific effect is insignificant.

Time dependence of gene silencing

As shown in Figure 5a, EGFP expression on the dots without siRNA and with control−siRNA increased during initial 4 days after cell seeding in the presence of FBS, reached the maximal expression level at day 4, and then gradually decreased afterward most likely due to plasmid metabolism (24). In contrast, a low level of EGFP expression was observed on the dots loaded with EGFP−siRNA throughout the culture period. The highest suppression was achieved 48 h after cell seeding, with a suppression efficiency of 91% compared to the fluorescence intensity determined at the same time points for cells transfected with control−siRNA. Similar time dependence was observed in the experiments in which cell were seeded in the absence of FBS (Fig. 5 b). The highest efficiency of gene silencing (80−90% compared to the results with control−siRNA) was achieved after 48 h of culture on the array. When control−siRNA was transfected, the expression of EGFP was lower in the absence of serum than in the presence of serum (open bars in Fig. 5 a and b). Although a reason for this result at this moment, the composition of lipid/siRNA/DNA might not be optimal for transferring pEGFP under the serum-free condition. However, it cannot be ruled out that control−siRNA might cause non-specific inhibition particularly in the absence of serum.

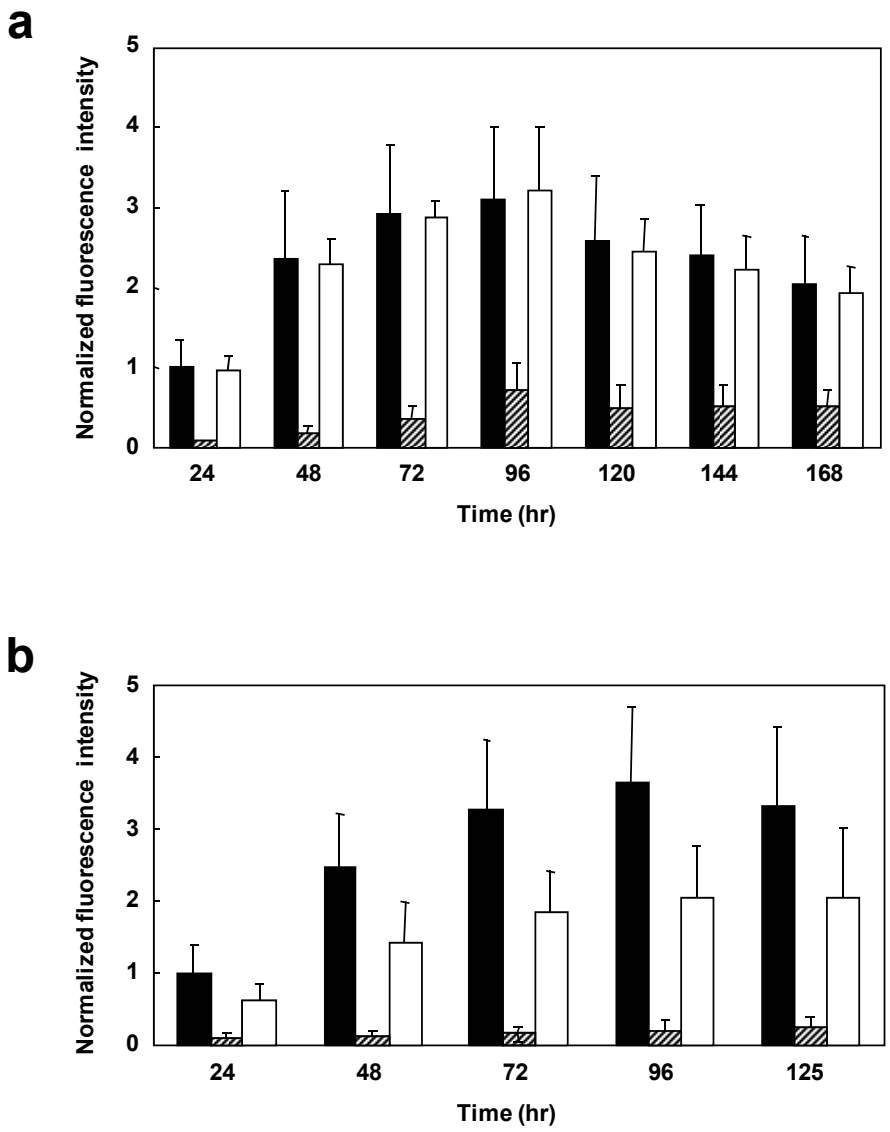

Figure 5. Time dependence of EGFP expression on the siRNA array. Cells were seeded in (a) the presence and (b) the absence of FBS (see Materials and Methods for details). Fluorescent intensities measured on the dots at various time points were normalized by that of control dot (no siRNA transfected) at 24 h. (▬): no siRNA transfected, (▨): transfected with EGFP–siRNA, (▭): transfected with control–siRNA. The data are expressed as mean ± standard deviation for n = 3.

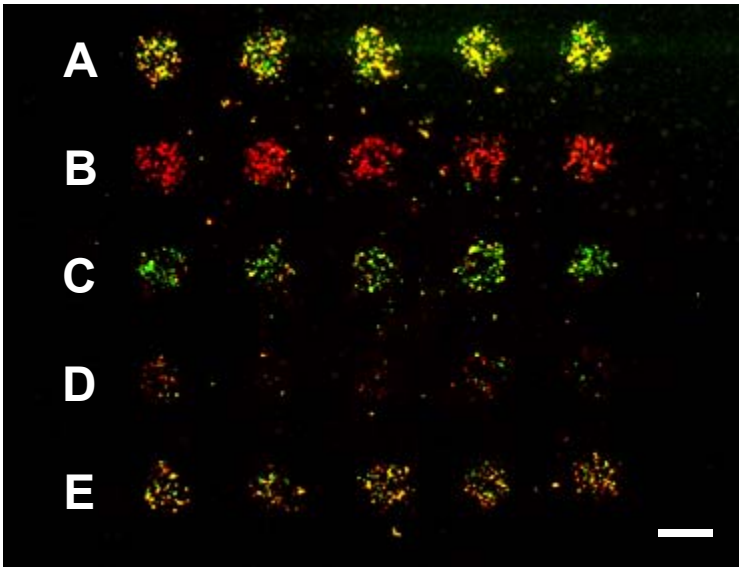

Figure 6. Parallel and dual silencing of gene expression on the siRNA array. The fluorescent images acquired using an interference filter for EGFP and DsRed were pseudo-colored and merged. Two plasmids, pEGFP and pDsRed, were loaded to all the dots (a) without any siRNA or together with (b) EGFP–siRNA, (c) DsRed–siRNA, (d) EGFP–siRNA plus DsRed–siRNA, and (E) control–siRNA. Bar = 500 μm.

Parallel and dual silencing

In this chapter, study was undertaken to examine the feasibility of the array method for the parallel experimentation in which two different siRNAs are introduced separately to the cells on different dots on a single array. In addition, attempts were made to simultaneously introduce different siRNAs to the cells on a single dot. The result is shown in Figure 6. All the dots were loaded with both plasmids, pEGFP and pDsRed. The siRNAs used here (EGFP–siRNA and DsRed–siRNA) were specific for the distinct sequences in the respective cDNA, and hence are not expected to interfere each other. As shown in Figure 6,

transfection of siRNA resulted in the reasonable gene expression profiles expected from the combinations of siRNAs and plasmids. This simple demonstration shows the feasibility of this method for use in parallel and/or dual silencing analysis on a single array platform.

DISCUSSION

In order to conduct array-based large-scale RNAi screens to distinguish peculiar phenotypes from the multitude of negative backgrounds, it is primarily important that the reliability and accuracy of phenotypic readouts are guaranteed. To realize such an assay method, cell-based siRNA arrays using processes for micropatterning and LBL assembly were prepared in this chapter. As demonstrated here, the siRNA arrays allowed to silence specific genes in a spatially restricted manner, which enabled to quantitatively determine silencing efficiency. The silencing efficiency determined for co-transfected EGFP gene reproducibly reached ca. 90% under the optimum conditions.

A key technology in the siRNA array preparation is an alkanethiol SAM that provides well-characterized functional surfaces for further modifications (14, 25). In combination with micropatterning techniques, the SAM finds a great opportunity to be applied in micro- and nanobiotechnology, especially in cell-based array technology (26–31). The UV-assisted patterning process used here is a simple and reproducible technique. The flexibility in pattern size and shape is of great advantage in restricting regions for siRNA loading over other methods such as, for instance, spotting by means of robotic arrayers. Using SAM, one can readily design distinctive surface chemistry between the patterns and the surrounding

areas, which consequently affords highly restrictions on the regions of siRNA loading and, in particular cases, cell adhesion.

The spots created on the SAM had an area of 0.79 mm^2 (1 mm in diameter), on which approximately 2500 HEK293 cells were grown at confluence. Although this size is rather large for the conventional microarrays, much smaller spots will probably affect the reliability of quantitative data obtained from a single spot. For quantitative study, the spot size should be carefully optimized depending on the cells used, because the confluent density is also a subject of cell types. In micropatterning of SAM, the size as well as the density of the spot can be easily changed by appropriately designing a photomask using the standard lithography-based technique.

One of the most important requirements for siRNA arrays is that nucleotides must be transiently loaded on the array before cell seeding. They were realized in this chapter by employing the LBL assembly process. The surface of COOH–SAM, possessing the negative charge under neutral conditions, attracts the LDR complex probably through electrostatic interactions, because the complexes formed with siRNA, plasmid DNA, and excess cationic lipid are expected to bare net positive charge. It is likely that the adsorption of the LDR complex overcompensates to generate cationically charged surface which, in turn, attracts excess anionic DNA to generate again an anionically charged surface. These alternate adsorption was repeated to obtain 5 layers consisting of the LDR complex and plasmid DNA. It was shown that the silencing of EGFP expression was restricted to the cells within the dot loaded with EGFP–siRNA, whereas EGFP expression in the cells at the surrounding regions outside the dot as well as those on the neighboring dots were not

affected by released EGFP–siRNA. This observation suggests that the leaching of siRNA out of the dot was not significant until cells were seeded and that the concentration of siRNA was too low to silence gene expression in the adjacent cells.

The concentration of siRNA in a solution used for LDR complex formation had a large effect on the level of gene silencing, with the optimum concentration of 1.0 μg/mL (Fig. 4). This effect is most likely due to the fact that higher concentration of siRNA gives rise to the larger loading on the dot. The loading of too much siRNA might enhance the introduction of siRNA into cells, initiating nonspecific inhibition of protein synthesis as in the case with control–siRNA. However, the large amount of siRNA seems to weaken cationic nature of the LDR complex, which in turn would retard transfection of cells with plasmid DNA, reducing the level of EGFP expression.

It was further demonstrated that the micropatterned SAM-based siRNA array allowed parallel and dual silencing of specific genes (Fig. 6). Taking into account the high silencing efficiency as well as the possibility of silencing endogenous genes, the array method presented here has potential as an excellent platform for large-scale RNAi screens. Moreover, assays using the siRNA array require neither the large number of cells nor the extremely expensive robotic machine for dispensing liquid. In addition, there is no difficulty in microscopic observation of living cells with an array format, in marked contrast to the assays using the conventional microplates.

In conclusion, the siRNA arrays prepared by means of micropatterning and LBL assembly processes enable to precisely restrict regions of gene silencing. This feature will facilitate obtaining quantitative data from cell-based RNAi screens on mammalian cells.

The flexibility of array design and the capability of controlling the cell adhesion area expand the future application of the siRNA arrays.

References

(1) Elbashir SM., Harborth J., Lendeckel W., Yalcin A., Weber K., Tuschl, T. (2001) Duplexes of 21-nucleotide RNAs mediate RNA interference in cultured mammalian cells. *Nature* **411** 494–498.

(2) Hammond SM., Caudy AA., Hannon GJ. (2001) Post-transcriptional gene silencing by double-stranded RNA. *Nat. Rev. Genet.* **2** 110–119.

(3) Leung RK., Whittaker PA. (2005) RNA interference: from gene silencing to gene-specific therapeutics. *Pharmacol Ther.* **107** 222–239.

(4) Boutros M., Kiger AA., Armknecht S., Kerr K., Hild M., Koch B., Hass SA., Paro R., Perrimon N. (2004) Genome-wide RNAi analysis of growth and viability in Drosophila cells. *Science* **303** 832–835.

(5) Ashrafi K., Chang FY., Watts JL., Fraser AG., Kamath RS., Ahringer J., Ruvkun G. (2003) Genome-wide RNAi analysis of *Caenorhabditis elegans* fat regulatory genes. *Nature* **421** 268–272.

(6) Chi JT., Chang HY., Wang NN., Chang DS., Dunphy N., Brown PO. (2003) Genomewide view of gene silencing by small interfering RNAs. *Proc. Natl. Acad. Sci. U.S.A.* **100** 6343–6346.

(7) Zheng L., Liu J., Batalov S., Zhou D., Orth A., Ding S., Schultz PG. (2004) An approach to genomewide screens of expressed small interfering RNAs in mammalian cells. *Proc. Natl. Acad. Sci. U.S.A.* **101** 135–140.

(8) Kumar R., Conklin DS., Mittal V. (2004) High-throughput selection of effective RNAi probes for gene silencing. *Gemone Res.* **13** 2333–2340.

(9) Silva JM., Mizuno H., Brady A., Lucito R., Hannon GJ. (2004) RNA interference microarrays: High-throughput loss-of-function genetics in mammalian cells. *Proc. Natl. Acad. Sci. U.S.A.* **101** 6548–6552.

(10) Mousses S., Caplen NJ., Cornelison R., Weaver D., Basik M., Hautaniemi S., Elkahioun AG., Lotufo RA., Choudary A., Dougherty ER., Suh E., Kallioniemi O. (2004) RNAi microarray analysis in cultured mammalian cells. *Genome Res.* **13** 2341–2347.

(11) Yoshikawa T., Uchimura E., Kishi M., Funeriu DP., Miyake M, Miyake J. (2004) Transfection microarray of human mesenchymal stem cells and on-chip siRNA gene knockdown. *J. Control. Release* **96** 227–232.

(12) Ziauddin J., Sabatini DM. (2001) Microarrays of cells expressing defined cDNAs. *Nature* **411** 107–110.

(13) Wheeler DB., Bailey SN., Guertin DA., Carprnter AE., Higgins CO., Sabatini DM. (2004) RNAi living-cell microarrays for loss-of-function screens in *Drosophila melanogaster* cells. *Nat. Methods* **1** 1–6.

(14) Bain CD., Troughton EB., Tao YT., Evall J., Whitesides GM., Nuzzo RG. (1989) Formation of monolayer films by the spontaneous assembly of organic thiols from solution onto gold. *J. Am. Chem. Soc.* **111** 321–335.

(15) Tarlov MJ., Burgess DRF., Gillen G. (1993) UV photopatterning of alkanethiolate monolayers self-assembled on gold and silver. *J. Am. Chem. Soc.* **115** 5305−5306.

(16) Huang J., Dahlgren DA., Hemminger JC. (1994) Photopatterning of self-Assembled alkanethiolate monolayers on gold: A simple monolayer photoresist utilizing aqueous chemistry. *Langmuir* **10** 626−628.

(17) Decher G. (1997) Fuzzy nanoassemblies: Toward layered polymeric multicomposites. *Science* **277** 1232−1237.

(18) Yamauchi F., Kato K., Iwata H. (2004) Micropatterned, self-assembled monolayers for fabrication of transfected cell microarrays. *Biochem. Biophys. Acta* **1672** 138−147.

(19) Lopez GP., Albers MW., Schreiber SL., Carroll R., Peralta E., Whitesides GM. (1993) Convenient methods for patterning the adhesion of mammalian cells to surfaces using self-assmbled monolayers of alkanethiols on gold. *J. Am. Chem. Soc.* **115** 5877−5878.

(20) Cooper E., Wiggs R., Hutt DA., Parker L., Leggett GJ., Parker TL. (1997) Rates of attachment of fibroblasts to self-assembled monolayers formed by the adsorption of alkylthiols onto gold surfaces. *J. Mater. Chem.* **7** 435−441.

(21) Haddow DB., France RM., Short RD., MacNeil S., Dawson RA., Leggett GJ., Cooper E. (1999) Comparison of proliferation and growth of human keratinocytes on plasma copolymers of acrylic acid/1,7-octadiene and self-assembled monolayers. *J. Biomed. Mater. Res.* **47** 379−387.

(22) McClary KB., Ugarova T., Grainger DW. (2000) Modulating fibroblast adhesion, spreading, and proliferation using self-assembled monolayer films of alkylthiolates on gold. *J. Biomed. Mater. Res.* **50** 428–439.

(23) Persengiev SP., Zhu X., Green MR. (2004) Nonspecific, concentration-dependent stimulation and repression of mammalian gene expression by small interfering RNAs (siRNAs). *RNA* **10** 12–18.

(24) Lechardeur D., Sohn KJ., Haardt M., Joshi PB., Monck M., Graham RW., Beatty B., Squire J., O'Brodovich H., Lukacs GL. (1999) Metabolic instability of plasmid DNA in the cytosol: a potential barrier to gene transfer. *Gene Ther*. **6** 482–497.

(25) Ulman A. (1996) Formation and structure of self-Assembled monolayers. *Chem. Rev.* **96** 1533–1554.

(26) Mrksich M., Dike LE., Tien J., Ingber DE., Whitesides GM. (1997) Using microcontact printing to pattern the attachment of mammalian cells to self-assembled monolayers of alkanethiolates on transparent films of gold and silver. *Exp. Cell Res.* **235** 305–313.

(27) Mrksich M., Whitesides GM. (1995) Patterning self-assembled monolayers using microcontact printing: A new technology for biosensors? *Trends Biotechnol.* **13** 228–235.

(28) Lopez GP., Biebuyck HA., Harter R., Kumar A., Whitesides GM. (1993) Fabrication and imaging of two-dimensional patterns of proteins adsorbed on self-

assembled monolayers by scanning electron microscopy. *J. Am. Chem. Soc.* **115** 10774–10781.

(29) Nelson BP., Grimsrud TE., Liles MR., Goodman RM., Corn RM. (2001) Surface plasmon resonance imaging measurements of DNA and RNA hybridization adsorption onto DNA microarrays. *Anal. Chem.* **73** 1–7.

(30) Ko IK., Kato K., Iwata H. (2005) Antibody microarray for correlating cell phenotype with surface marker. *Biomaterials* **6** 687–696.

(31) Kato K., Sato H., Iwata H. (2005) Immobilization of histidine-tagged recombinant proteins onto micropatterned surfaces for cell-based functional assays. *Langmuir* **21** 7071–7075.

Chapter 2

Use of microarrays in transfectionof mammalian cells with dicer-digested small interfering RNAs

INTRODUCTION

Small interfering RNA (siRNA) has emerged as a powerful tool for analyzing genomic functions (1). When introduced in mammalian cells, siRNA triggers the post-transcriptional degradation of messenger RNA (mRNA) with a homologous sequence to suppress its translation. This technique enables the silencing of specific genes at a cellular level, providing much simpler means for the loss-of-function study compared with the conventional knockout animal technique. The simplicity further provides the possibility of high-throughput functional genomics study that is a central challenge in current life sciences (2).

To implement high-throughput functional studies, transfection cell microarrays have been developed by several research groups (3–9). These microarrays were designed to transfer a panel of complementary DNA (cDNA) expression constructs (3–6) or siRNAs (6–8 and Chapter 1) individually into mammalian cells. Microarrays designed for siRNA transfection display synthetic siRNAs (21–27 nt in length). Because the efficiency of gene silencing greatly depends on the target sequences within mRNA, optimal targets are

selected using empirically customized algorithms (9, 10). However, target optimization is time-consuming and not viable in principle for mRNA with unknown sequences. These problems make it difficult to perform knockdown experiments for the large set of DNA transcripts.

This chapter aimed at fabricating microarrays that display siRNAs prepared from cDNA templates. The preparation of siRNA involves the transcription of cDNA to generate double-stranded RNAs (dsRNA) followed by digestion with endoribonuclease, dicer (11–13). Because the digestion products contain siRNAs (21–25 nt in length) with various sequences targeting either segment of mRNA, optimization of target sequence is not necessary. Effective d-siRNA can be prepared within a day, whereas chemical synthesis with target optimization requires a couple of weeks and, by rough estimation, costs hundred times more. The simplicity and efficiency, as well as cost effectiveness, of d-siRNA are great advantage especially in large-scale loss-of-function study. In particular, Kittler et al (14) prepared 5,305 endoribonuclease-digested siRNAs and used them to screen for genes required for the division of human cells.

In this chapter, the micropattern of a self-assembled monolayer (SAM) created on the glass-based substrate was utilized for the site-addressable loading of dicer-digested siRNA (d-siRNA). The concentration of individual siRNAs loaded onto a single spot is expected to be smaller with d-siRNA than with synthetic siRNA. Therefore, this chapter examined whether efficient transfection could be achieved using d-siRNA on transfection cell arrays. It will be demonstrated that the sequence heterogeneity of d-siRNA has minor effects on the silencing efficiency in mammalian cells.

EXPERIMENTAL

Preparation of patterned SAM

A glass substrate with a micropatterned SAM was prepared as before (15 and Chapter 1). In brief, a glass plate (22 × 26 × 0.5 mm, Matsunami Glass Industries, Ltd., Osaka, Japan) was immersed in piranha solution [7:3 (v/v) mixture of 96% H_2SO_4 and 30% H_2O_2] for 5 min at room temperature to remove impurities and then was washed with 2-propanol and water. Thin layers of chromium (thickness: 1 nm) and gold (thickness: 49 nm) were sequentially deposited onto the purified glass plate using a vacuum evaporator (V–KS200, Osaka Vacuum Instruments, Osaka, Japan). Immediately after deposition, the plate was immersed in 1 mM solution of 1-hexadecanethiol (Tokyo Kasei Kogyo Co., Tokyo, Japan) in ethanol at room temperature for 24 h to allow the formation of a methyl-terminated SAM (CH_3–SAM) on gold. The plate was washed with ethanol and water to remove unreacted alkanethiols, and was dried under a stream of dried nitrogen gas.

For micropatterning, the glass plate having a CH_3–SAM was overlaid with a photomask and irradiated with ultraviolet light through the photomask from an ultra-high-pressure mercury lamp (500 W, Optical Modulex SX–UI500HQ, Ushio Inc., Osaka, Japan). The photomask was made of a quartz plate deposited with a thick chromium layer having 5 × 5 circular holes with a diameter of 1 mm. After 2 h irradiation, the plate was washed with ethanol and water to remove photo-cleaved alkanethiols and immersed immediately in 1 mM solution 11-mercapto-1-undecanoic acid (Aldrich) in ethanol. The plate was kept in the solution for 2 h at room temperature to allow the formation of a carboxylic acid-terminated SAM (COOH–SAM) within the UV-radiated spots. Finally the plate was washed with

ethanol and water to remove unreacted alkanethiols and was dried under a stream of nitrogen gas.

Plasmids

Plasmids used were pEGFP-C1, pDsRed2-C1 and pEGFP-Actin (all from Clontech) which coded enhanced green fluorescent protein (EGFP), red fluorescent protein (DsRed) and β-actin, respectively, under the control of human cytomegalovirus promoter. These plasmids were amplified in *Escherichia coli* DH5α (Toyobo, Osaka, Japan) and purified using Plasmid Maxiprep Kit (Qiagen).

Preparation of d-siRNA

The procedure of d-siRNA preparation is shown in Figure. 1. The cDNAs of EGFP, DsRed and β-actin were amplified by polymerase chain reaction (PCR) using pEGFP-C1, pDsRed2-C1 and pEGFP-Actin as templates. Forward and reverse primers containing SP6 or T7 promoter sequences were used (Table 1). The conditions of thermal cycling were as follows: 35 cycles, denaturation at 94 ^{o}C for 30 sec, annealing at 55 ^{o}C for 1 min, and extension at 72 ^{o}C for 1 min. The amplified cDNAs were purified using MiniElute PCR Purification Kit (Qiagen). The following procedures for the preparation of d-siRNA were conducted using Knock-down siRNA Kit (Spring Bioscience, CA). In brief, the cDNA was transcribed to single-stranded RNA (ssRNA) using T7 or SP6 RNA polymerase, and then sense and antisense ssRNAs were annealed to obtain double-stranded RNA (dsRNA). After purification, the dsRNA was digested with recombinant human dicer at 37 ^{o}C. The digestion products were purified using a spin column followed by

phenol/chloroform/isoamyl alcohol extraction and ethanol precipitation. Finally the purified d-siRNA was dissolved in Tris-EDTA (TE) buffer (pH 8.0). The molecular weight distribution of d-siRNA was analyzed quantitatively by agarose gel electrophoresis. As a control, nonspecific siRNA (control siRNA; Qiagen) was used. The sequences of the control siRNA were as follows: sense, 5'-UUCUCCGAACGUGUCACGUdTdT-3'; antisense, 5'-ACGUGACACGUUCGGAGAAdTdT-3'.

The amount of d-siRNA loaded on spots

To determine the amount of d-siRNA loaded to the spot, a tracer of rhodamine-conjugated siRNA (GFP-siRNA-Rho, Qiagen) was mixed with non-labeled d-siRNA and plasmid DNA. These nucleic acids were loaded to the micropatterned substrate. The fluorescent image of the spots was recorded with a stereo microscope (MZ FL III, Leica) equipped with a cooled-CCD camera (ORCA-ER; Hamamatsu Photonics K. K., Shizuoka, Japan). A fluorescent intensity was measured for a single spot using an AQUA-Lite digital imaging software (Hamamatsu Photonics). The fluorescent intensity was converted to the amount of d-siRNA using a calibration curve obtained by depositing GFP-siRNA-Rho of known amounts to a spot. The data were expressed as mean ± standard deviation for n = 5.

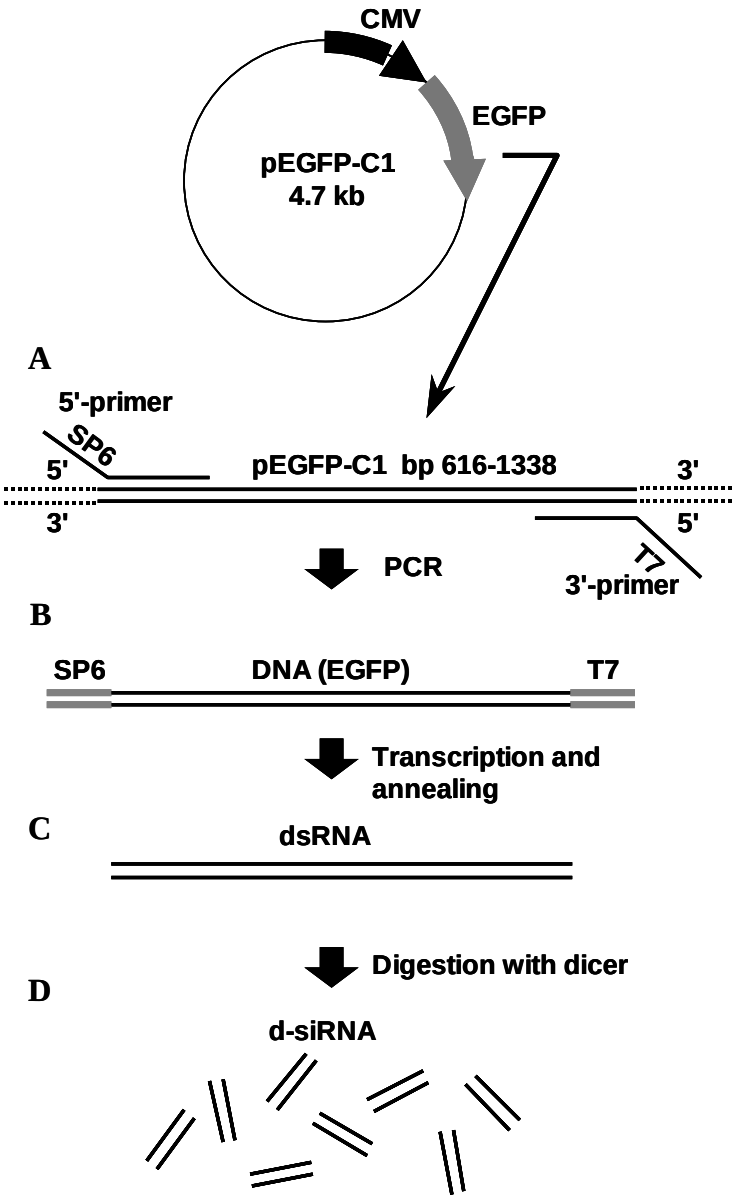

Figure 1. Scheme for the preparation of d-siRNA specific for EGFP. (A) pEGFP-C1 used as a template. (B) Amplification of EGFP gene by PCR. (C) Transcription and annealing to obtain dsRNA. (D) Digestion of dsRNA with dicer to yield d-siRNA.

Table 1. Primers Used for the PCR Amplification of cDNA

DNA	Sequence[a]
EGFP (Fw)[b]	5'-AGAGATTTAGGTGACACTATAGAAGAGGTGAGCAAGGGCGAGGAGCT-3'
EGFP (Rv)[b]	5'-AAGGTAATACGACTCACTATAGGGAGAGAGTCCGGACTTGTACAGCT-3'
DsRed (Fw)[c]	5'-AGAGATTTAGGTGACACTATAGAAGAGTCATGCGCTTCAAGGTGCGC-3'
DsRed (Rv)[c]	5'-AAGGTAATACGACTCACTATAGGGAGACCACGATGGTGTAGTCCTCG-3'
β-Actin(Fw)[d]	5'-AGAGATTTAGGTGACACTATAGAAGAGGTGATGGTGGGCATGGGTCA-3'
β-Actin(Rv)[d]	5'-AAGGTAATACGACTCACTATAGGGAGAAAGGAGAAGCTGTGCTACGT-3'

[a]Sequences underlined represent SP6 and T7 promoter sequences added to forward and reverse primers, respectively. Sequences in bold represent cDNA specific regions. [b]Designed for the full-length cDNA of EGFP. [c]Designed for DsRed 644-1227. [d]Designed for β-actin 200–710. Fw: forward primer, Rv: reverse primer.

d-siRNA loading on microarrays

d-siRNA (0–20 μg/mL), plasmid DNA (200 μg/mL), and LipofectAMINE2000 (0.3 mg/mL; Invitrogen) were mixed in Opti-MEM (Gibco). The mixture was kept at room temperature for 20 min to allow the formation of electrolyte complexes between the anionic nucleic acids and the cationic lipid. The solution of the complexes was pipetted to the COOH-terminated SAM spots (200 nL per spot). After incubation for 5 min, the solution was aspirated. Finally, the entire surface of the plate was washed with phosphate-buffered saline (PBS) and used immediately without drying.

Gene silencing on microarrays

Human embryonic kidney 293 (HEK293) cells were obtained from Health Science Research Resources Bank, Osaka, Japan, and grown in minimal essential medium (MEM;

Gibco) containing 10% fetal bovine serum (FBS), 100 U/mL penicillin, and 0.1 mg/mL streptomycin at 37 °C under 5% CO_2. The cells were harvested by trypsin digestion and seeded to the d-siRNA-loaded microarray at 6.7×10^4 cells/cm^2. The cells were incubated at 37 °C under 5% CO_2 to allow cell adhesion and transfection. Cells were observed with an epifluorescence microscope (Olympus, Tokyo, Japan) and a stereo microscope every 24 h after cell seeding. The fluorescent intensity of EGFP was measured for the entire areas of every spot. The efficiency of gene silencing (suppression efficiency) was determined according to the following equation:

$$\text{Suppression efficiency (\%)} = [\ 1 - (\ I_{\text{specific}} / I_{\text{control}}\ )\ ] \times 100$$

where I_{specific} and I_{control} are the fluorescent intensities of EGFP measured for the spot on which plasmid DNA was cotransfected with the specific d-siRNA or control siRNA, respectively. All the data presented in this chapter are the average of three independent experiments.

RESULTS

Preparation of d-siRNA microarray

As shown in Figure 2A, dsRNA could be prepared by in vitro transcription of cDNA (723 bp for full length nucleotides encoding EGFP) followed by the annealing of sense and antisense strands of ssRNAs. dsRNA corresponding to 644–1227 DsRed gene was digested

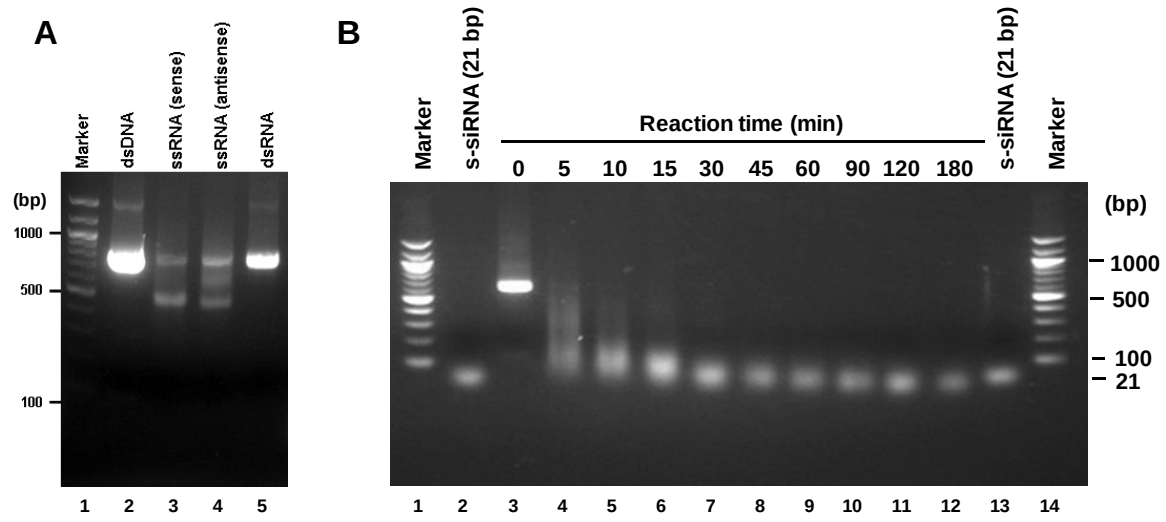

Figure 2. Agarose gel electrophoresis of the products obtained after each step of d-siRNA preparation. (A) cDNA encoding EGFP sequence (723 bp) used as a template was transcribed to generate sense and antisense strands of ssRNA and annealed. Lane 1: molecular weight standard, lane 2: template DNA, lanes 3 and 4: ssRNA (sense and antisense strands, respectively) transcribed from the DNA template, lane 5: dsRNA obtained by annealing the ssRNAs. (B) d-siRNA obtained by digesting dsRNA (638 bp) with dicer. dsRNA was prepared using a cDNA template for the sequence of DsRed. Lane 1 and 14: molecular weight standard, lanes 2 and 13: synthetic siRNA with a length of 21 bp (synthetic siRNA as control), lanes 3–12: dsRNA digested for various time periods as indicated above the image.

by recombinant human dicer for various time periods. Agarose gel electrophoresis of digested products (Fig. 2B) showed that the length of RNAs was gradually decreased with digestion time and that it took more than 1 hr to generate small dsRNA with a length of less than 30 bp. In mammalian cells, interferon response leading to cell apoptosis is initiated

upon introduction of dsRNA with a length of more than 30 bp (16, 17). Therefore, d-siRNA obtained by digesting dsRNA for 1 hr was used in the later experiments.

As shown in Figure 3, the amount of d-siRNA loaded to the COOH-SAM spots increased with an increase in the concentration of d-siRNA. The loading of d-siRNA reached 39.8 ± 15 ng/cm^2 when 20 μg/mL d-siRNA solution was used. This loading is comparable to the case in which synthetic siRNA was loaded by the layer-by-layer assembly process (38 ± 11 ng/cm^2) (see Chapter 1).

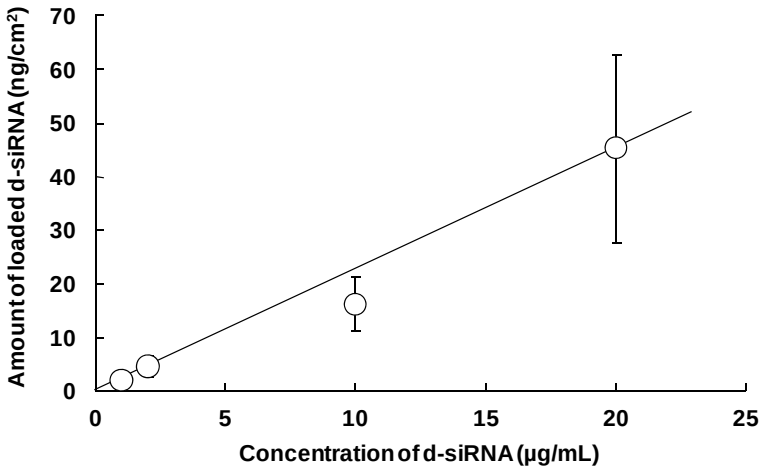

Figure 3. The amount of d-siRNA loaded to COOH-SAM. The amount of d-siRNA loaded on spots was measured by rhodamine labeled siRNA. The data are plotted as a function of d-siRNA concentration in a solution used for the preparation of DNA-RNA-lipid complexes.

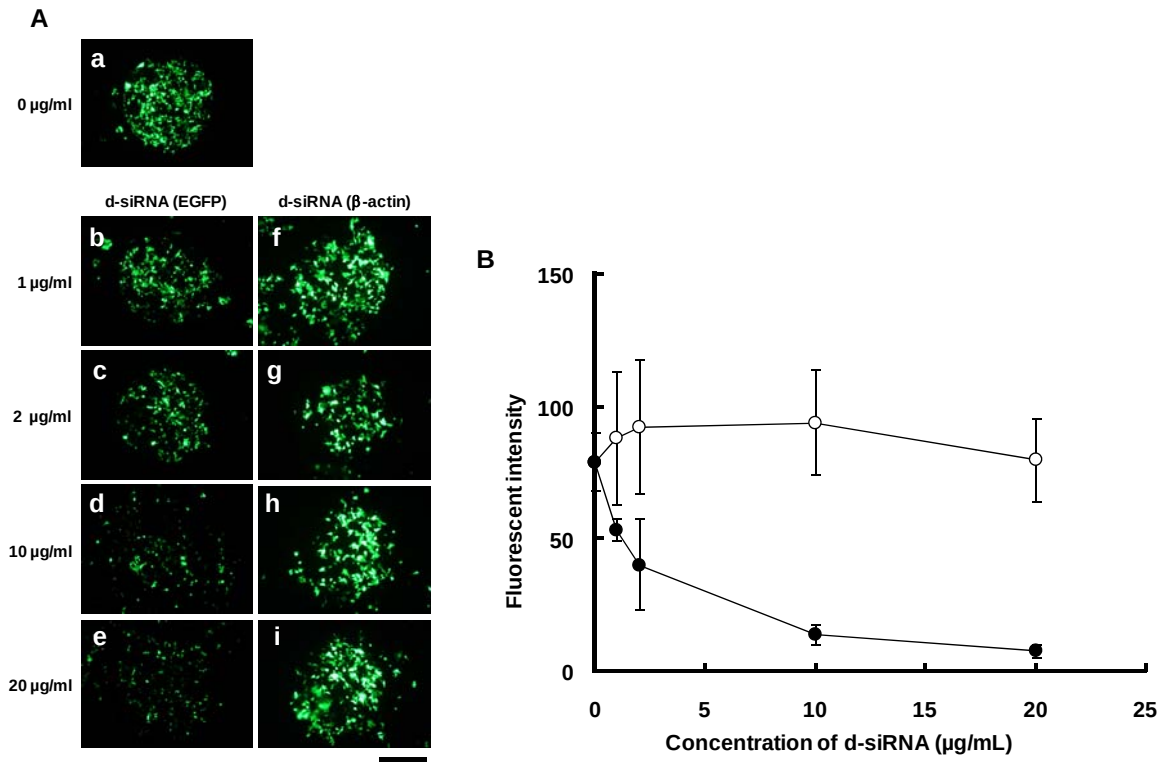

Figure. 4. Sequence specific gene silencing on the d-siRNA loaded spots. (A) The representative photographs are shown for the HEK293 transfected with (a) plasmid alone and plasmid plus d-siRNA specific for (b–e) EGFP and (f–i) β-actin. The photographs were acquired 48 h after cell seeding. Scale bar: 500 μm. (B) Fluorescent intensity of EGFP expressed in HEK293 as a function of d-siRNA concentration in a solution used for the preparation of DNA-RNA-lipid complexes. The d-siRNAs used were specific for (●) EGFP and (○) β-actin. The data are expressed as mean ± standard deviation for n = 3.

Gene silencing on d-siRNA microarrays

HEK293 cells were seeded to the microarray that displayed d-siRNAs specific for EGFP and β-actin, together with pEGFP-C1, as separate spots. In Figure 2, the representative photographs are shown for cells 48 h after seeding. According to the previous chapter, loaded DNA-RNA-lipid complexes most likely are taken up by the cells through endocytosis. The expression of EGFP was silenced on the spots loaded with d-siRNA prepared by digesting EGFP-specific dsRNA (Fig. 4A b–e). The series of photographs (Fig. 4A b–e) show that EGFP expression was suppressed in a loading-dependent manner, with the highest suppression efficiency found at 20 μg/mL of d-siRNA. On the other hand, cells on the spots with d-siRNA specific for β-actin (Fig. 4A f–i) expressed EGFP at a level similar to the control cells transfected only with the plasmid (Fig. 4A a and Fig. 4B). Cells present on the regions around spots exhibited no sign of EGFP expression. These results show that EGFP gene is silenced by d-siRNA in sequence and spatially specific manners on the microarray. In separate experiments, gene silencing was examined in HEK293 cells stably expressing EGFP. The cells were cultured on the microarray on which d-siRNA-lipid complexes lacking plasmid DNA were loaded. However, silencing of EGFP expression could not be observed (data not shown), probably due to the inappropriate composition of the complexes.

As shown in Figure. 5, EGFP expression on the spots with no d-siRNA (plasmid alone) reached the maximal level 5 days after cell seeding, and gradually decreased after a 5-day culture on the microarray, most likely due to plasmid degradation (18). On the other hand, a relatively low level of EGFP expression was observed continuously on the spots with EGFP-specific d-siRNA during any time periods examined, although suppression

efficiency was varied depending on the amount of loaded d-siRNA. In fact, 10 and 20 μg/mL d-siRNA solutions gave rise to more than 90% suppression efficiency at any time points.

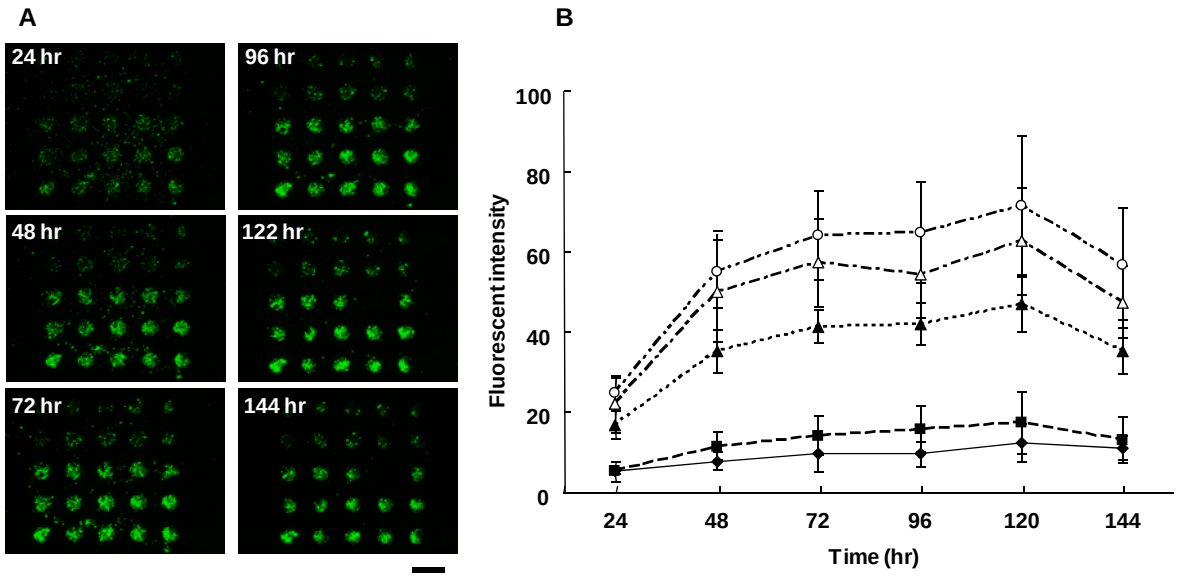

Figure 5. Time dependence of EGFP expression in HEK293 cells transfected on the d-siRNA microarray. (A) Fluorescent images of the entire microarray that displayed the spots with different d-siRNAs. d-siRNAs were loaded under the same condition to the five spots on the same line of the microarray. d-siRNA concentration was, from bottom to up, (○) 0, (●) 1, (▲) 2, (■) 10, and (♦) 20 μg/mL. Six photographs were recorded for the same microarray at different time points as indicated in the photographs. Cells were totally detached from one of the spots (middle right of the microarray) upon replacing the medium with PBS for imaging 122 h after seeding. Scale bar: 2 mm. (B) Fluorescent intensity of EGFP expressed in HEK293 cells on the d-siRNA microarray shown in A. The average intensities are expressed as mean ± standard deviation for n = 4. The data for the fourth line from the right side was omitted because cells were totally detached from one of the spots on the line due to medium disturbance during culture.

DISCUSSION

High-throughput functional genomics studies require new methodologies that permit the parallel modification of specific gene expression. Transfection cell microarray technology provides practical means to carry out such studies. Several research groups have developed transfection cell microarrays that allow silencing of a large set of genes by siRNA (Chapters 1 and 6–8). In order to extend the usefulness of transfection cell microarrays, siRNAs prepared by digesting dsRNA with endoribonuclease were used in this chapter.

The endoribonuclease digestion of dsRNA transcribed from cDNA yields the library of short dsRNA fragments with a length of 21–25 nt. All fragments target their homologous sequences in mRNA, and some of them exhibit gene silencing activity (11–13). In contrast to the preparation of siRNA by chemical synthesis, the method employed here does not require the optimization of target sequences in advance. Taking advantage of this feature, Zhu and Jiang (19) identified a protein essential for midzone formation and cytokinesis in HeLa cells. Tan et al (20) also used d-siRNA to inhibit the replication of hepatitis B virus in mammalian cells. More importantly, as exemplified in the study by Kittler et al (14), a large set of d-siRNAs can be prepared rapidly and cost-effectively for use in functional screening for genes. To demonstrate that this microarray-based approach is feasible for high-throughput assays, to show that the dicer approach works for multiple genes is further needed.

The results of this chapter revealed that the amount of loaded d-siRNAs was similar to those described in Chapter 1 for synthetic siRNA. As a platform for the preparation of

transfection cell microarrays, a micropatterned SAM that displayed the array of carboxylic acid-terminated spots was utilized. As in Chapter 1, d-siRNA and plasmid DNA were loaded onto these spots by the process in which the surface of negatively charged COOH-SAM attracted the d-siRNA-plasmid-lipid complex through electrostatic interactions because the complexes formed with excess cationic lipid bared net positive charge. As a result (Fig. 3), d-siRNA could be load onto the spot at a density similar to synthetic siRNA.

It is supposed that the concentration of individual siRNAs loaded on a single spot would be lower with d-siRNA than with synthetic siRNA. However, it has been reported that pooling of siRNAs maintained efficient silencing of specific target gene (13). In particular, d-siRNA gave rise to a silencing efficiency at a level similar to that reported for synthetic siRNA (Chapter 1), suggesting that the loaded spot contains a sufficient amount of different effective d-siRNA. It was also observed that the silencing efficiency was dependent on the amount of RNA loading. This is probably due to the effect that higher loading enhances the introduction of siRNA into cells. Similar tendency for synthetic siRNA (Chapter 1) and plasmid DNA (5) were observed. It was also reported that the pooling of siRNA serves to reduce off-target effects. Because cross-silencing requires sufficient copies of RNA with a high level of sequence similarity to the off-target mRNA, it is expected that the library of d-siRNAs contains a reduced number of small RNA with off-target effects (21–23).

In conclusion, d-siRNA can be suitably applied to transfection cell arrays. Heterogeneity of d-siRNA in sequence has minor effects on the loading of siRNA onto the array and its transfer to cultured mammalian cells. The unique feature of d-siRNA, such as no requirement of target selection, cost effectiveness, and negligible off-target effects, are

of great advantage to the preparation of transfection cell arrays for use in large-scale functional screening for genes in a high-throughput manner.

References

(1) Elbashir SM., Harborth J., Lendeckel W., Yalcin A., Weber K., Tuschl, T. (2001) Duplexes of 21-nucleotide RNAs mediate RNA interference in cultured mammalian cells. *Nature* **411** 494–498.

(2) Kamath RS., Fraser AG., Dong Y., Poulin G., Durbin R., Gotta M., Kanapin A., Bot NL., Moreno S., Sohmann M., Welchman DP., Zipperlen P., Ahringer J. (2003) Systematic functional analysis of the *Caenorhabditis elegans* genome using RNAi, *Nature* **421** 231–237.

(3) Ziauddin J., Sabatini DM. (2001) Microarrays of cells expressing defined cDNAs. *Nature* **411** 107–110.

(4) Yamauchi F., Kato K., Iwata H. (2004) Micropatterned, self-assembled monolayers for fabrication of transfected cell microarrays. *Biochim. Biophys. Acta* **1672** 138–147.

(5) Yamauchi F., Kato K., Iwata H. (2004) Spatially and temporally controlled gene transfer by electroporation into adherent cells on plasmid DNA-loaded electrodes. *Nucleic Acids Res.* **32** e187.

(6) Yoshikawa T., Uchimura E., Kishi M., Funeriu DP., Miyake M., Miyake J. (2004) Transfection microarray of human mesenchymal stem cells and on-chip siRNA gene knockdown. *J. Control. Release* **96** 227–232.

(7) Mousses S., Caplen N., Cornelison R., Weaver D., Basik M., Hautaniemi S., Elkahloun AG., Lotufo RA., Choudary ER., Suh E., Kallioniemi O. (2003) RNAi microarray analysis in cultured mammalian cells. *Genome Res.* **13** 2341–2347.

(8) Kumar R., Conklin DS., Mittal V. (2003) High-throughput selection of effective

RNAi probes for gene silencing. *Genome Res.* **13** 2333–2340.

(9) Reynold A.s, Leake D., Boese Q., Scaringe S., Marshall WS., Khvorova A. (2004) Rational siRNA design for RNA interference. *Nat. Biotechnol.* **22** 326–330.

(10) Pei Y., Tuschl T. (2006) On the art of identifying effective and specific siRNAs. *Nat. Methods* **3** 670–676.

(11) Yang D., Buchholz F., Huang Z. Goga A., Chen CY., Brodsky FM., Bishop JM. (2002) Short RNA duplexes produced by hydrolysis with *Escherichia coli* RNase III mediate effective RNA interference in mammalian cells. *Proc. Natl. Acad. Sci. U.S.A.* **99** 9942–9947.

(12) Myers JW., Jones JT., Meyer T., Ferrell JE. (2003) Recombinant Dicer efficiently converts large dsRNAs into siRNAs suitable for gene silencing. *Nat. Biotechnol.* **21** 324–328.

(13) Buchholz F., Kittler R. Slabicki M., Theis M. (2006) Enzymatically prepared RNAi libraries. *Nat. Methods* **3** 696–700.

(14) Kittler R., Putz G., Pelletier L., Poser I., Heninger AK., Drechsel D., Fischer S., Konstantinova I., Habermann B., Grabner H., Yaspo ML., Himmelbauer H., Korn B., Neugebauer K., Pisabarro MT., Buchholz F. (2004) An endoribonuclease-prepared siRNA screen in human cells identifies genes essential for cell division. *Nature* **432** 1036–1040.

(15) Tarlov MJ., Burgess DRF., Gillen G. (1993) UV photopatterning of alkanethiolate monolayers self-assembled on gold and silver. *J. Am. Chem. Soc.* **115** 5305−5306.

(16) Manche L., Green SR., Schmedt C., Mathews MB. (1992) Interactions between double- stranded RNA regulators and the protein kinase DAI. *Mol. Cell. Biol.* **12** 5238–5248.

(17) Minks MA., West DK., Benvin S., Baglioni C. (1979) Structural requirements of double-stranded RNA for the activation of 2',5'-oligo(A) polymerase and protein kinase of interferon-treated HeLa cells. *J. Biol. Chem.* **254** 10180–10183.

(18) Lechardeur D., Sohn KJ., Haardt M., Joshi PB., Monck M., Graham RW., Beatty B., Squire J., O'Brodovich H., Lukacs GL. (1999) Metabolic instability of plasmid DNA in the cytosol: A potential barrier to gene transfer. *Gene Ther.* **6** 482–497.

(19) Zhu C., Jiang W. (2005) Cell cycle-dependent translocation of PRC1 on the spindle by Kif4 is essential for midzone formation and cytokinesis. *Proc. Natl. Acad. Sci. U.S.A.* **102** 343–348.

(20) Xuan B., Qian Z., Hong J., Huang W. (2006) EsiRNAs inhibit Hepatitis B virus replication in mice model more efficiently than synthesized siRNAs. *Virus Res.* **118** 150–155.

(21) Birmingham A., Anderson EM., Reynolds A., Ilsley-Tyree D., Leake D., Fedorov Y., Baskerville S., Maksimova E., Robinson K., Karpilow J., Marshall WS., Khvorova A. (2006) 3' UTR seed matches, but not overall identity, are associated with RNAi off-targets. *Nat. Methods* **3** 199–204.

(22) Lin X., Ruan X., Anderson MG., McDowell JA., Kroeger PE., Fesik SW., Shen Y. (2005) siRNA-mediated off-target gene silencing triggered by a 7 nt complementation. *Nucleic Acids Res.* **33** 4527–4535.

(23) Jackson AL., Burchard J., Schelter J., Chau BN., Cleary M., Lim L., Linsley PS. (2005) Widespread siRNA "off-target" transcript silencing mediated by seed region sequence complementarity. *RNA* **12** 1179–1187.

Chapter 3

Electroporation microarray for parallel transfer of small interfering RNA into mammalian cells

INTRODUCTION

Electroporation is a physical method that allows transfer of biomacromolecules such as nucleic acids and proteins into living cells. The transfer is through micropores transiently created in a cell membrane upon application of electric pulses (1). Because of excellent efficiency, the method has been widely used for study of gene functions in a variety of organisms ranging from prokaryotes to eukaryotes (1).

Recently, electroporation was further applied to cell-based microarrays that permit transfer of multiple expression constructs simultaneously and individually into mammalian cells (2, 3). In this method, cells are cultured on an electrode on which plasmid vectors are loaded in an array format. Upon application of an electric pulse, cells incorporate the loaded plasmids in a spatially-controlled manner. Because of its applicability to high-throughput analysis with reasonably high transfection efficiency, the method provides a promising means of analyzing multiple gene functions (2, 4).

Small interfering RNA (siRNA) is a double-stranded RNA of ~21 nucleotides (5). When introduced into cells, siRNA triggers RNA interference (RNAi) by which gene expression is specifically silenced (6). Because of its simplicity compared to the

conventional knockout technique, RNAi has frequently been used to study gene functions in living mammalian cells, most effectively on a large-scale (7–10). Although techniques have been reported for parallel electroporation of siRNAs into mammalian cells in a 96-well format (11, 12), the microarray-based electroporation of siRNA has never been reported. In the microarray-based method in which siRNAs are loaded onto a small plate as microspots prior to cell seeding, a total system will be much more miniaturized than the techniques using microplates. This feature allows reduction of the amount of chemicals, DNAs, cells, and media required for large-scale assays. In addition, the microarray format makes it easy to observe cells using standard optical microscopes and to detect small differences in fluorescent intensities between conditions. It can be expected that these features facilitate a substantial increase in the throughput of functional analysis and the reliability of the data obtained, as demonstrated by previous studies on plasmid-based microarrays (2, 3). Microelectrode arrays have also been reported for spatially-controlled electroporation (13–15). Although this technique enables application and recording of electric potential in a spatially controlled manner, parallel transfection with multiple nucleic acids would not be straightforward, unlike the microarrays previously developed (2, 3).

To extend the usefulness of microarray-based electroporation, this method is applied here to the transfer of siRNA into mammalian cells. siRNA was ionically adsorbed on an electrode surface that had been modified with a cationic polymer. This article deals with the fundamental aspects of siRNA loading onto a cationically-modified electrode, and the electric pulse-triggered transfer of siRNA into human embryonic kidney cells, HEK293, cultured directly on the surfaces. Then, this technique is combined with a micropatterned

electrode to demonstrate the potential of this method for creating transfected cell microarrays.

EXPERIMENTAL

siRNA

All siRNAs were purchased from Qiagen, Hilden, Germany. The sequences of siRNA specific for enhanced green fluorescent protein (GFP-siRNA) and non-specific siRNA (control-siRNA) were as follows: GFP-siRNA, (sense) 5'-GCAAGCUGACCCUGAA GUUCAU-3' and (antisense) 5'-GAACUUCAGGGUCAGCUUGCCG-3'; control-siRNA, (sense) 5'-UUCUCCGAACGUGUCACGUdTdT-3' and (antisense) 5'-ACGUGACAC GUUCGGAGAAdTdT-3'. Rhodamine-labeled siRNA specific for EGFP (EGFP-siRNA-Rho) was used for the determination of siRNA loading.

Electrode and siRNA loading

A glass plate (24 mm × 26 mm × 1.5 mm; Matsunami Glass, Osaka, Japan) was treated with a Piranha solution (concentrated sulfuric acid : hydrogen peroxide = 7 : 3 by volume) at room temperature for 5 min to remove impurities. The cleaned glass plate was thoroughly washed with deionized water and 2-propanol, and dried under a stream of nitrogen gas. In a continuous process, a thin primer layer of chromium (thickness: 1 nm) was deposited onto the glass surface using a thermal evaporator (V-KS200; Osaka Vacuum Instruments, Osaka, Japan), followed by a gold layer (thickness 199 nm for infrared (IR) absorption spectroscopy and for counter electrodes (anode); or 49 nm for other

experiments). Immediately after deposition, the plate was immersed in 1 mM 11-mercaptoundecanoic acid (Aldrich, Milwaukee, WI) solution in ethanol at room temperature for 24 h to form a self-assembled monolayer (SAM) on the gold-evaporated glass plate. The plate was then washed with ethanol and water, and dried under a stream of nitrogen gas.

Branched polyethyleneimine (PEI; Aldrich) with a weight-averaged molecular weight of 2000 g/mol was dissolved in phosphate buffered saline (PBS) to a concentration of 1%. The solution pH was adjusted to 7.4 with HCl. The glass-based gold electrode bearing a SAM of carboxylic acid-terminated alkanethiol (COOH-SAM) was exposed to the PEI solution and kept for 30 min at room temperature to electrostatically adsorb PEI on to the surface. The plate was then washed with water to remove weakly adsorbed PEI, sterilized with 70% ethanol, and air-dried in a sterile laminar flow hood. Under sterile conditions, the plate modified with PEI was then exposed to siRNA solution (0–50 μg/mL) in PBS (pH 7.4) at room temperature for 2 h to adsorb siRNA onto the surface. The resulting siRNA-loaded glass plate was washed with PBS to remove weakly-bound siRNA, and immediately used for later experiments.

IR reflection absorption spectroscopy (IR-RAS)

IR-RAS spectra of PEI- adsorbed and siRNA-adsorbed SAMs were recorded with a Spectrum One (Perkin Elmer, Waltham, MA) equipped a mercury-cadmium-telluride detector and a RAS sampling accessory (Harrick Scientific Co., Ossining, NY) at a resolution of 4 cm^{-1} with an accumulation of 256 scans (3). All samples for IR-RAS analysis were prepared using a glass plate with a thick gold layer (199 nm) so as to attain

sufficient reflection of IR light. Prior to the analysis, sample surfaces were rinsed once with pure water and dried under vacuum. A bare gold surface was used as a reference.

Determination of siRNA loading

Rhodamine-labeled siRNA was loaded onto the electrode as described above. The concentrations of siRNA were 0.1, 1.0, 10, and 50 μg/mL. The electrode was then observed with a fluorescence stereomicroscope (MZ FL III, Leica, Solms, Germany) equipped with a cooled-CCD camera (ORCA-ER; Hamamatsu Photonics, Hamamatsu, Japan). Fluorescence intensity was measured using AQUA-Lite digital imaging software (Hamamatsu Photonics) and converted into the amount of siRNA using a calibration curve obtained by depositing known amounts of rhodamine-labeled siRNA on to the electrode. The data were expressed as mean ± standard deviation for n = 3. The loading of siRNA was further determined in the same fashion after electric pulsing (see below for pulsing conditions).

Cell culture

Human embryonic kidney cells, HEK293, were obtained from Health Science Research Resources Bank, Osaka, Japan. HEK293 cells that stably express destabilized GFP were generated by transforming HEK293 cells with the pd2EGFP-N1 plasmid (Clontech, Palo Alto, CA). Stable clones, d2EGFP-HEK, were selected by antibiotic resistance (500 μg/mL G418). The cells were maintained in minimal essential medium (MEM; Invitrogen, Carlsbad, CA, USA) supplemented with 10% fetal bovine serum (FBS), 100 U/mL penicillin, and 100 μg/mL streptomycin at 37 ^{o}C under 5% CO_2 atmosphere.

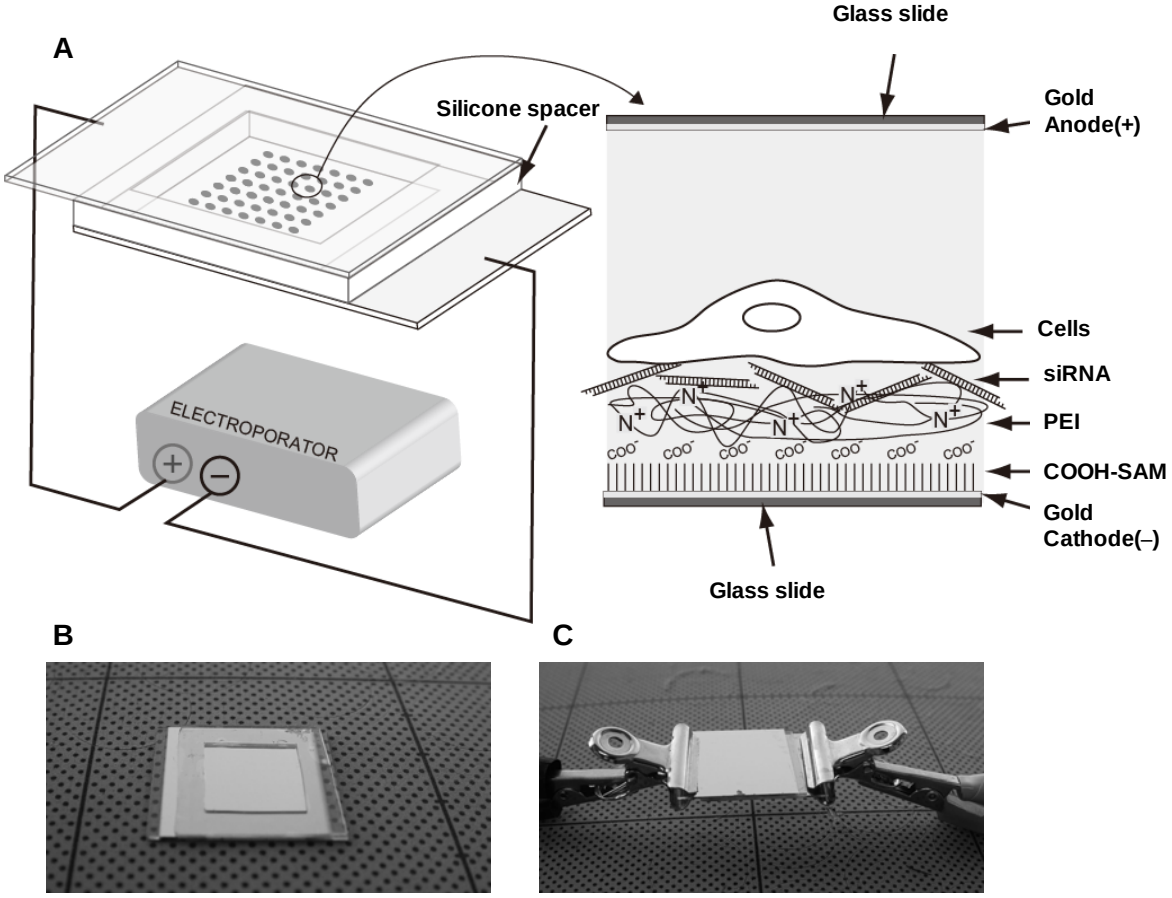

Figure 1. (A) Schematic drawings of the electroporation setup. Drawings are not to scale. Photographs of (B) a basement electrode with a silicone frame, (C) basement and upper electrode connected to a pulse generator.

Electroporation on siRNA-loaded electrodes

A sterilized silicone rubber frame (inner area, 14 mm × 14 mm; thickness, 0.5 mm) was adhered to the siRNA-loaded electrode to confine the cell culture region (Fig. 1). d2EGFP-HEK cells were seeded onto the siRNA-loaded surface within the frame at a density of 60,000 cells/cm^2. The plate was placed in a 35-mm polystyrene cell culture dish, and cells

were cultured in MEM supplemented with 10% FBS, 100 U/mL penicillin, and 100 μg/mL streptomycin at 37 ^{o}C under 5% CO_2 atmosphere to allow cell attachment to the electrode. After 24 h (cell density reached 80–90% confluence), the inner space of the silicone frame was washed with PBS to eliminate non-adhering cells, and filled with cold PBS at 4 ^{o}C. As a counter electrode, a glass plate with a 199-nm thick gold layer was placed on the silicone frame with the gold surface down at a distance of 0.5 mm above the siRNA-loaded electrode (Fig. 1). The lower (cathode) and upper (anode) electrodes were connected to a pulse generator (Gene Pulser Xcell, Bio-Rad, Hercules, CA, USA). Cells on the electrode were treated with a single electric pulse at the field strength of 240 V/cm for a duration of 10 msc. After 5-min incubation at room temperature, PBS was replaced with MEM supplemented with 10% FBS, 100 U/mL penicillin, and 100 μg/mL streptomycin. The cells were further cultured for 48 h and then observed with an epifluorescence microscope (BX-51; Olympus, Tokyo, Japan).

Flow cytometry

Cells were harvested by trypsinization 48 h after electroporation and washed with cold PBS. The expression of EGFP was analyzed with a flow cytometer (FACS Caliber, Becton-Dickinson, Franklin Lakes, NJ). Data from approximately 20,000 cells were used to generate a histogram. For quantitative analysis, geometrical mean fluorescence was determined from the histograms.

Electroporation on microarrays

A micropatterned SAM was prepared as in Chapter 1. In brief, the SAM of 1-hexadecanethiol formed on gold was irradiated with ultraviolet light through a chromium photomask that had an array of circular windows (1 mm in diameter). By this procedure, the alkanethiol monolayer was eliminated from the irradiated spots. The SAM of 11-mercaptoundecanoic acid was then formed within these spots to obtain a micropatterned surface. The array of the spots (6 × 7 matrix) was arranged in the center of an electrode so that the outermost spots were located approximately 2 mm from the silicone rubber frame. This is because relatively less efficient transfection of cells was occasionally observed on the peripheral part of an electrode near the silicone rubber frame. The adsorption of PEI and the loading of siRNA were carried out as described above, but siRNA solutions were manually pipetted on to the spots. Cell culture, electroporation, and microscopic observation were conducted as described above.

RESULTS

Loading of siRNA

The results of IR-RAS analysis are shown in Figure 2. A strong absorption band at 1718 cm^{-1} is seen in the spectrum of COOH-SAM (Fig. 2A). This absorption is assigned to the stretching vibration of C═O contained in 11-mercaptoundecanoic acid. In the spectrum for the PEI-treated surface (Fig. 2B), new peaks appeared at 1675, 1542, and 1410 cm^{-1}. These peaks are assigned to amines (16), indicating the presence of PEI. After exposure to

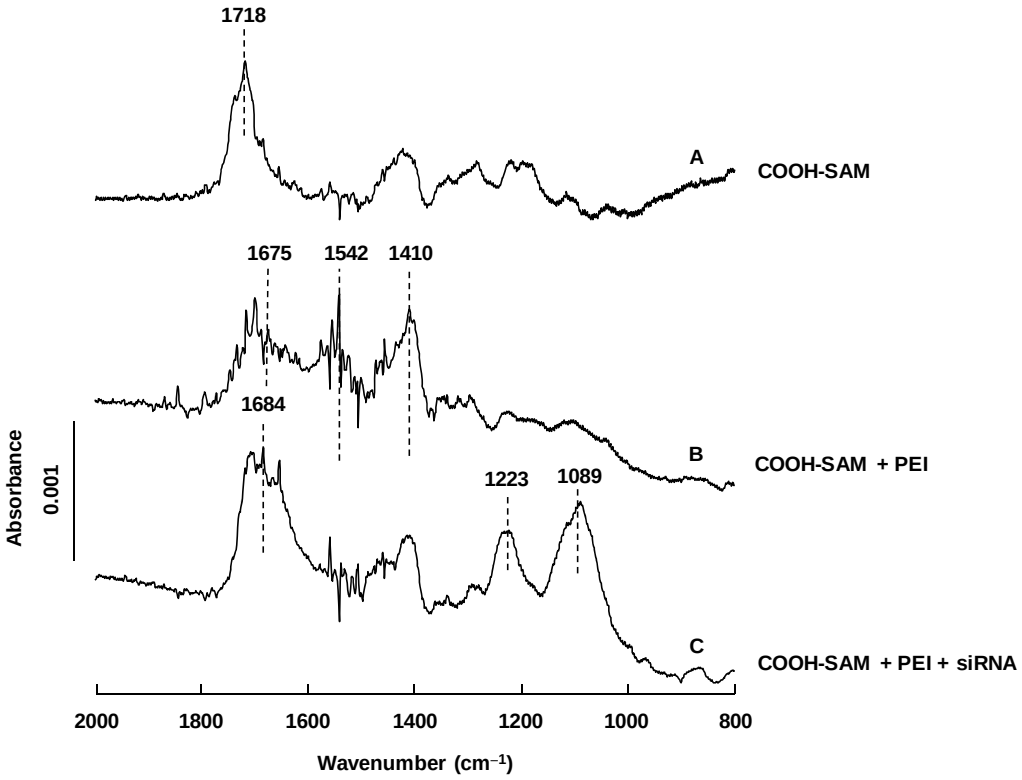

Figure 2. Representative results of IR-RAS analysis for (A) an electrode with COOH-SAM, (B) an electrode with COOH-SAM and PEI, and (C) an electrode with COOH-SAM, PEI, and GFP-siRNA. siRNA was adsorbed from a solution of 50 μg/mL. The original spectra are split for clarity. The Y-axis indicates intensity in arbitrary units. Some peaks are not well assigned to the stretching vibration of C=O(1600–1750 cm^{-1}), C6=C6 in guanine (1684 cm^{-1}). Peaks: 1675, 1542, and 1410 cm^{-1}, stretching vibration of amines; and, 1089 and 1223 cm^{-1}, symmetrical and antisymmetrical stretching, respectively, of phosphate.

siRNA (Fig. 2C), additional absorption is seen in the 1600–1750 cm^{-1} regions; this is assigned to the vibration of C=O contained in the base of RNA (17). For instance, C6=O6 in guanine is known to exhibit a stretching absorption peak at 1684 cm^{-1}. The strong absorption peaks are attributed, respectively, to the symmetric stretching at 1089 cm^{-1} and

antisymmetric stretching at 1223 cm^{-1} of phosphate in ribonucleotides (18). These results as a whole provide the evidence that a COOH-SAM was formed on the gold electrode and that PEI and siRNA were adsorbed sequentially onto the SAM.

Figure 3A shows the amount of siRNA adsorbed to the PEI-modified electrode. As can be seen, increases in the concentration of siRNA gave rise to larger amounts of adsorbed siRNA, reaching 31.4 ± 10 ng/cm^2 when 50 μg/mL siRNA solution was used.

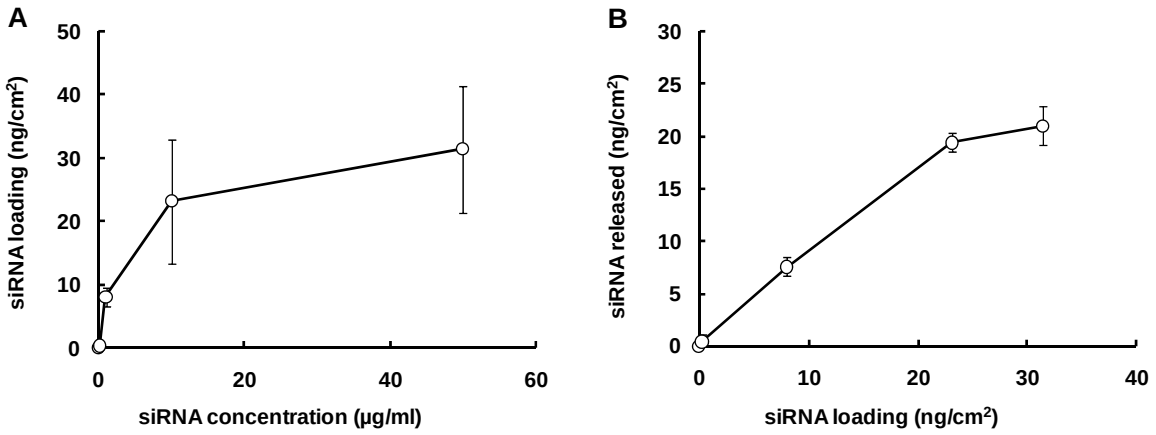

Figure 3. (A) The amount of rhodamine-conjugated siRNA adsorbed by the PEI electrode from 0.1, 1, 10, and 50 μg/mL solutions. Fluorescence intensity was determined from the microphotographs of the array and converted to the amount of siRNA using a calibration curve. The data are expressed as mean ± standard deviation for n = 3. (B) The amount of rhodamine-conjugated siRNA released upon electric pulsing at a field strength of 240 V/cm. The data are expressed as mean ± standard deviation for n = 3.

Release of siRNA upon electric pulsing

The amount of siRNA released from the electrode was determined as a difference between the amounts of siRNA existing on the electrode before and after application of a single electric pulse at a field strength of 240 V/cm. The results are shown in Figure 3B. The graph indicates that siRNA was released in a loading dependent manner.

Gene silencing on siRNA-loaded surfaces

d2EGFP-HEK cells were cultured on the siRNA-loaded surfaces. It was observed that cells adhered to and spread on the siRNA-loaded electrode. Preliminary experiments showed that PEI with a molecular weight of 25,000 or 750,000 g/mol gave rise to slight impairments in regard to cell adhesion (data not shown), compared with the case with PEI of 2000 g/mol. When an electric pulse was applied to the cells at the field strength of 240 V/cm, cell morphology was changed from spreading shapes into round ones. These cells still adhered to the surface and returned to spreading shapes within 12 h. Though the timescale of such morphological changes was not studied in detail, firm adhesion of cells was crucial for efficient transfer of siRNA into cells. Cell viability was approximately 90% when assessed by trypan blue exclusion tests immediately after electric pulsing at 240 V/cm. An electric pulse at higher field strengths (> 300 V/cm) resulted in detached and severely damaged cells. In separate experiments using plasmid-loaded electrodes, it was observed that reverse polarity (the basement electrode with cells was used as anode, while the upper electrode was used as cathode) resulted in inefficient transfection because of severe damage to cells (data not shown).

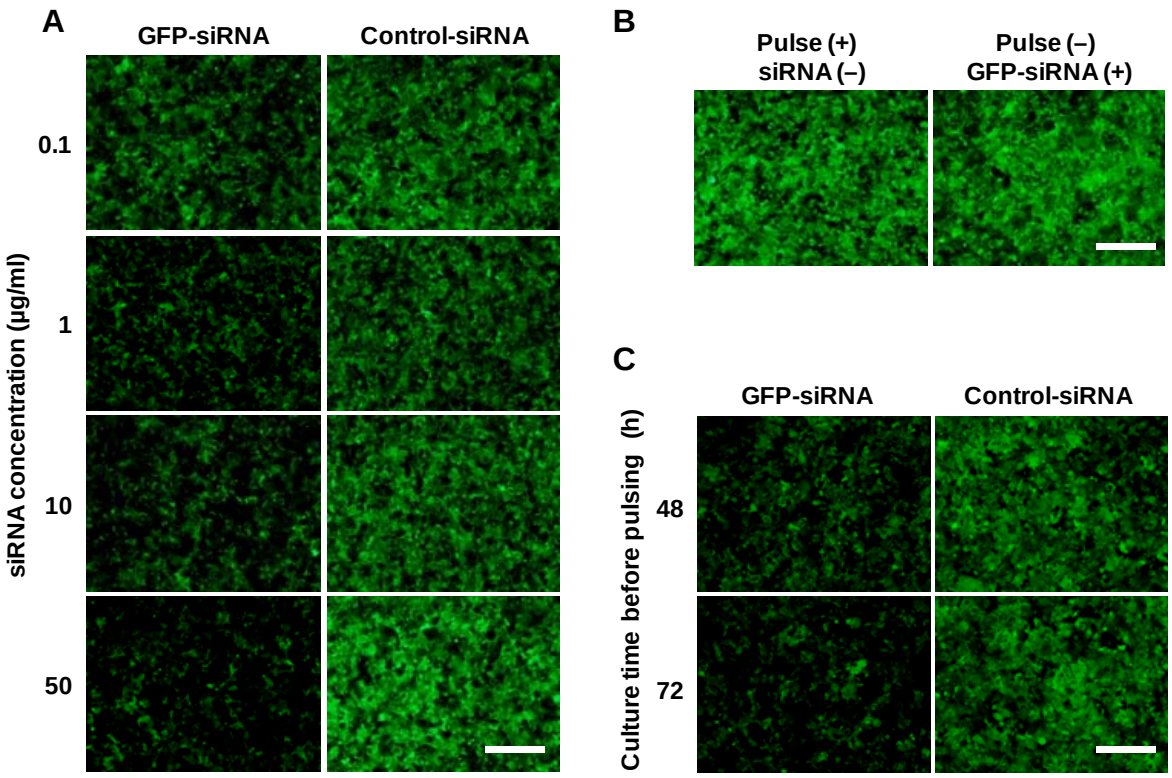

Figure 4. (A) Fluorescence microphotographs of d2EGFP-HEK cells electroporated on the electrodes loaded with various amounts of (left) GFP-siRNA and (right) control-siRNA. The concentration of siRNA in the solution used for loading is indicated at the left of the photographs. (B) Fluorescence microphotographs of (left) cells pulsed on the electrode onto which no siRNA was adsorbed and (right) cells cultured on the GFP-siRNA-loaded electrode for two days without electric pulsing. (C) The effect of culture periods before pulsing. Fluorescence microphotographs of cells pulsed on the electrodes onto which (left) GFP-siRNA or (right) control-siRNA was adsorbed from 50 μg/mL siRNA solutions. The culture periods are indicated on the left of the photographs. The photographs were recorded 48 h after pulsing. Scale bar: 500 μm for (A) to (C).

Figure 4A shows the representative fluorescent microphotographs of d2EGFP-HEK cells cultured on the siRNA-loaded surfaces for 24 h followed by electric pulsing at 240 V/cm. These images were acquired 48 h after pulsing. On the surface with GFP-siRNA, the fluorescence from EGFP was reduced in a dose-dependent manner. The observed reduction was not due to a decrease in the number of EGFP-expressing cells in an exclusive basis, but to the attenuation of expression level in most of the cells. On the other hand, EGFP expression remained unaffected on the surface with control-siRNA at any loading. The level of EGFP expression in the cells pulsed on the surfaces with control-siRNA was almost identical to levels in intact d2EGFP-HEK or in cells pulsed on the electrode on which no siRNA was adsorbed (Fig. 4 B). These results suggest that EGFP gene is silenced on application of an electric pulse in a sequence-specific manner on the GFP-siRNA-loaded electrode. Importantly, when cells were cultured on the siRNA-loaded surface for two days without electric pulsing, no decrease in GFP expression was observed (Fig. 4B), indicating that electric pulsing was necessary to achieve gene silencing. Electric pulsing at 48 and 72 h after cell seeding resulted also in significant reduction in the level of GFP expression (Fig. 4 C). These results suggest that the loaded siRNA retained their gene silencing activity for 3 days under a cell culture environment, showing the versatility of the method for transferring siRNA at the desired moment with equivalent results.

The expression of EGFP was further analyzed by flow cytometry (Fig. 5). Figures 5A and B shows that EGFP expression in d2EGFP-HEK was reduced by electric pulsing on the electrode loaded with GFP-siRNA. The histogram for cells pulsed on the electrode with control-siRNA (Fig. 5 C) is similar to that for d2EGFP-HEK (Fig. 5 D). As shown in Fig. 5 E, fluorescent intensity was significantly different between the two cases. Silencing

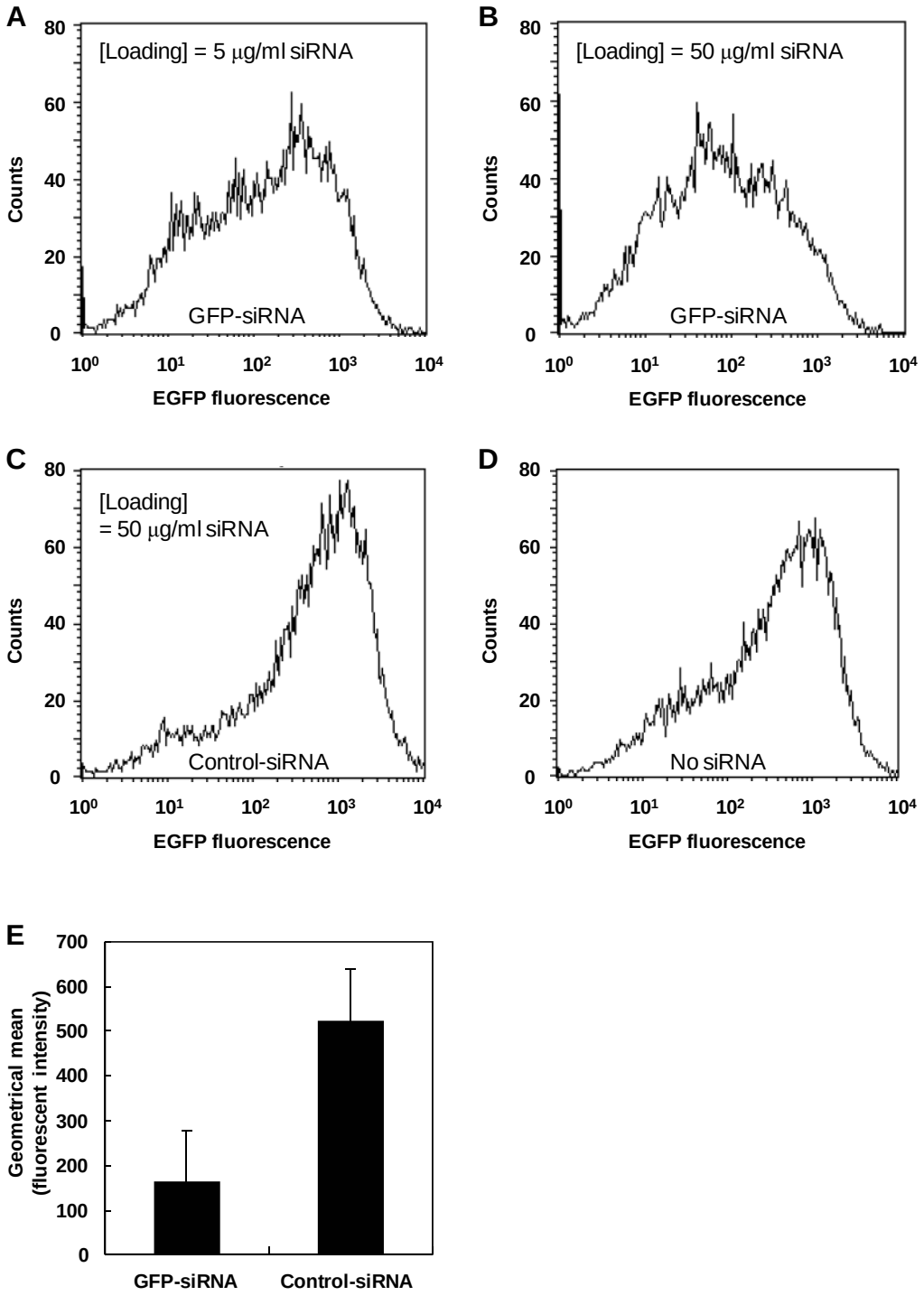
A
[Loading] = 5 μg/ml siRNA
GFP-siRNA
Counts
EGFP fluorescence
B
[Loading] = 50 μg/ml siRNA
GFP-siRNA
Counts
EGFP fluorescence
C
[Loading]
= 50 μg/ml siRNA
Control-siRNA
Counts
EGFP fluorescence
D
No siRNA
Counts
EGFP fluorescence
E
Geometrical mean
(fluorescent intensity)
GFP-siRNA
Control-siRNA

efficiency, defined as a ratio of EGFP fluorescence on the electrode with EGFP-siRNA to that on the electrode with control-siRNA, was approximately 70% for the condition of 50 μg/mL siRNA. These results indicate again that the electroporation of GFP-siRNA triggered the sequence-specific silencing of the EGFP gene. Fig. 5 also shows that reduction in EGFP expression was much more noticeable on the electrode prepared with 50 μg/mL siRNA solution (Fig. 5B) than that prepared with 5 μg/mL siRNA (Fig. 5A).

Gene silencing on siRNA loaded microarray

A microarray was prepared by loading GFP-siRNA and control-siRNA onto different spots on a single electrode. d2EGFP-HEK cells adhered uniformly to the entire surface of the microarray. When observed 48 h after electric pulsing at a field strength of 240 V/cm, cells on the spots with GFP-siRNA exhibited the reduced expression of EGFP with a similar extent between spots (Figs. 6 A and B). The silencing effect was restricted to the GFP-siRNA-loaded spots, with a normal level of the EGFP expression in cells on the

---

Figure 5. Flow cytometric analysis of d2EGFP-HEK cells pulsed at a field strength of 240 V/cm on electrodes loaded with (A, B) GFP-siRNA and (C) control-siRNA. siRNA was adsorbed from (A) 5 and (B, C) 50 μg/mL solutions. A curve in (D) represents a histogram for d2EGFP-HEK cells cultured on a PEI-adsorbed surface lacking siRNA and electrically pulsed at 240 V/cm. (E) Geometric mean fluorescence determined from histograms for the experiments in which 50 μg/mL siRNA solution was used. The data were expressed as mean ± standard deviation for n = 3 (control) or 5 (GFP).

surrounding regions where no siRNA was loaded. In contrast, cells on the spots with control-siRNA (Fig. 6 A and B) expressed EGFP at a similar level to the surrounding cells. As shown in Figure. 6 C, the EGFP expression was suppressed by 70% on the spots with GFP-siRNA compared with the spots with control-siRNA.

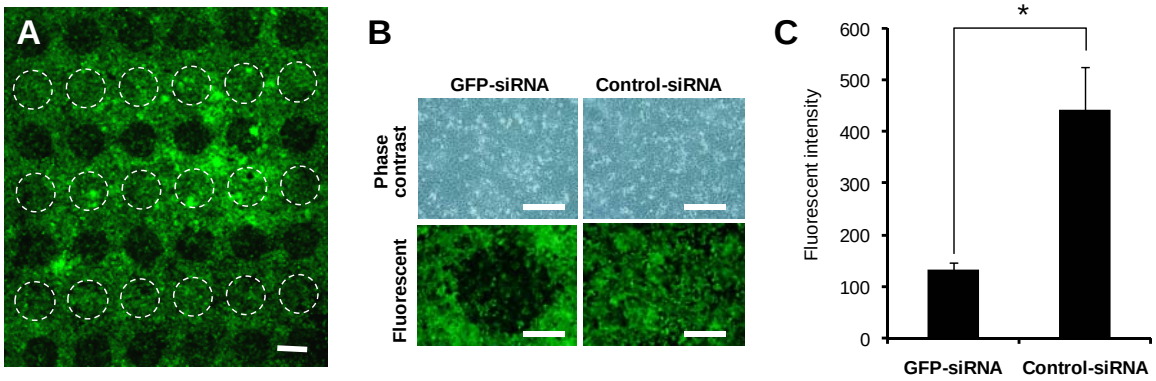

Figure 6. Electroporation of siRNA on the microarray. (A) Low magnification fluorescence image of d2EGFP-HEK cells electroporated on the microarray that displayed 42 spots arrayed in a 6 × 7 matrix. The image was recorded 48 h after electric pulsing at 240 V/cm. GFP-siRNA was loaded to spots (dark spots) on odd lines from the top; control-siRNA (highlighted with dashed circles) was loaded on even lines. (B) Higher magnification image of cells in (A). Phase-contrast and fluorescence microphotographs are shown for d2EGFP-HEK cells electroporated on the spots with (left) GFP-siRNA and (right) control-siRNA. Scale bar: (A) 1 mm and (B) 500 μm. (C) Fluorescence intensity of d2EGFP-HEK cells electroporated on the spots with GFP-siRNA and control-siRNA. Intensity was measured 48 h after electroporation. The data are expressed as mean ± standard deviation for 12 spots on two independent microarrays. *Asterisks* indicate statistical significance ($p < 0.05$) by Student's t-test.

DISCUSSION

Because of the excellent efficiency, electroporation is used to transfer nucleic acids into mammalian cells in a wide range of biological studies. Normally, electric pulses are applied to cell suspensions to temporally destabilize cell membranes, allowing uptake of exogenous DNA (typically plasmid DNA) present in a medium into the cytosol (19–21). Recently, electroporation has been frequently used to transfer siRNA into mammalian cells (22). It appears that the mechanism just described partially explains the surface-mediated electroporation reported in this chapter. However, in this method, siRNA must become detached from the electrode prior to permeating through the electrically-destabilized membranes. The release of siRNA is also effectively achieved by an electric pulse (Fig. 3). An important difference from conventional electroporation, typically performed at 1–10 kV/cm, is that this method allows for a much lower field strength. Cells on an electrode are significantly damaged by an elevated electric field, and it was found that the ideal conditions exist in a small window (220–280 V/cm), with the optimum field strength of ~ 240 V/cm in agreement with a previously study using a similar electroporation setup (3). Field strengths below or beyond this window resulted in considerably lower efficiency of gene silencing.

Other conditions that have an effect on transfection efficiency include the number and duration of electric pulses and the density of cells on the electrode. For these parameters, the conditions optimized in previous studies (2, 3, 23) for the electroporation of plasmid DNA were adopted here.

From comparison of the amount of released siRNA (Fig. 3) and the efficiency of gene silencing (Figs. 4 and 5), it is suggested that the availability of siRNA for cells is the most critical determinant of transfection efficiency. The local concentration of released siRNA may be relatively high at the basal face of cells and restricted within the spots. However, at present, it is not clear how loaded siRNA is released from the electrode upon electric pulsing. Nevertheless, Niu and Knoll reported that a poly(ethylene glycol)-tethered SAM was delaminated from gold by exerting small electric potential (24), and such might be the case here.

Another important aspect of a method is the use of electrostatic interactions between COOH-SAM and PEI, and PEI and siRNA for loading siRNA. It is expected that, similar to the case with plasmid DNA (25), polyelectrolyte complex formation serves to prevent the release and nuclease degradation of siRNA before electric pulsing. However, the loading of siRNA (~30 ng/cm^2) was approximately one tenth than that of plasmid DNA [typically 300 ng/cm^2 (2)]. This is plausibly because of the smaller molecular weight of siRNA (~1.5 × 10^3 g/mol) compared with plasmid DNA (for instance, molecular weight of pEGFP-C1 is ~3 × 10^6 g/mol).

This chapter demonstrates that siRNA can be transferred from the surface of an electrode into cells cultured on the electrode upon application of an electric pulse. This method could also be applied to the micropatterned surface, which permits the parallel introduction of siRNAs into mammalian cells. The electric pulse-triggered method is effective for silencing an endogenous gene, indicating higher efficiency of the present method compared with the lipid-mediated method (Chapter 1). These findings lead to

conclude that the electroporation microarray provides a potential platform for parallel loss-of-function studies using siRNA.

References

(1) Chang DC., Chassy BM., Saunders JA., Sowers AE. (1992) Guide to Elecrtroporation and Electrofusion, Academic Press, San Diego.

(2) Yamauchi F., Kato K., Iwata H. (2004) Spatially and temporally controlled gene transfer by electroporation into adherent cells on plasmid DNA-loaded electrodes. *Nucleic Acids Res.* **32** e187.

(3) Inoue Y., Fujimoto H., Ogino T., Iwata H. (2008) Site-specific gene transfer with high efficiency onto a carbon nanotube-loaded electrode. *J. R. Soc. Interface.* **5** 909-918.

(4) Yamauchi F., Okada M., Kato K., Jakt LM., Iwata H. (2007) Array-based functional screening for genes that regulate vascular endothelial differentiation of Flk1-positive progenitors derived from embryonic stem cells. *Biochim. Biophys. Acta* **1770** 1085–1097.

(5) Elbashir SM., Harborth J., Lendeckel W., Yalcin A., Weber K., Tuschl, T. (2001) Duplexes of 21-nucleotide RNAs mediate RNA interference in cultured mammalian cells. *Nature* **411** 494–498.

(6) Fire A., Xu SQ., Montgomery MK, Kostas SA., Driver SE., Mello CC. (1998) Potent and specific genetic interference by double-stranded RNA in *Caenorhabditis elegans*. *Nature* **391** 806–811.

(7) Kittler R., Putz G., Pelletier L., Poser I., Heninger AK., Drechsel D., Fischer S., Konstantinova I., Habermann B., Grabner H., Yaspo ML., Himmelbauer H., Korn B., Neugebauer K., Pisabarro MT., Buchholz F. (2004) An endoribonuclease-prepared siRNA screen in human cells identifies genes essential for cell division. *Nature* **432** 1036–1040.

(8) Berns K., Hijmans EM., Mullenders J., Brummelkamp TR., Velds A., Heimerikx

M., Kerkhoven RM., Madiredjo M., Nijkamp W., Weigelt B., Agami R., Ge W., Cavet G., Linsley PS., Beijersbergen RL., Bernards R. (2004) A large-scale RNAi screen in human cells identifies new components of the p53 pathway. *Nature* **428** 431–437.

(9) Paddison PJ., Silva JM., Conklin DS., Schlabach M., Li M, Aruleba S., Balija V., O'Shaughnessy A., Gnoj L., Scobie K., Chang K., Westbrook T., Cleary M., Sachidanandam R., McCombie WR., Elledge SJ., Hannkn G. (2004) A resource for large-scale RNA-interference-based screens in mammals. *Nature* **428** 427–431.

(10) Pelkmans L., Fava E., Grabner H., Hannus M., Habermann B., Krausz E., Zerial M. (2005) Genome-wide analysis of human kinases in clathrin- and caveolae/raft-mediated endocytosis. *Nature* **436** 78–86.

(11) Mousses S., Caplen N., Cornelison R., Weaver D., Basik M., Hautaniemi S., Elkahloun AG., Lotufo RA., Choudary ER., Suh E., Kallioniemi O. (2003) RNAi microarray analysis in cultured mammalian cells. *Genome Res.* **13** 2341–2347.

(12) Ovcharenko D., Jarvis R., Hunicke-Smith S., Brown D. (2005) High-throughput RNAi screening in vitro: From cell lines to primary cells. *RNA* **11** 985–993.

(13) Lin YC., Li M., Wu CC. (2004) Simulation and experimental demonstration of the electric field assisted electroporation microchip for *in vitro* gene delivery enhancement. *Lab Chip* **4** 104–108.

(14) Jain T., Muthuswamy J. (2007) Bio-chip for spatially controlled transfection of nucleic acid payloads into cells in a culture. *Lab Chip* **7** 1004–1011.

(15) Jain T., Muthuswamy J. (2008) Microelectrode array (MEA) platform for targeted neuronal transfection and recording. *IEE. Trans. Biomed. Eng.* **55** 827–832.

(16) Chaufer B., Rabiller-Baudry M., Bouguen A., Labbé JP., Quémerais A. (2000)

Spectroscopic characterization of zirconia coated by polymers with amine groups. *Langmuir* **16** 1852–1860.

(17) Banyay M., Sarkar M., Gräslund A. (2003) A library of IR bands of nucleic acids in solution. *Biophys. Chem.* **104** 477–488.

(18) Liquier J., Akhebat A., Taillandier E. (1991) Characterization by FTIR spectroscopy of the oligoribonucleotide duplexes r(A-U)6 and r(A-U)8. *Spectrochim. Acta* **47A** 177–186.

(19) Kinoshita K., Tsong TY. (1978) Survival of sucrose-loaded erythrocytes in the circulation. *Nature* **272** 258–260.

(20) Wong TK., Neumann E. (1982) Electric field mediated gene transfer. *Biochem. Biophys. Res. Commun.* **107** 584–587.

(21) Tsong TY. (1991) Electroporation of cell membrane. *Biophys. J.* **60** 297–306.

(22) Wilson JA, Jayasena S, Khvorona A, Sabatinos S, Rodrigue-Gervais IG, Arya S, Sarangi F, Harris-Brandts M., .Beaulieu S., Richardson CD. (2003) RNA interference blocks gene expression and RNA synthesis from hepatitis C replicons propagated in human liver cells. *Proc. Natl. Acad. Sci .U.S.A.* **100** 2783–2788.

(23) Yamauchi F., Kato K., Iwata H. (2005) Layer-by-layer assembly of poly(ethyleneimine) and plasmid DNA onto transparent indium-tin oxide electrodes for temporally and spatially specific gene transfer. *Langmuir* **21** 8360–8367.

(24) Niu L., Knoll W. (2007) Electrochemically addressable functionalization and parallel readout of a DNA biosensor array. *Anal. Chem.* **79** 2695–2702.

(25) Yamauchi F., Koyamatsu Y., Kato K., Iwata H. (2006) Layer-by-layer assembly of cationic lipid and plasmid DNA onto gold surface for stent-assisted gene transfer.

Biomaterials **27** 3497–3504.

Chapter 4

Layer-by-layer assembly of small interfering RNA and poly(ethyleneimine) for substrate-mediated electroporation with high efficiency

INTRODUCTION

Small interfering RNA (siRNA) is double-stranded RNA of 21–25 nucleotides with a sequence homologous to the specific region of messenger RNA (mRNA) (1). The introduction of siRNA into mammalian cells triggers RNA interference by which the expression of a specific gene is silenced by degradation of mRNA (2). Due to the simplicity of siRNA-triggered knockdown compare to the conventional knockout technique, siRNA is recognized as a versatile tool for the analysis of gene functions (3, 4), especially for high-throughput knockdown experiments using transfection microarrays (5, 6).

Functional studies using siRNA-based microarrays rely primarily on two factors. First, the intrinsic efficiency of siRNA for gene silencing is required to be high enough for assessing the effect of gene silencing. The efficiency is greatly dependent on targeted sequences within mRNA (7). The libraries of siRNAs generated by digesting double-stranded RNA by endoribonuclease are suitably used to conduct knockdown experiments on microarrays for the large set of DNA transcripts, as demonstrated in Chapter 2. Secondary, the transfection efficiency of siRNAs must be sufficiently high for reducing

false negative data. As demonstrated in Chapter 3, electroporation provides an efficient method for transferring siRNA from microarrays into cultured mammalian cells.

However, further improvement of transfection efficiency may improve the reliability and reproducibility of knockdown experiments on siRNA microarrays. According to previous chapters, siRNA loading on electroporation microarrays seems to be one of the most important parameters that have influence on transfection efficiency. For this reason, the present chapter aimed at increasing the loading of siRNA on electroporation microarrays for the improved efficiency of transfection and hence the elevated suppression of gene expression. In this chapter, the layer-by-layer (LBL) assembly technique (8) was examined to amply deposit siRNA onto a microarray. The LBL assembly process has been widely utilized in the creation of functional surfaces (9–11), including the fabrication of electroporation microarrays loaded with plasmid DNA (12).

In this chapter, the LBL technique was employed to construct a multilayer consisting of cationic polymer, poly(ethyleneimine) (PEI), and anionic polymer, siRNA, on the surface of a gold electrode. PEIs with different molecular architectures were examined in an attempt to increase the loading of siRNA. The surfaces with PEI/siRNA multilayers were characterized by infrared reflection-adsorption (IR-RAS) spectroscopy and surface plasmon resonance (SPR) analysis. The combination of cells stably transformed with an enhanced green fluorescent protein (EGFP) gene and EGF-specific siRNA were used to examine the effect of siRNA loading on the silencing of an endogenous gene.

EXPERIMENTAL

siRNA and PEI

Two siRNAs, GFP-siRNA and control-siRNA, were purchased from Qiagen. GFP-siRNA had an ability to knockdown EGFP gene (sense, 5'-GCAAGCUGACCCUGAAGU UCAU-3'; antisense, 5'-GAACUUCAGGGUCAGCUUGCCG-3'), while control-siRNA had no silencing effect (sense, 5'-UUCUCCGAACGUGUCACGUdTdT-3'; antisense, 5'-ACGUGACACGUUCGGAGAAdTdT-3'). The linear and branched forms of PEI were purchased from Aldrich Chemical Co., Milwaukee, WI. The number-averaged molecular weight was 2500 and 25000 for linear PEI, and 2000 and 25000 for branched PEI.

Cell culture

Cells used were human embryonic kidney cell line, d2EGFP-HEK, stably expressing destabilized EGFP (see Chapter 3 for the establishment). These cells were routinely maintained in a minimal essential medium (MEM; Invitrogen Corp., Carlsbad, CA, USA) supplemented with 10% fetal bovine serum, 100 U/mL penicillin, and 100 μg/mL streptomycin at 37 °C under 5% CO_2 atmosphere.

Preparation of electrodes by LBL assmebly

As described in Chapter 1, a self-assembled monolayer (SAM) of carboxylic acid-terminated alkanethiol was formed on a glass plate. In brief, a glass plate (26 mm × 22 mm × 0.5 mm, Matsunami Glass Industries, Ltd., Osaka, Japan) was treated with a Piranha solution (concentrated H_2SO_4 : 30% H_2O_2 = 7 : 3 by volume) at room temperature for 5 min

to remove impurities. The cleaned glass plate was thoroughly washed with deionized water and 2-propanol, and dried under a stream of nitrogen gas. A thin primer layer of chromium (thickness: 1 nm) was deposited onto the glass surface using a thermal evaporator (V-KS200, Osaka Vacuum Instruments, Osaka, Japan), and then a gold layer (thickness: 49 nm) was further deposited on top of the chromium layer in a continuous process. Immediately after deposition, the plate was immersed in 1 mM 11-mercaptoundecanoic acid (Aldrich Chemical Co.) solution in ethanol at room temperature to form a carboxylic acid-terminated SAM (COOH-SAM) on gold. After 24 h, the plate was washed with ethanol and water, and dried under a stream of nitrogen gas.

PEI was dissolved in phosphate buffered saline (PBS) to a concentration of 0.1%. The solution was adjusted to pH 7.4 with HCl. An electrode bearing COOH-SAM was immersed in the PEI solution for 30 min at room temperature to ionically adsorb PEI onto the electrode. Then the plate was washed with water to remove weakly adsorbed PEI. Subsequently, the PEI-adsorbed surface was exposed to 5 μg/mL siRNA solution in PBS (pH 7.4) for 20 min at room temperature to ionically adsorb siRNA onto the surface, followed by washing with PBS. The sequential adsorption of PEI and siRNA was repeated up to 5 times to obtain a multilayer. Finally, the electrode with the multilayer was washed with PBS and immediately used for later experiments.

Infrared reflection absorption spectroscopy (IR-RAS)

IR-RAS spectra of PEI- and siRNA-adsorbed onto an electrode were recorded with Spectrum One (PerkinElmer, Waltham, MA) equipped a mercury-cadmium-telluride detector and a RAS sampling accessory (Harrick Scientific Co., Ossining, NY) at a

resolution of 4 cm^{-1} with an accumulation of 256 scans. All samples for IR-RAS analysis were prepared using a glass plate with a thick gold layer (199 nm) so as to attain sufficient reflection of IR light. Prior to analysis, sample surfaces were rinsed once with pure water and dried under vacuum. A bare gold surface was used as reference.

Surface plasmon resonance (SPR) analysis

As reported previously (13), an in-house SPR instrument was used for analyzing the adsorption of siRNA and PEI on an electrode. The electrode baring COOH-SAM was mounted on a glass prism together with a flow cell. PBS solutions of PEI (0.1%) and siRNA (5 μg/mL) were sequentially introduced into the flow cell. In each step, solutions were halted within the flow cell for 20 min, followed by streaming of pure PBS for 5 min to washout non-adsorbed PEI or siRNA. During these procedures, light reflectance was continuously monitored at a constant incident angle 0.5 degree smaller than the resonance angle. Finally the observed reflectance was converted to the shift of the resonance angle. All measurements were performed at 30 °C. To determine the surface density of PEI and siRNA, a resonance angular shift was converted to the surface density assuming the unit angular shift of 0.5 μg/cm^2/DA (14).

Electroporation

An electroporation setup is shown in Scheme 1. A sterilized silicone rubber frame of a thickness of 0.5 mm was adhered to the electrode for restricting a cell culture region and keep distance between the basement and upper electrodes. The siRNA-loaded electrode

was first washed with PBS followed by plating of d2EGFP-HEK cells within the frame at a density of 45000 cells/cm^2. The cells were cultured at 37 °C under 5% CO_2 atmosphere to adhere on the electrode. After incubation for 24 h, the electrode surface within the frame was washed with PBS to eliminate no-adhering cells and then filled with cold PBS. A counter electrode (a glass plate bearing a gold layer of 199 nm in thickness) was placed on

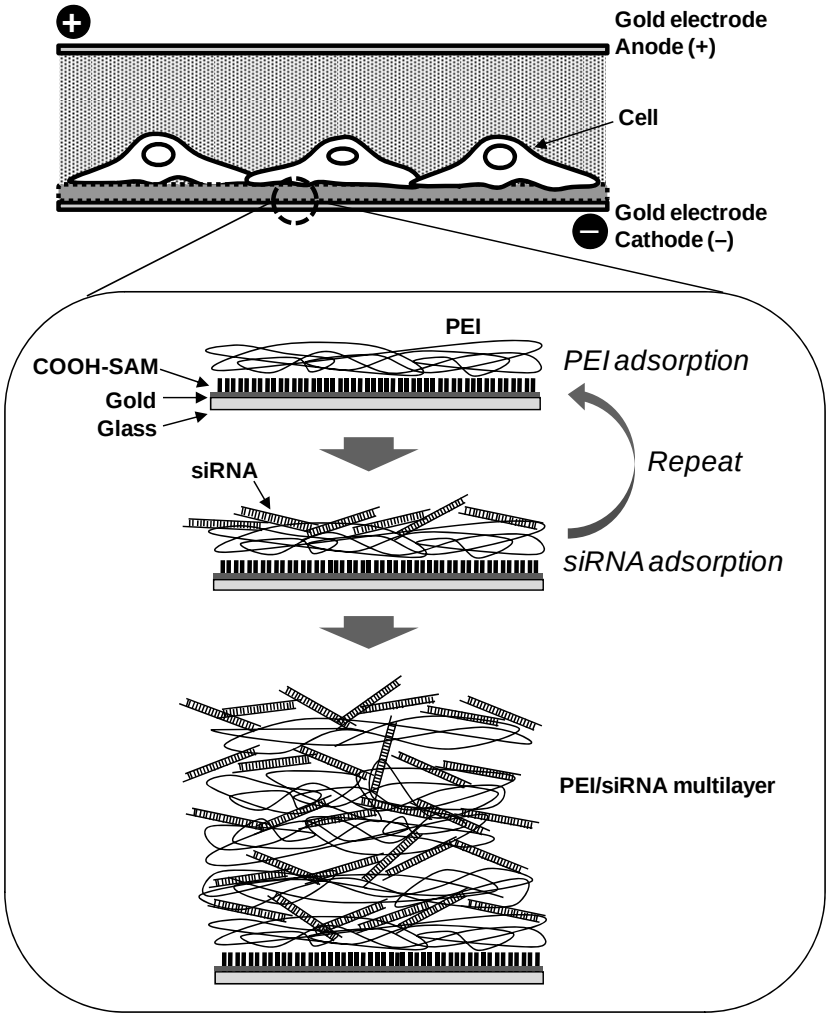

Scheme 1. Schematic representation for the electroporation setup.

the silicone frame, and both of the electrodes were connected to pulse generator (Gene Pulser Xcell, Bio-Rad, Hercules, CA). Then, the cells were treated with a single pulse at the field strength of 240 V/cm for a duration of 10 msec. Five minutes after electric pulsing, PBS was replaced with MEM supplemented with 10% FBS, 100 U/mL penicillin, and 100 μg/mL streptomycin. Cells were further cultured for 48 h at 37 ^{o}C under 5% CO_2 atmosphere. To evaluate the suppression of EGFP expression, cells were observed with an epifluorescence microscope (BX-51, Olympus, Tokyo, Japan).

Flow cytometry

Cells were harvested from an electrode by trypsinization 48 h after electroporation and washed with cold PBS. The expression of EGFP was analyzed with a flow cytometer (FACS Caliber, Becton-Dickinson, Franklin Lakes, NJ). Data from approximately 20,000 cells were used to generate a histogram. For the quantitative analysis, geometrical mean fluorescence was determined from the histograms.

RESULTS

Effect of PEI structure

Figure 1 shows fluorescent microphotographs of d2EGFP-HEK cells electroporated on the electrodes that had a monolayer consisting of GFP-siRNA and PEI. The branched and linear forms of PEI of two different molecular weights were used to compare the effects on

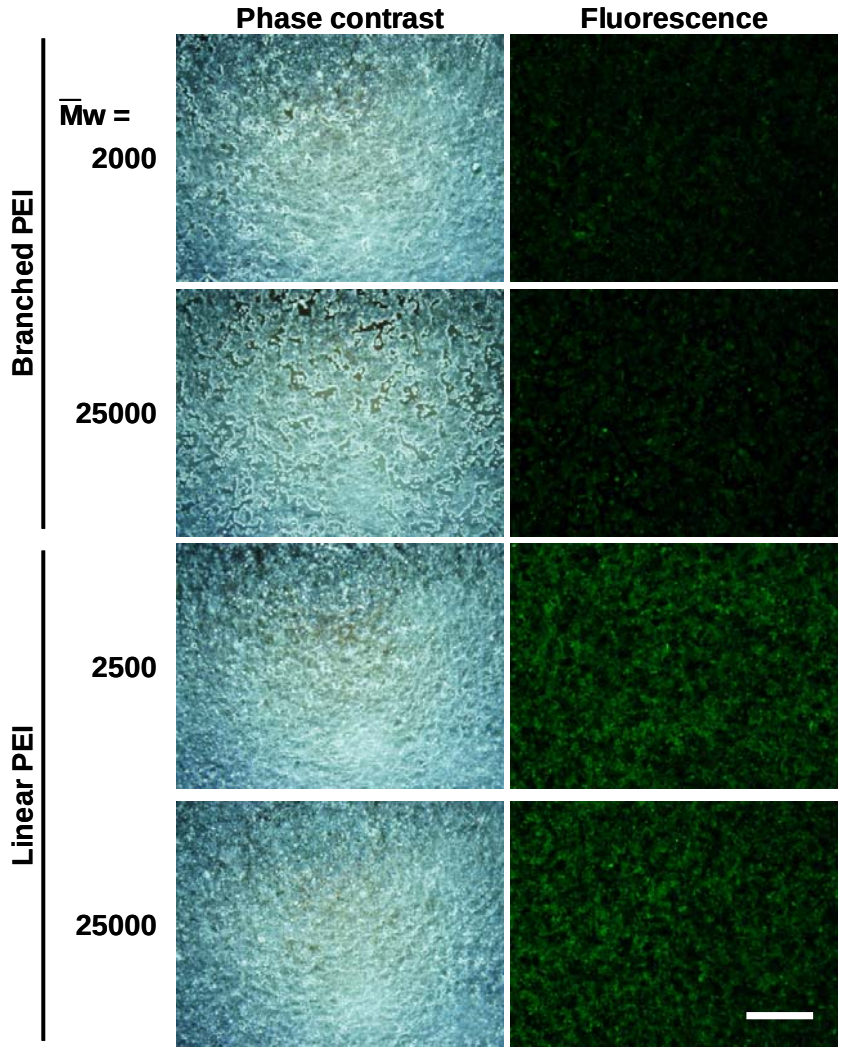

Figure 1. Phase contrast (left) and fluorescent (right) microphotographs of EGFP-HEK cells electroporated on the GFP-siRNA-loaded electrodes. Branched PEI (Mw = 2000 or 25000) or linear PEI (Mw = 2500 or 25000) was adsorbed from their 0.1% solution to an electrode, and then GFP-siRNA (50 μg/mL) was adsorbed to the PEI-adsorbed surface. Bar: 1 mm.

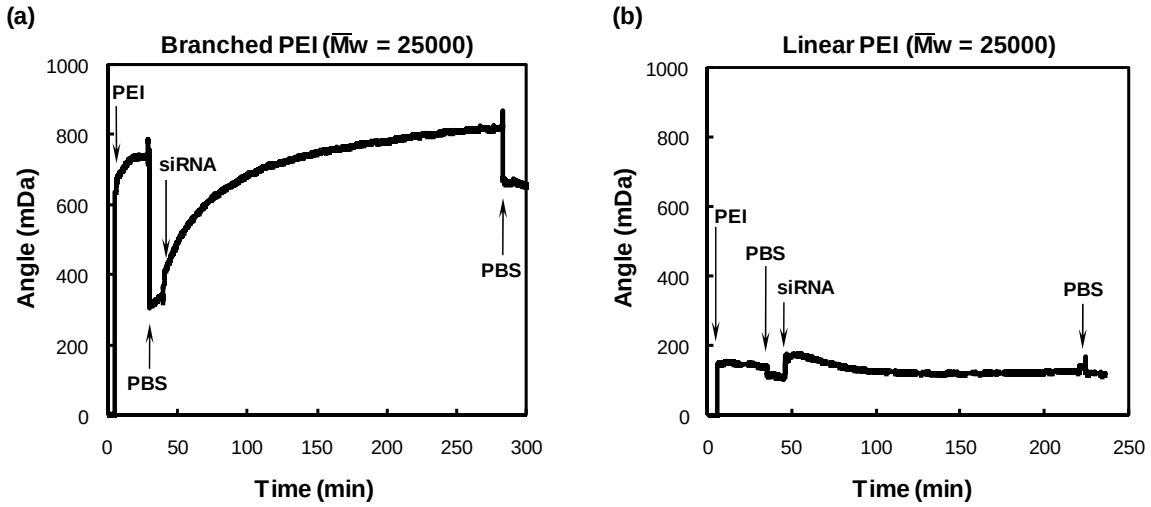

Figure 2. SPR sensorgrams recorded during the exposure of the COOH-SAM-bearing electrode sequentially to the solution of 0.1% PEI and 5 μg/mL GFP-siRNA. Cationic polymers used were (a) branched PEI (Mw = 25000) and (b) linear PEI (Mw = 25000).

gene silencing. As can be seen in the phase contrast microphotographs, the difference in molecular architecture had little effects on the adhesion and growth of cells. However, in fluorescent microphotographs, it is seen that EGFP expression is suppressed much more with the branched PEIs than the linear ones. The effect of molecular weigh of PEI was not obvious in fluorescent microphotographs.

Figure 2 shows SPR sensorgrams recorded for the sequential adsorption of PEI and GFP-siRNA onto an electrode bearing COOH-SAM. The observed sifts of a resonance angle indicate the adsorption of PEI onto the COOH-SAM and siRNA onto the PEI-adsorbed surface. Figure 2 clearly shows that the angle shifts due to the adsorption of both PEI and siRNA were larger with branched form of PEI than the linear form. This result

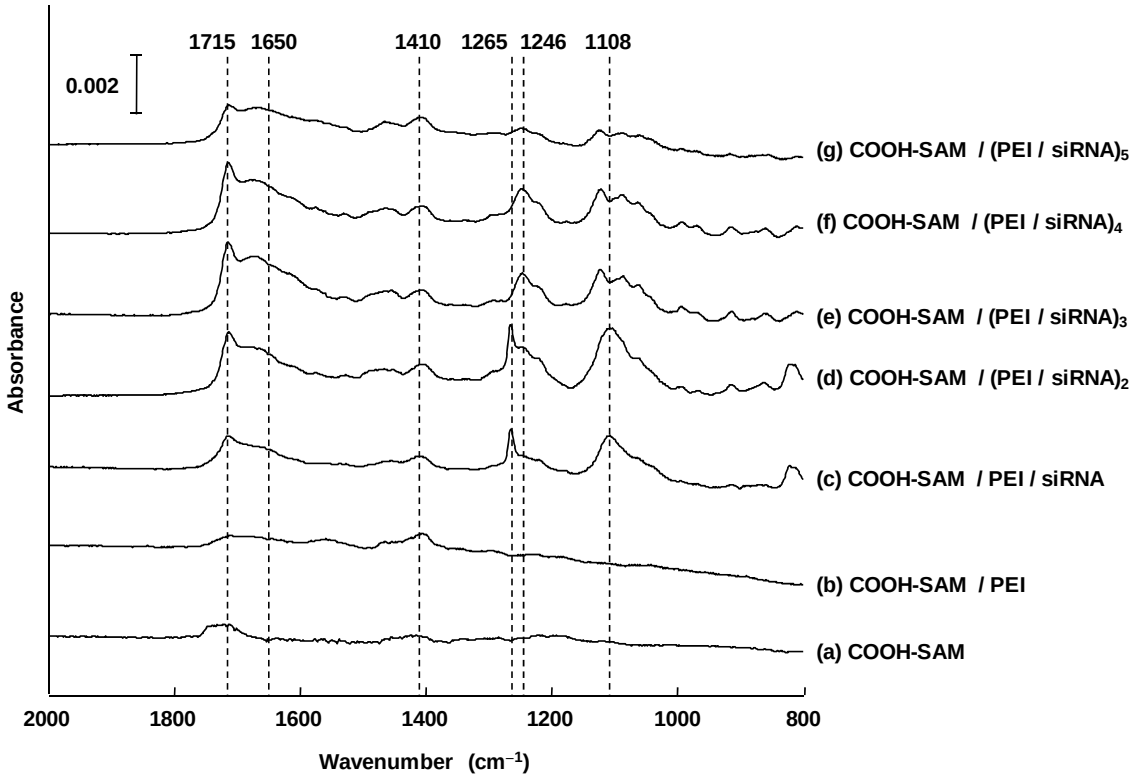

Figure 3. IR-RAS spectra recorded for electrodes with (a) COOH-SAM, (b) COOH-SAM and PEI, (c) COOH-SAM, PEI, and GFP-siRNA, (d) COOH-SAM and $(PEI/siRNA)_2$, (e) COOH-SAM and $(PEI/siRNA)_3$, (f) COOH-SAM and $(PEI/siRNA)_4$, (g) COOH-SAM, and $(PEI/siRNA)_5$. Solutions containing 0.1% branched PEI (Mw = 25000) and 5 μg/ml siRNA were used for sequential adsorption.

indicates that the branched PEI gave rise to larger loading of siRNA. It is likely that the higher adsorption capacity of the branched PEI is the basis for the elevated efficacy of gene silencing by siRNA as demonstrated in Figure 1. According to the results described above, the branched PEI of the molecular weight of 25000 was used in the later experiments.

LBL assembly of PEI and siRNA

In order to increase the amount of siRNA and hence enhance the silencing efficiency, the LBL assembly technique was applied to the loading of siRNA onto an electrode. The surface of electrodes that had various numbers of a PEI/siRNA layer was analyzed with IR-RAS. The results are shown in Figure 3. The broad peak at 1710–1725 cm^{-1} seen in the spectrum of COOH-SAM (Fig. 3 a) is assigned to the stretching vibration of C═O contained in 11-mercaptoundecanoic acid. In the spectrum for the PEI-adsorbed surface (Fig. 3 b), a new peak assigned to amine (15) appeared at 1410 cm^{-1}, which indicates the presence of PEI. After exposure to siRNA solution (Fig. 3 c), additional absorption is seen at 1650–1730 cm^{-1} (C═O vibration of bases) (16), 1108 cm^{-1} (symmetric stretching of phosphate), and 1246–1265 cm^{-1} (antisymmetric stretching of phosphate) (15), providing the evidence for the adsorption of siRNA. The infrared absorption bands due to PEI and siRNA are seen in the spectra obtained after repeated adsorption cycles (Fig. 3 d–g). These results demonstrate the adsorption of PEI and siRNA.

To quantitatively characterize the adsorption layer, SPR analysis was performed for the LBL assembly process. Figure 4 shows the SPR sensorgrams recorded during the alternative adsorption of branched PEI (Mw = 25000) and GFP-siRNA onto an electrode bearing COOH-SAM. Cumulative loading was determined from the resonance angular shifts observed after PBS washing following each adsorption step. In Figure 4 b, the data are plotted as a function of adsorption numbers. As can be seen, the loading of siRNA increases with an increasing number of adsorption cycles.

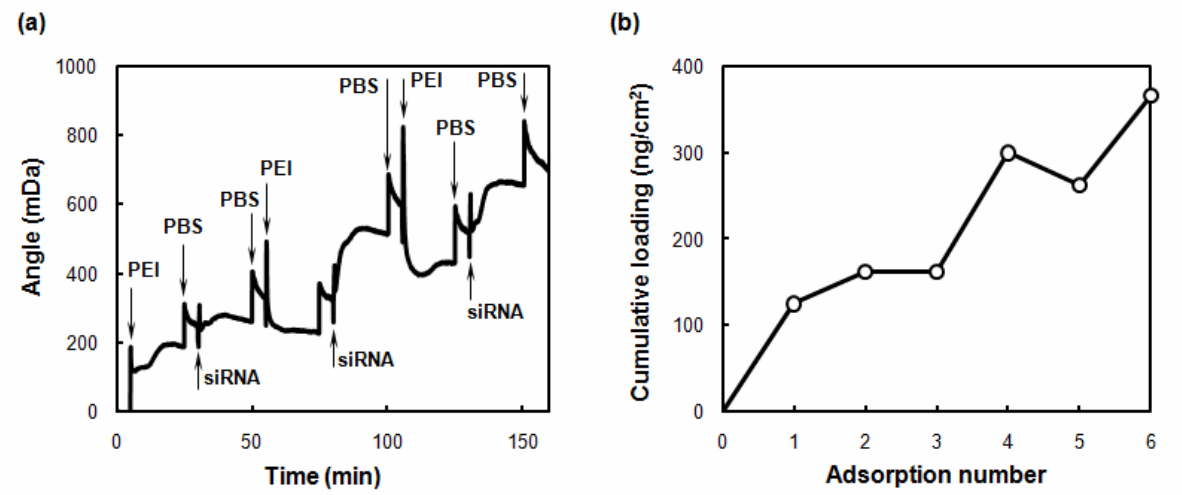

Figure 4. SPR sensorgram recorded during the alternate exposure of the COO-SAM-bearing electrode to the solutions of 0.1% branched PEI (Mw = 25000) and 5 μg/mL GFP-siRNA. After each adsorption step, PBS was circulated over the surface to wash out unbound PEI and siRNA. (b) Cumulative loading of PEI and siRNA determined from the sensorgram in (a).

Gene silencing on siRNA multilayers

Figure 5 shows the representative microphotographs of d2EGFP-HEK cells transfected on the electrodes that possessed 1–5 layers of PEI/GFP-siRNA or PEI/control-siRNA. On the electrodes prepared with control-siRNA, EGFP expression remained unaffected in any layer number. In contrast, fluorescence from EGFP was reduced on the electrodes with GFP-siRNA. The observed reduction in fluorescence was dependent upon layer numbers. An increase in the layer numbers gave rise to more reduction in EGFP expression.

The expression of EGFP was further analyzed by flow cytometry. The geometrical mean fluorescence was determined for various conditions and normalized by the data for the electrode with a single PEI/control-siRNA layer. The results are shown in Figure 6. On

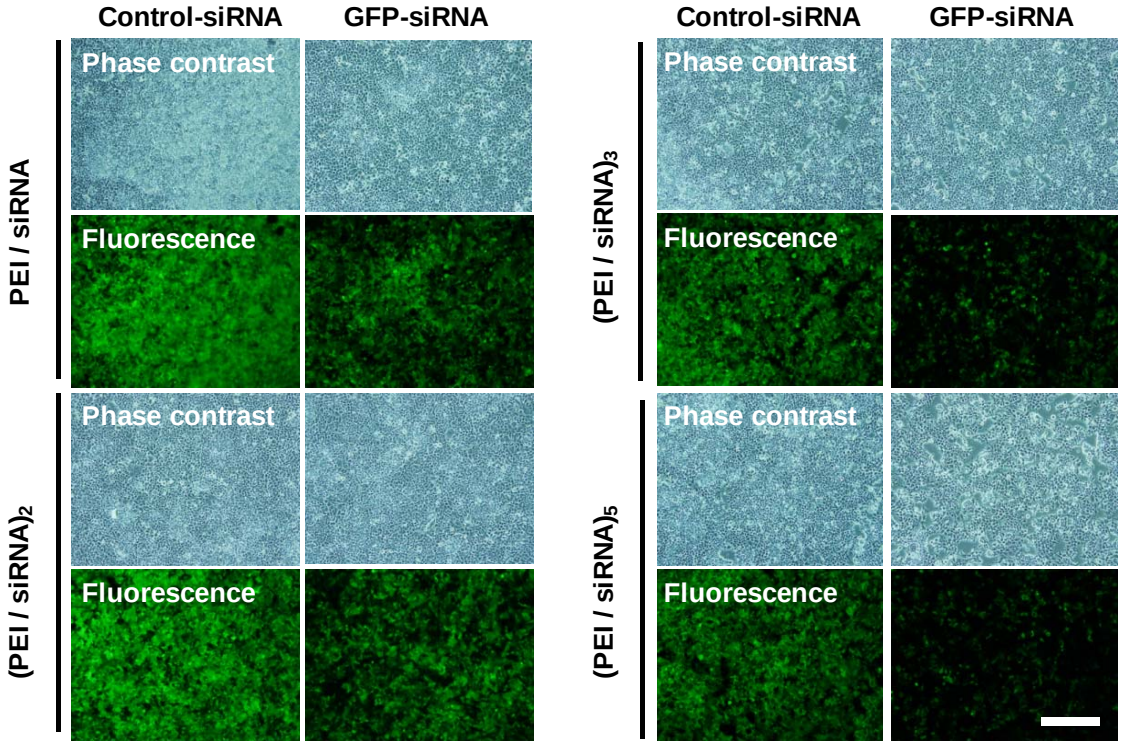

Figure 5. Phase contrast and fluorescent microphotographs of d2EGFP-HEK cells electroporated on the electrodes with (left) PEI/control-siRNA or (right) PEI/GFP-siRNA multilayers. Bar: 500 μm.

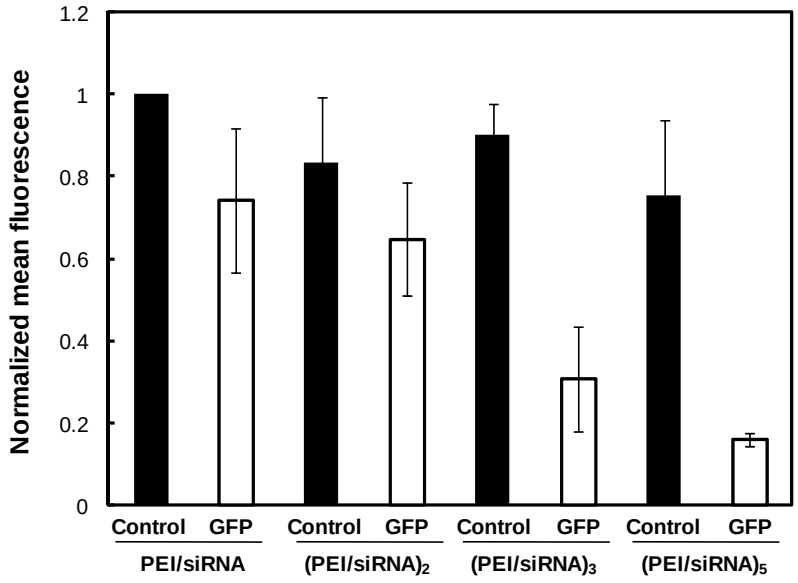

Figure 6. Mean fluorescence determined by flow cytometry for cells electroporated on the electrodes with (■) PEI/control-siRNA and (□) PEI/GFP-siRNA multilayers. The data are normalized by that for the electrode with a single layer of PEI/control-siRNA and expressed as mean ± standard deviation for n = 3.

the electrodes with control-siRNA, cells strongly expressed EGFP with no significant dependency on the layer numbers. To the contrary, on the electrodes prepared with GFP-siRNA, EGFP expression was reduced in a layer number-dependent manner. On the electrode with $(PEI/GFP\text{-}siRNA)_5$, EGFP fluorescence was reduced by 85% compared to the result obtained from the electrode with a single PEI/control-siRNA layer.

DISCUSSION

To increase the amount of siRNA loaded onto an electrode, the LBL assembly technique was used for adsorb anionic siRNA and cationic PEI on a gold electrode. IR-RAS and SPR analyses of the siRNA-loaded electrode revealed that siRNA loading increased with the cycle numbers of PEI and isRNA adsorption. It was further demonstrated that, when EGFP-expressing cells were electroporated on the GFP-siRNA-loaded electrode, the gene silencing effect was enhanced by increasing the siRNA loading by the LBL assembly in an adsorption cycle- dependent manner.

The LBL assembly technique was reported by Decher (8) and Iwata et al. (17), and applied in a variety of fields including biotechnology (18–23). This technique has been utilized for loading DNA on the material surfaces for controlled release of DNA (18, 19) and surface-mediated gene transfer into living cells (Chapters 1–3, 21–23). Recently, Recksiedler et al. reported the fabrication of thin multilayered films consisting of poly(anilineboronic acid) and single-stranded RNA (24). In present chapter, the LBL assembly technique is successfully applied to amply deposit siRNA on an electrode for efficient electroporation. The amount of loaded siRNA reached ca. 400 ng/cm^2 after three cycles of PEI/siRNA adsorption (Fig. 4). This amount is comparable to the surface density of plasmid DNA (500–600 ng/cm^2) deposited in a similar fashion onto an anionically-modified indium-tin oxide electrode (12).

In the LBL assembly, the formation of a thin multilayer involves the interaction between polycations and polyanions at ionic surfaces. The technique utilizes the overcompensation of negative or positive charges previously fixed on the surface. The

results obtained in this chapter show that the branched form of PEI gives rise to much efficient deposition of PEI itself and siRNA than the linear PEI does. This finding suggests that charge compensation at surface effectively takes place with the branched PEI. This is probably related to the steric effect of branched PEI, although further mechanistic study is needed to understand in more detail. Another concern is that branched PEI contains primary, secondary, and tertiary amines while linear PEI contains only primary and secondary amines. In spite of such a structural difference, it was reported that pK_a and the dissociation constants are similar between these polymers (25).

It is likely that enhanced gene silencing on the electrode prepared by the LBL assembly of PEI and siRNA is due to the elevated availability of siRNA for cells upon electric pulsing. The higher loading of siRNA might yield the higher amount of siRNA locally released from the surface and then transferred into adjacent cells. Chapters 1 and 2 also demonstrated a similar dependence among the siRNA loading, the amount of released siRNA, and silencing efficiency.

In conclusion, it is demonstrated that the LBL assembly of branched PEI and siRNA facilitates to increase siRNA loading on an electrode, and accordingly intensifies the gene silencing effect of siRNA in the cells electroporated on the electrode. The method described here is simple and effective, and possibly applicable to the fabrication of siRNA-loaded electroporation microarrays. This feature will accelerate the large-scale study of gene functions using cell-based transfection microarrays.

References

(1) Fire A., Xu SQ., Montgomery MK., Kostas SA., Driver SE., Mello CC. (1998) Potent and specific genetic interference by double-stranded RNA in *Caenorhabditis elegans*. *Nature* **391** 806–811.

(2) Elbashir SM., Harborth J., Lendeckel W., Yalcin A., Weber K., Tuschl T. (2001) Duplexes of 21-nucleotide RNAs mediate RNA interference in cultured mammalian cells. *Nature* **411** 494–498.

(3) Hannon J. (2002) RNA interference. *Nature* **418** 244–251.

(4) Echeverri CJ. Perrimon N. (2006) High-throughput RNAi screening in cultured cells: a user's guide. *Nat. Rev. Genet.* **7** 373–384.

(5) Wheeler DB., Bailey SN., Guertin DA., Carpenter AE., Higgins CO., Sabatini DM. (2004) RNAi living-cell microarrays for loss-of-function screens in *Drosophila melanogaster* cells. *Nat. Method* **1** 1–6.

(6) Carpenter AE., Sabatini DM. (2004) Systematic genome-wide screens of gene function. *Nat. Rev. Genet.* **5** 11–22.

(7) Reynolds A., Leake D., Boese Q., Scaringe S., Marshall WS., Khvorova A. (2004) Rational siRNA design for RNA interference. *Nat. Biotechnol.* **22** 326–330.

(8) Decher G. (1997) Fuzzy nanoassemblies: Toward layered polymeric multicomposites. *Science* **277** 1232–1237.

(9) Jewell CM., Lynn DM. (2008) Multilayered polyelectrolyte assemblies as platforms for the delivery of DNA and other nucleic acid-based therapeutics. *Adv. Drug Delivery Rev.* **60** 979–999.

(10) Schwinte P., Voegel JC., Picart C., Haikel Y., Schaaf P., Szalontai B. (2001) Stabilization effects of various polyelectrolyte multilayer films on the structure of adsorbed/embedded fibronectin molecules: An ATR-FTIR study. *J. Phys. Chem.* **105** 11906–11916.

(11) Sukhorukov GB., Montrel MM., Petrov AL., Shabarchina LI., Sukhorukov BI. (1996) Multilayer films containing immobilized nucleic acids. Their structure and possibilities in biosensor applications. *Biosens. Bioelectron.* **11** 913–922.

(12) Yamauchi F., Kato K., Iwata H. (2005) Layer-by-layer assembly of poly(ethyleneimine) and plasmid DNA onto transparent indium-tin oxide electrodes for temporally and spatially specific gene transfer. *Langmiur* **21** 8360–8367.

(13) Hirata I., Morimoto Y., Murakami Y., Iwata H., Kitano E., Kitamura H., Ikada Y. (2000) Study of complement activation on well-defined surfaces using surface plasmon resonance. *Colloid. Surf. B Biointerf.* **18** 285–292.

(14) Knoll W. (1991) Polymer thin films and interfaces characterized with evanescent light. *Makromol. Chem.* **192** 2827–2856.

(15) Chaufer B., Rabiller-Baudry M., Bouguen A., Labbé JP., Quémerais A. (2000) Spectroscopic characterization of zirconia coated by polymers with amine groups. *Langmuir* **16** 1852–1860.

(16) Banyay M., Sarkar M., Gräslund A. (2003) A library of IR bands of nucleic acids in solution. *Biophys. Chem.* **104** 477–488.

(17) Iwata H., Takagi T., Kobayashi K., Oka T., Tsuji T., Ito F. (1994) Strategy for developing microbeads applicable to islet xenotransplantation into a spontaneous diabetic NOD mouse. *J. Biomed. Mater. Res.* **28** 1201–1207.

(18) Jewell CM. Lynn DM. (2008) Multilayered polyelectrolyte assemblies as platforms for the delivery of DNA and other nucleic acid-based therapeutics. *Adv. Drug Deliv. Rev.* **60** 979–999.

(19) Zhang J., Chua LS., Lynn DM. (2004) Multilayered thin films that sustain the release of functional DNA under physiological conditions. *Langmiur* **20** 8015–8021.

(20) Ren KF., Ji J., Shen JC. (2006) Construction and emzymatic degradation of multilayered poly-L-lysin/DNA films. *Biomaterials* **27** 1152–1159.

(21) Jewell CM., Zhang J., Fredin NJ., Lynn DM. (2005) Multilayered polyelectrolyte films promote the direct and localized delivery of DNA to cells. *J. Control. Release* **106** 214–223.

(22) Yamauchi F., Koyamatsu Y., Kato K., Iwata H. (2006) Layer-by-layer assembly of cationic lipid and plasmid DNA onto gold surface for stent-assisted gene transfer. *Biomaterials* **27** 3497–3504.

(23) Yamauchi F., Kato K., Iwata H. (2004) Micropatterned, self-assembled monolayers for fabrication of transfected cell microarrays. *Biochim. Biophys. Acta* **1672** 138–147.

(24) Recksiedler CL., Deore BA., Freund MS. (2006) A novel layer-by-layer approach for the fabrication of conducting polymer/RNA multilayer films for controlled release. *Langmiur* **22** 2811–2815.

(25) Kobayashi S., Hiroishi K., Tokunoh M., Saegusa T. (1987) Chelating properties of linear and branched poly(ethylenimines). *Macromolecules* **20** 1496–1500.

Chapter 5

Prolonged durability of electroporation microarrays by saccharide addition to nucleic acids

INTRODUCTION

Microarrays capable of transferring multiple nucleic acids in parallel have been developed as high-throughput analytical tools for conducting gain-of-function study using expression constructs (1–4) or loss-of-function study using small interfering RNAs (siRNAs) (5, 6, Chapters 1 and 2). Several research groups reported the results of feasibility studies using transfection microarrays (7, 8, 9), most of which demonstrated the profound potential of this technology in functional genomics research.

The usefulness of transfection microarrays greatly relies on the efficiency of transfection. To enhance the efficiency, cationic lipids have been utilized as complexes with nucleic acids (1). Other systems with much higher efficiency employ electric pulses to trigger the release of nucleic acids from an array and their translocation into cells (3, 4, Chapter 3). These methods enable to transfer nucleic acids into cells to a reasonable level for functional studies. However, transfection efficiency is considerably reduced during the storage of microarrays. This underlines the needs for appropriate methods to store microarrays. Such methods will be critically important especially for distributing microarrays as commercial products.

It is assumed that the major cause of reduction in transfection efficiency is the desiccation of nucleic acids complexed with cationic polymers. To address this desiccation problem, experiments were carried out in this chapter to examine the effects of various saccharides and sugar alcohols added to plasmid DNA. Trehalose (saccharides) and glycerol (sugar alcohol) have been widely used as excellent moisture retention agents. This is due to hydroxyl groups that strongly interact with water molecules via hydrogen bonding (10–13). In this chapter, plasmid DNA was mixed with various saccharides and sugar alcohols with different structures and molecular sizes and then arrayed onto a cationically-modified electrode. These compositions were screened for their potential to preserve the efficiency of electric pulse-triggered transfection after the storage of microarrays under various conditions. Similar experiments were further carried out to study the effect of saccharides and sugar alcohols for the durability of siRNA-loaded microarrays.

EXPERIMENTAL

Nucleic acids and chemicals

Plasmid DNA used was pEGFP (pEGFP-C1, Clontech, Palo Alto, CA, U.S.A.) which encoded enhanced green fluorescent protein (EGFP). siRNAs were purchased from Qiagen. GFP-siRNA (sense; 5'-GCAAGCUGACCCUGAAGUUCAU-3', antisense; 5'-GAACUUCAGGGUCAGCUUGCCG-3') was designed for silencing EGFP gene, while control siRNA (sense; 5'-UUCUCCGAACGUGUCACGUdTdT-3', antisense; 5'-

ACGUGACACGUUCGGAGAAdTdT-3') had no silencing effect. Saccharides and sugar alcohols including monosaccharides (glucose and fructose), disaccharides (trehalose and sucrose), and trisaccharide (raffinose) were purchased from Wako Pure Chemical Industries, Osaka, Japan. Glycerol was purchased from Nacalai Tesque, Kyoto, Japan. Poly(ethyleneimine) (PEI, average molecular weight = 2000) and 11-mercaptoundecanoic acid were purchased from Aldrich.

Cell culture

Human embryonic kidney cell line HEK293 was obtained from Health Science Research Resources Bank, Osaka, Japan. As demonstrated in Chapter 3, d2EGFP-HEK that stably expressed a destabilized green fluorescent protein was generated by transforming HEK293 with pd2EGFP-C1 (Clontech, Palo Alto, CA) followed by cloning in a medium containing 500 μg/mL G418. These cells were routinely maintained in a minimal essential medium (MEM, Invitrogen, Carlsbad, CA) supplemented with 10% fetal bovine serum (FBS), 100 U/mL penicillin, and 100 μg/mL streptomycin at 37 °C under 5% CO_2 atmosphere.

Surface plasmon resonance (SPR) analysis

To analyze the adsorption of plasmid DNA onto an electrode, a SPR instrument was used as before (14). A glass-based gold electrode bearing a self-assembled monolayer of 11-mercaptoundecanoic acid (COOH-SAM) on the surface was mounted onto a triangular prism with a flow cell. Then, phosphate buffered saline (PBS, pH 7.4) containing 10

mg/mL PEI was circulated over the COOH-SAM at 30 °C for 1 h followed by circulation of PBS containing 5 μg/mL plasmid DNA with (0.1–10%, w/v) or without additives. During these procedures, light reflectance was continuously monitored at a constant incident angle 0.5 degree smaller than the resonance angle of the COOH-SAM. Finally the observed reflectance was converted to the shift of the resonance angle.

Preparation and storage of microarrays

All procedures including the preparation of a gold electrode, the formation of a self-assembled monolayer (SAM), and the adsorption of PEI onto the SAM were performed as reported before (3, 4). In brief, thin layers of chromium (thickness: 1 nm) and gold (thickness: 49 nm) were sequentially deposited onto a cleaned glass plate (BK7, 25 mm × 25 mm × 1 mm, Arteglass Associates, Kyoto, Japan). The plate was immersed in 1 mM 11-mercaptoundecanoic acid solution in ethanol at room temperature for 24 h to form a carboxylic acid-terminated SAM (COOH-SAM) on gold. The gold electrode bearing COOH-SAM was exposed to 1% (w/v) PEI solution in PBS (pH 7.4) at room temperature for 30 min to ionically adsorb PEI onto the electrode. The electrode was washed with water to remove weakly adsorbed PEI and then dried. The solutions of plasmid DNA or siRNA were spotted using a SPRinter® microarrayer (Toyobo, Osaka, Japan). This apparatus was equipped with a spotting pin (diameter: 500 μm) for dispensing a droplet (~10 nL) of aqueous solution in a 96-spot format within the area of 1.2 cm × 0.8 cm of flat substrates. The spotted solutions contained 50 μg/mL nucleic acids (pEGFP-C1, GFP-siRNA, or control-siRNA) and 0–10% (w/v) additives. Spotting was carried out at 60–80% relative

humidity and room temperature. The time required for preparing a single microarray was different depending on array design and multiplicity but in the most typical case approximately 1 h. The nucleic acid-loaded electrodes were stored at –20, 4, or 25 °C for 7, 30, or 180 days in sealed polystyrene containers.

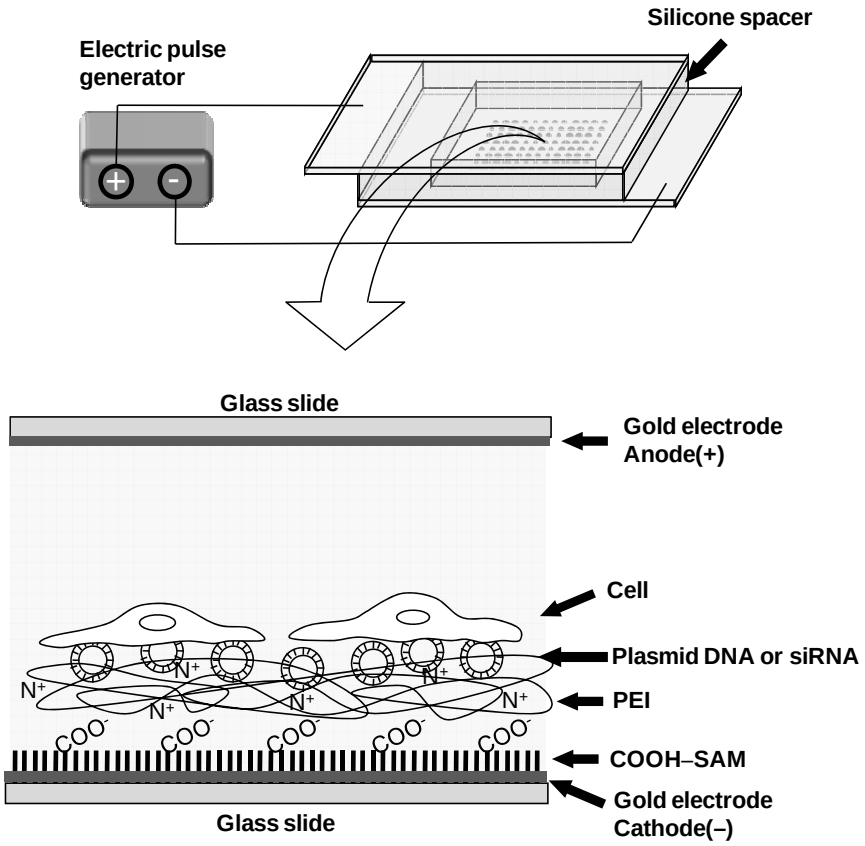

Scheme 1. Schematic drawings for the electroporation setup. Drawings are not to scale.

Electroporation

Electroporation was performed as reported before (3, 4) using an experimental setup shown in Scheme 1. In brief, a sterilized silicone frame of 0.5 mm in thickness was

attached to the electrode to restrict cell culture region and keep distance between electrodes. The nucleic acid-loaded electrode was washed with PBS followed by plating HEK293 or d2EGFP-HEK cells within the frame at a density of 45,000 cells/cm^2. The cells were cultured for 24 h to attach them to the electrode. After washing the electrode with PBS to eliminate non-adhering cells, the silicone frame was filled with cold PBS, and a counter electrode (a glass plate bearing a 199 nm-thick gold layer on one side) was placed on the silicone frame. Both electrodes were connected to a pulse generator (Gene Pulser Xcell, BioRad, Hercules, CA). Then, cells were treated with a single electric pulse at the field strengths of 260 V/cm for a duration of 10 msec. After pulsing and subsequent incubation for 5 min at room temperature, PBS was replaced with MEM containing 10% FBS, 100 U/mL penicillin, and 100 μg/mL streptomycin, and the cells were further cultured. At 48 h after electroporation, a fluorescent image of the entire microarray was acquired using a fluorescence stereomicroscope (Leica MZ FLIII, Solms, Germany) equipped with a cooled CCD camera (ORCA-ER, Hamamatsu Photonics Hamamatsu, Japan). A fluorescent intensity was measured for every spot using an AQUA-Lite digital imaging software (Hamamatsu Photonics).

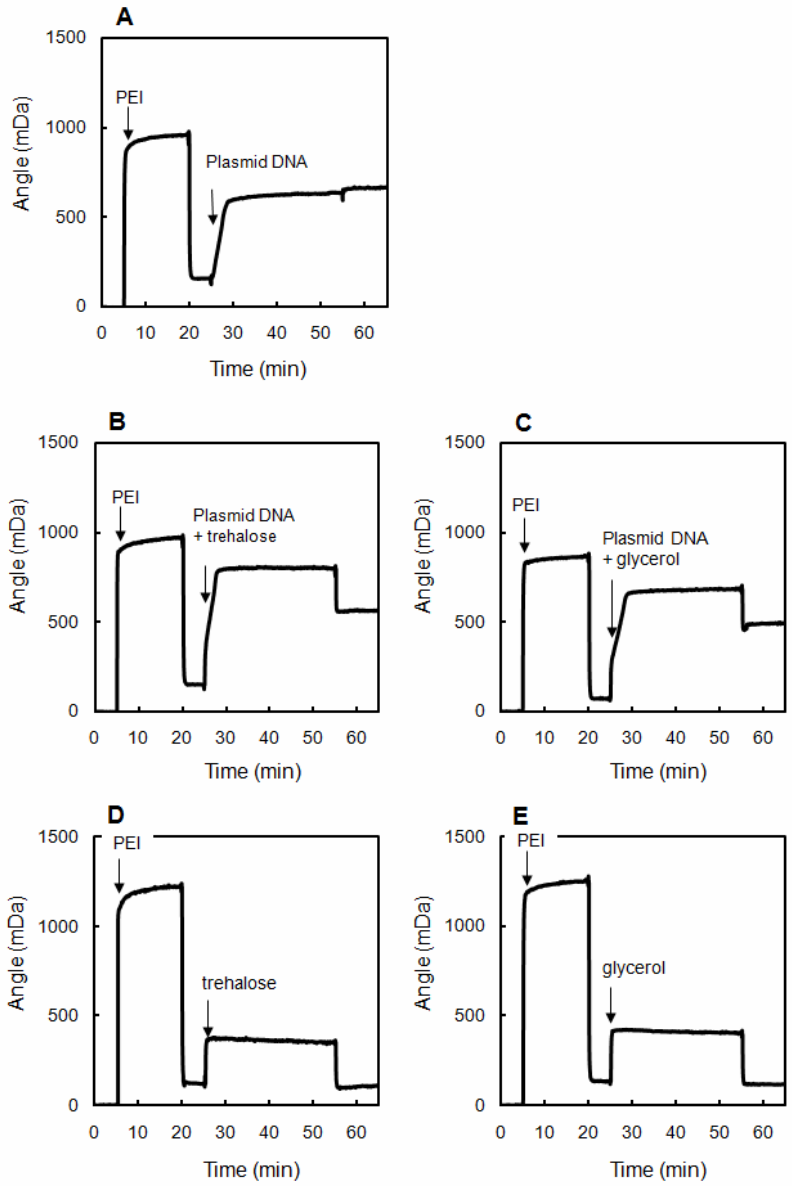

Figure 1. SPR sensorgrams recorded during the exposure of COOH-SAM to PEI solution and subsequent exposure to the solution of plasmid DNA with or without additives. (A) DNA alone, (B) trehalose with DNA, (C) glycerol with DNA, (D) trehalose alone, and (E) glycerol alone. [PEI], [glycerol], and [trehalose] = 10 mg/mL, [DNA] = (A–C) 5 μg/mL, (D and E) 0 μg/mL.

RESULTS

Adsorption of plasmid in the presence of additives

Figure 1 A shows an SPR sensorgram obtained during the adsorption of PEI onto a COOH-SAM followed by adsorption of plasmid DNA to the PEI-adsorbed SAM. The shift of the resonance angle (ca. 100 mDA) was observed by exposing the COOH-SAM to a PEI solution. Subsequent exposure to a plasmid solution resulted in the further sift of the resonance angle (ca. 400 mDA). The observed angular shifts indicate the adsorption of PEI and DNA.

The effect of additives on the adsorption of plasmid was also studied by SPR analysis. The representative data are shown in Figure 1 B–E for the case with glycerol and trehalose. The addition of these additives to DNA solution gave rise to similar angular shifts to that observed for the control experiment just described (Fig. 1 B and C). As shown in Figure 1 D and E, no angular shit was observed when a single solution of these additives was used, suggesting that these additives do not interfere with DNA adsorption onto the PEI-adsorbed SAM. A similar result was obtained in the case of ethylene glycol (Fig. 2).

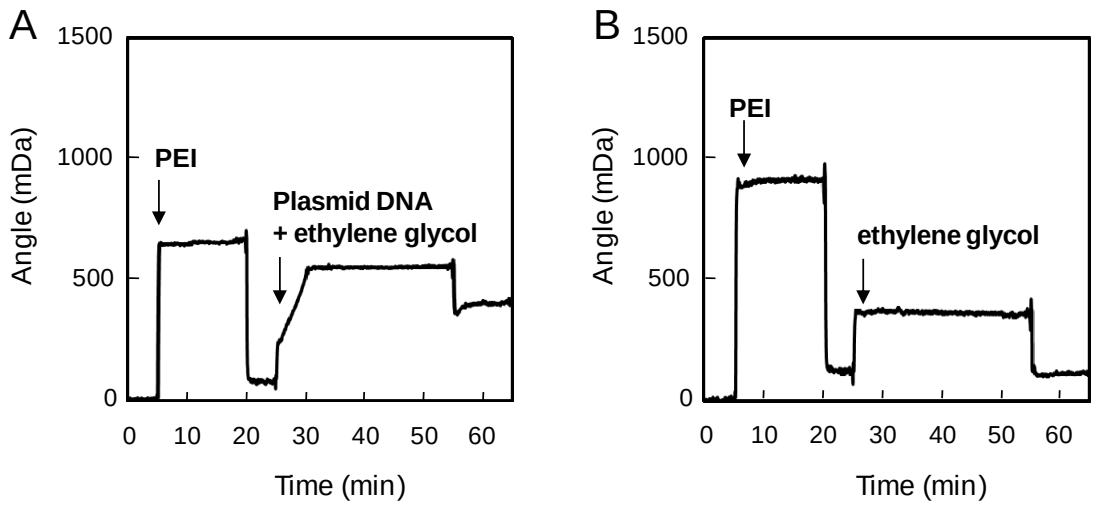

Figure 2. SPR sensorgrams recorded during the exposure of the COOH-SAM surface to PEI solution and subsequent exposure to the solution of ethylene glycol (A) with and (B) without plasmid DNA. [PEI], [ethylene glycol] = 10 mg/mL. [DNA] = (A) 5 μg/mL, (B) 0 μg/mL.

Effects of additives on the durability of plasmid-loaded microarrays

It was observed that, without additives, the solution of plasmid DNA dried up on the substrate immediately after spotting. On the other hand, the addition of additives served to prevent desiccation of plasmid solution during spotting. During storage at 4 and –20 °C, all droplets containing additives maintained their size during 30-day storage. However, at 25 ^{o}C, the droplets containing glycerol or ethylene glycol were totally desiccated during 30-day storage. Other additives including glucose, fructose, trehalose, sucrose, and raffinose markedly prolonged the time before total desiccation at 25 °C.

A

—	Glu0.1	Glu1.0	Glu10	—	Fru0.1	Fru1.0	Fru10	—	Tre0.1	Tre1.0	Tre10
—	Suc0.1	Suc1.0	Suc10	—	Raf0.1	Raf1.0	Raf10	—	Gly0.1	Gly1.0	Gly10
Tre0.1	Tre1.0	Tre10	—	Glu0.1	Glu1.0	Glu10	—	Fru0.1	Fru1.0	Fru10	—
Gly0.1	Gly1.0	Gly10	—	Suc0.1	Suc1.0	Suc10	—	Raf0.1	Raf1.0	Raf10	—
Fru1.0	Fru10	—	Tre0.1	Tre1.0	Tre10	—	Glu0.1	Glu1.0	Glu10	—	Fru0.1
Raf1.0	Raf10	—	Gly0.1	Gly1.0	Gly10	—	Suc0.1	Suc1.0	Suc10	—	Raf0.1
Glu10	—	Fru0.1	Fru1.0	Fru10	—	Tre0.1	Tre1.0	Tre10	—	Glu0.1	Glu1.0
Suc10	—	Raf0.1	Raf1.0	Raf10	—	Gly0.1	Gly1.0	Gly10	—	Suc0.1	Suc1.0

B

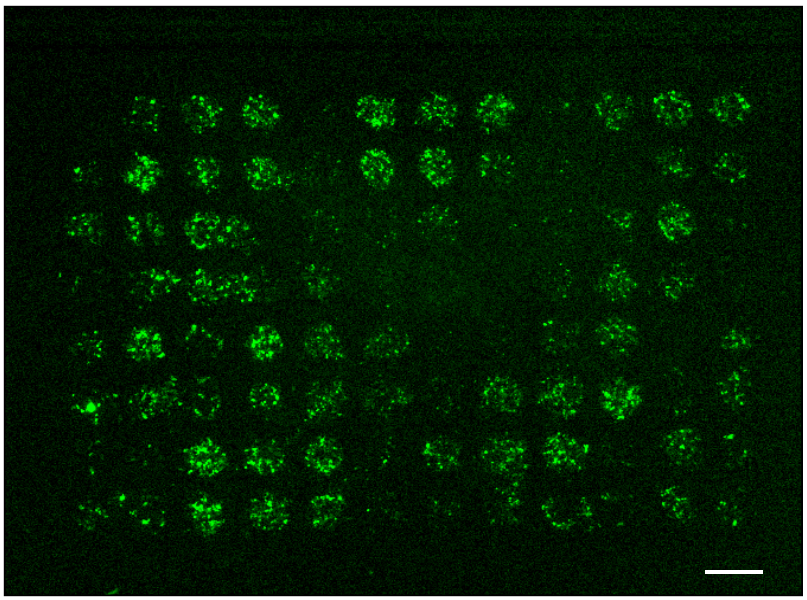

Figure 3. Electroporation of plasmid DNA into cells on a microarray. The microarray was used immediately after preparation without storage. (A) Identification of spots. Glu; glucose, Fru; fructose, Tre; trehalose, Suc; sucrose, Raf; raffinose, Gly; glycerol. Numbers following the abbreviations represent the concentration of additives (w/v). Bars (—) represents no additives. (B) Fluorescent image of cells electroporated on the microarray. Cells were seeded to an entire electrode within the silicone frame immediately after microarray preparation. An electric pulse was applied to cells 24 h after seeding. Cells were imaged 48 hr after electroporation (i.e. 72 hr after seeding). Bar: 1 mm.

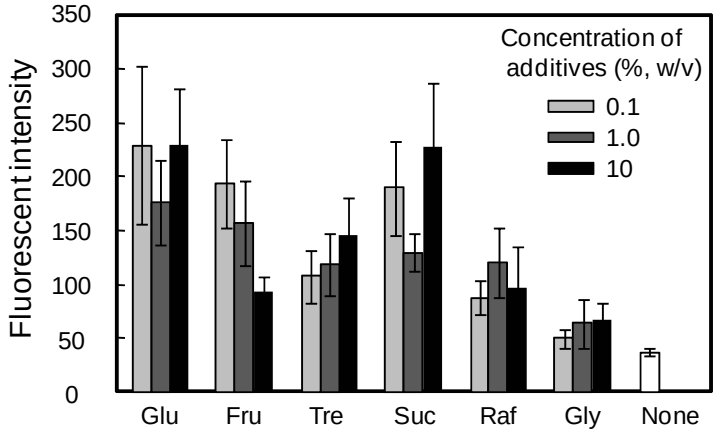

Figure 4. Quantitative evaluation of EGFP expressed in cells electroporated on a microarray. Cells were seeded immediately after microarray preparation. An electric pulse was applied to the cells 24 h after seeding. The cells were imaged after additional culture for 48 h. Glu; glucose, Fru; fructose, Tre; trehalose, Suc; sucrose, Raf; raffinose, Gly; glycerol, None; no additives. Data are expressed as mean ± standard error of the mean (n = 4).

Figure 3 shows the low magnification fluorescent image of HEK293 cells transfected on the microarray on which pEGFP was loaded with various additives in a 96-spot format. Cells were seeded to the microarray immediately after preparation without storage periods. As can be seen, EGFP was expressed to different levels depending on the spot identities. Fluorescent intensities determined for each condition are shown in Figure 4. It is seen that fluorescent intensity is significantly higher on the spots with saccharides than on those

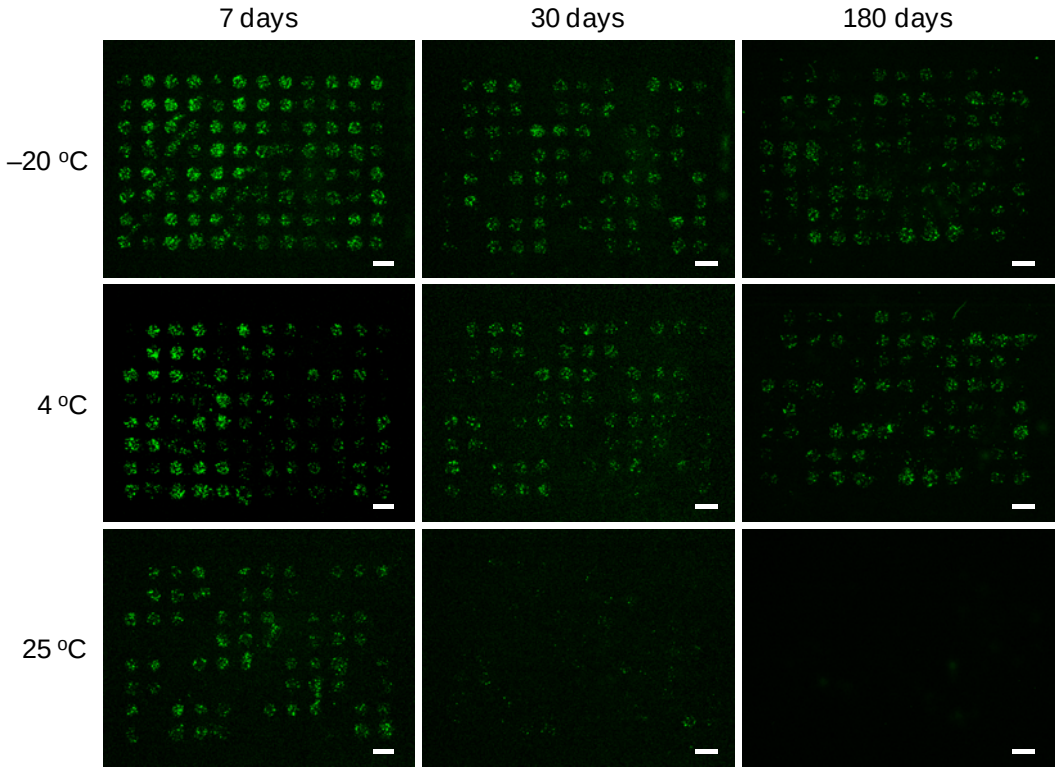

Figure 5. Fluorescent images of cells electroporated on microarrays. Microarrays were stored under various conditions, and then cells were seeded to the microarray. The identification of spots is the same as in Figure 3. Bars: 1 mm.

without additives. These results indicate that the addition of the saccharides significantly improved the efficiency of EGFP expression. In many cases, but not all, the effects of saccharides are enhanced with an increasing concentration of these additives. On the other hand, the addition of glycerol had insignificant effects on transfection efficiency compared to the control spots without additives.

Electroporation was performed after storage at various temperatures (–20, 4, or 25 °C) for different time periods (7, 30, or 180 days). Though saccharides or sugar alcohol were added to plasmid solutions, the pulsing conditions optimized in Chapter 3 for conventional transfection microarrays without additives was adopted here. According to the results of SPR analysis (Fig. 1), it is expected that, by washing the microarray with PBS prior to cell seeding, these additives are removed from the spots, leaving plasmid-loaded spots similar to those on previous microarrays prepared without additives. In fact, cells adhered well on every spot on the microarrays, with no sign of adverse effects caused by residual additives.

Figure 5 shows the fluorescent images of microarrays acquired 48 h after electroporation. Generally, storage at higher temperature and/or for longer periods resulted in much more attenuation in EGFP expression. Figure 6 shows fluorescent intensities determined for every condition. Data are not shown for storage at 25 °C for 30 and 180 days because EGFP expression was hardly detected on all the spots. Under any other storage conditions, the lowest expression of EGFP was observed on the spots with plasmid alone among the spots on the microarray. It is seen that EGFP is most efficiently expressed on the spots with monosaccharides (glucose, fructose), disaccharides (trehalose, sucrose) and trisaccharide (raffinose), indicating the promotive effect of these additives. In contrast, glycerol (sugar alcohol) exhibited no effects on transfection efficiency. As shown in Figure 7, the promotive effect was observed with other saccharides (galactose, maltose, and lactose), while moderate or less effects were seen with sugar alcohols (sorbitole, ethylene glycol), polysaccharide (dextran), and polypeptide (gelatin). In many cases, the promotive

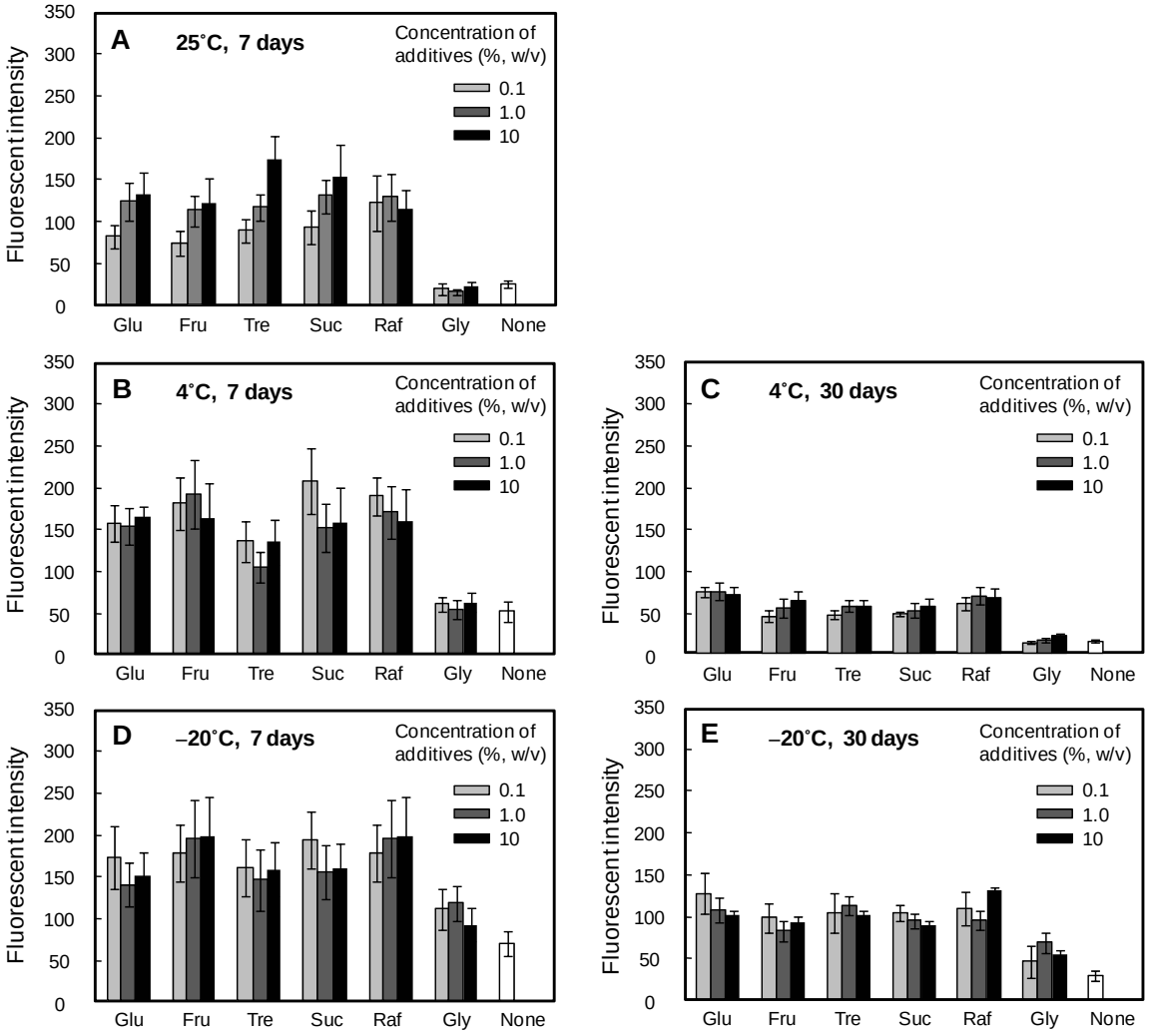

Figure 6. Quantitative evaluation of EGFP expressed in cells electroporated on the microarrays. Microarrays were stored (A) at 25 °C for 7 days, 4 °C for (B) 7 or (C) 30 days, and –20°C for (D) 7 or (E) 30 days. Glu; glucose, Fru; fructose, Tre; trehalose, Suc; sucrose, Raf; raffinose, Gly; glycerol, None; no additives. Data are expressed as mean ± standard error of the mean (n = 6).

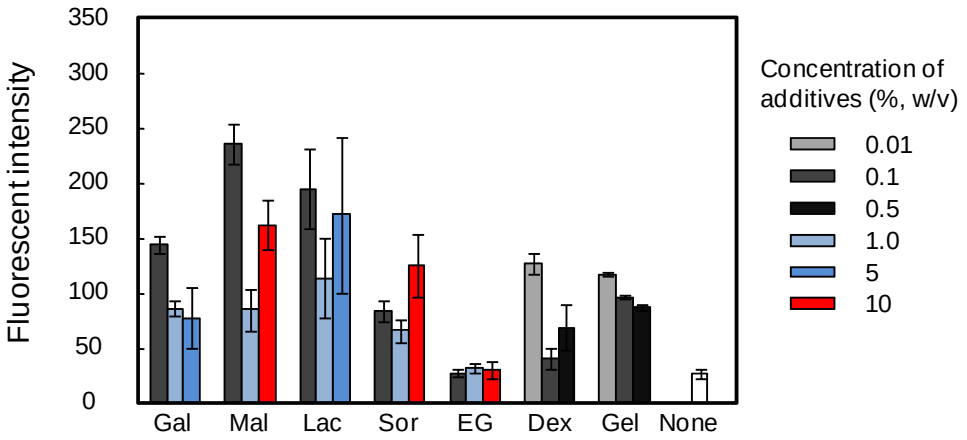

Figure 7. Quantitative evaluation of EGFP expression in cells electroporated on plasmid DNA-loaded microarrays. Microarrays were stored at 25 °C for 7 days. Gal; galactose, Mal; maltose, Lac; Lactose, Sor; sorbitole, EG; ethylene glycol, Dex; dextran, Gel; gelatin, None; no additives. Data are expressed as mean ± standard error of the mean (n = 6).

effect was enhanced with an increasing concentration of additives, though these differences were statistically insignificant.

Effects of additives on the durability of siRNA-loaded microarrays

siRNA-loaded microarrays were prepared by a similar fashion as for plasmid-loaded microarrays. The microarrays were stored at 25 °C for 7 days prior to cell seeding. To investigate the efficiency of gene silencing, HEK293 cells stably expressing EGFP (d2EGFP-HEK) were electroporated on the microarray. Figure 8 shows a fluorescent image acquired 48 h after electroporation. Silencing efficiency can be defined as a ratio of EGFP

A

— GFP	— Control	Glu GFP	Glu Control	Fru GFP	Fru Control	Suc GFP	Suc Control	Tre GFP	Tre Control	Gly GFP	Gly Control
Gly Control	— GFP	— Control	Glu GFP	Glu Control	Fru GFP	Fru Control	Suc GFP	Suc Control	Tre GFP	Tre Control	Gly GFP
Gly GFP	Gly Control	— GFP	— Control	Glu GFP	Glu Control	Fru GFP	Fru Control	Suc GFP	Suc Control	Tre GFP	Tre Control
Tre Control	Gly GFP	Gly Control	— GFP	— Control	Glu GFP	Glu Control	Fru GFP	Fru Control	Suc GFP	Suc Control	Tre GFP
Tre GFP	Tre Control	Gly GFP	Gly Control	— GFP	— Control	Glu GFP	Glu Control	Fru GFP	Fru Control	Suc GFP	Suc Control
Suc Control	Tre GFP	Tre Control	Gly GFP	Gly Control	— GFP	— Control	Glu GFP	Glu Control	Fru GFP	Fru Control	Suc GFP
Suc GFP	Suc Control	Tre GFP	Tre Control	Gly GFP	Gly Control	— GFP	— Control	Glu GFP	Glu Control	Fru GFP	Fru Control
Fru Control	Suc GFP	Suc Control	Tre GFP	Tre Control	Gly GFP	Gly Control	— GFP	— Control	Glu GFP	Glu Control	Fru GFP

B

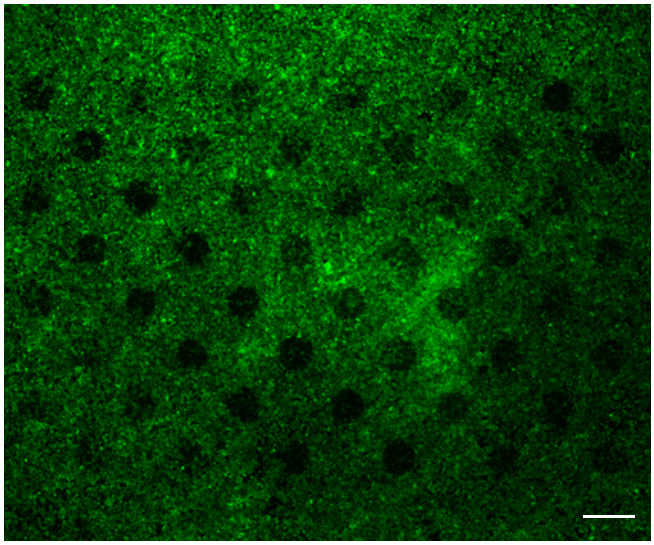

C

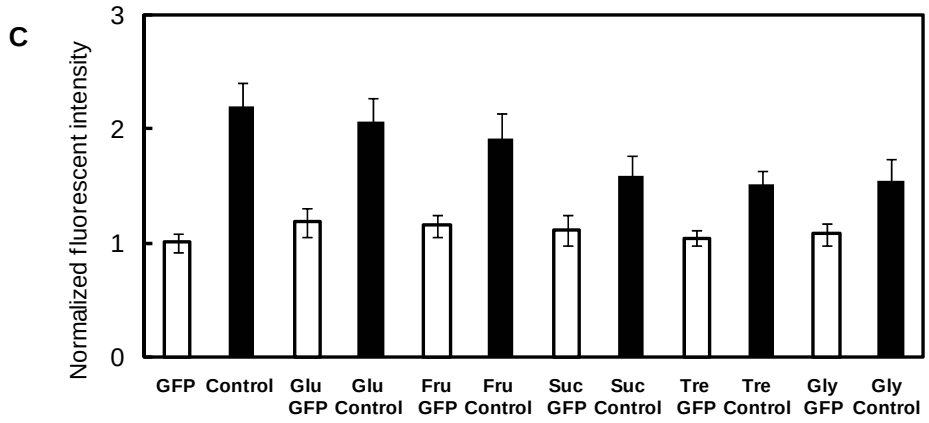

expression on the spots with EGFP-siRNA to that on the spots with control-siRNA. Strikingly, even after storage at 25 °C for 7 days, silencing efficiency was almost similar between conditions. This result indicates that the additives have no positive effects on the preservation of transfection efficiency.

DISCUSSION

It is assumed that the reduction in transfection efficiency during the storage of microarrays is caused by the evaporation of water from spotted droplets. As a result, polyelectrolyte complexes formed at surface between plasmid DNA and PEI seem to reduce their solubility. This is similar to the phenomenon that water soluble polyelectrolyte complexes occasionally turn to be insoluble upon desiccation (15). Because transformation of cells requires detachment of DNA and/or DNA/PEI complex from the microarray surface upon electric pulsing, insolubility of the complexes would reduce their availability for cells

---

Figure 8. The effect of additives on the silencing of EGFP expression by siRNA electroporated on the microarray that had been stored at 25 °C for 7 days. (A) Identification of spots. Glu; glucose, Fru; fructose, Tre; trehalose, Suc; sucrose, Raf; raffinose, Gly; glycerol, GFP; GFP-siRNA, and Control; control-siRNA. The concentration of additives was 10 % (w/v). Data are expressed as mean ± standard error of the mean (n = 16). (B) Fluorescent images of the microarray. Bar: 1 mm. (C) Quantitative evaluation of EGFP expression in cells electroporated on microarrays. Data were normalized by the result for

the spot on which GFP-siRNA was electroporated without additives. Data are expressed as mean ± standard error of the mean (n = 16).

and hence transfection efficiency (3). It may be unlikely that desiccation affects the structural integrity of plasmid DNA, since, in recombinant DNA technology, plasmids are frequently dried up in the course of purification with no adverse effects on transfection efficiency (16). Storage at low temperature might also had a promotive effect on the preservation of transfection efficiency by minimizing nuclease degradation of loaded DNA.

It was observed that the addition of saccharides and sugar alcohols to plasmid solution reduced the rate of desiccation. This is due to the effect that these compounds interact with water molecules via hydrogen bonding (10–13,17), elevating the enthalpy of water evaporation (18–20). Therefore, the droplets of plasmid solution containing saccharides and sugar alcohols remain their moisture contents for longer periods than those containing no additives. It was shown that transfection efficiency was improved by reducing storage temperature and/or periods. This can also be explained by the moisture contents remaining high in the droplets. Presumably, the observed difference in the effects between various additives is dependent on their potential to interact with water molecules. It is demonstrated here that monosaccharides such as glucose and fructose and disaccharides such as trehalose and sucrose are the most potent additives for the prolonged durability of plasmid-loaded microarrays.

The peculiar effect was observed when saccharides and sugar alcohol were used in the preparation of siRNA-loaded microarrays. These additives have no effect on the preservation of transfection efficiency, suggesting that the water evaporation from siRNA solution has minor affects on electroporation. Because siRNA consists of short nucleotides

(22 residues in the case of EGFP-siRNA), siRNA might remain sufficiently soluble even after desiccation on microarrays and might be easily detached from the surface upon electric pulsing.

It may be concluded that, when added to plasmid DNA solution, saccharides and sugar alcohols serve to reduce the rate of water evaporation from the droplets of plasmid solution during microarray preparation and its storage. As a result, the durability of plasmid-loaded microarrays is significantly prolonged. However, this effect is dependent on the type of additives. Monosaccharides and disaccharides provide most excellent results in regard to transfection efficiency after storage of microarrays. With these additives, microarrays could be stored for up to 30 days at –20 °C with no considerable reduction in transfection efficiency. In contrast, the addition of saccharides and sugar alcohols has no positive effects on the preservation of transfection efficiency during storage of siRNA-loaded microarrays.

References

(1) Ziauddin J., Sabatini DM. (2001) Microarrays of cells expressing defined cDNAs. *Nature* **411** 107–110.

(2) Yamauchi F., Kato K., Iwata H. (2004) Micropatterned, self-assembled monolayers for fabrication of transfected cell microarrays. *Biochem. Biophys. Acta* **1672** 138–147.

(3) Yamauchi, F., Kato, K., Iwata, H. (2004) Spatially and temporally controlled gene transfer by electroporation into adherent cells on plasmid DNA-loaded electrodes. *Nucleic Acids Res.* **32** e187.

(4) Inoue, Y., Fujimoto, H., Ogino, T., Iwata, H. (2008) Site-specific gene transfer with high efficiency onto a carbon nanotube-loaded electrode. *J. R. Soc. Interface* **5** 909–918.

(5) Mousses, S., Caplen, N., Cornelison, R., Weaver, D., Basik, M., Hautaniemi, S., Elkahloun, AG., Lotufo, RA., Choudary, ER., Suh, E., and Kallioniemi, O. (2003) RNAi microarray analysis in cultureed mammalian cells. *Genome Res.* **13** 2341–2347.

(6) Kumar R., Conklin DS., Mittal V. (2004) High-throughput selection of effective RNAi probes for gene silencing. *Gemone Res.* **13** 2333–2340.

(7) Mannherz, O., Mertens, D., Hahn, M., Lichter, P. (2006) Functional screening for proapoptotic genes by reverse transfection cell array technology. *Genomics* **87** 665–672.

(8) Yamauchi, F., Okada, M., Kato, K., Jakt, LM., Iwata, H. (2007) Array-based functional screening for genes that regulate vascular endothelial differentiation of Flk-1-

positive progenitors derived from embryonic stem cells. *Biochim. Biophys. Acta.* **1770** 1085–1097.

(9) Fiebitz, A., Nyarsik, L., Haendler, B., Hu, YH, Wagner, F., Thamm, S., Lehrach, H., Janitz, M., Vanhecke, D. (2008) High-throughput mammalian two-hybrid screening for protein-protein interactions using transfected cell arrays. *BMC Genomics* **9** 68.

(10) Kawai, H., Sakurai, M., Inoue, Y., Chujo, R., Kobayashi, S. (1992) Hydration of oligosaccharides: Anomalous hydration ability of trehalose. *Cryobiology* **29** 599–606.

(11) Uedaira, H., Ishimura, M., Tsuda, S., Uedaira, H. (1990) Hydration of oligosaccharides. *Bull. Chem. Soc. Jpn.* **63** 3376–3379.

(12) Dashnau, JL., Nucci, NV., Sharp, KA., Vanderkooi, JM. (2006) Hydrogen bonding and the cryoprotective properties of glycerol/water mixtures. *J. Phys. Chem. B* **110** 13670–13677.

(13) Brady, JW., Schmidt, RK. (1993) The role of hydrogen bonding in carbohydrates: Molecular dynamics simulations of maltose in aqueous solution. *J. Phys. Chem.* **97** 958–966.

(14) Hirata, I., Morimoto, Y., Murakami, Y., Iwata, H., Kitano, E., Kitamura, H., Ikada, Y. (2000) Study of complement activation on well-defined surfaces using surface plasmon resonance. *Colloid. Surf. B Biointerf.* **18** 285–292.

(15) Anchordoquy, TJ., Girouard, LG., Carpenter, JF., Kroll, DJ. (1998) Stability of lipid/DNA complexes during agitation and freeze-thawing. *J. Pharm. Sci.* **87** 1046-1051.

(16) Sambrook, J., Fritsch, EF., Maniatis, T. (1989) Molecular Cloning A laboratory manual, second edition. Book. 1,chapter 1., Cold Spring Harbor Laboratory Press: New York.

(17) Molinero, V., Cagin, T., Goddard, WA. (2003) Sugar, water and free volume networks in concentrated sucrose solution. *Chem. Phys. Lett.* **377** 469–474.

(18) Yamamoto, S., Morihiro, T., Ariyoshi, K, Aktas, T. (2005) Effects of surface concentration on drying behavior of carbohydrate solutions. *Drying Technology* **23** 1319–1330.

(19) Potts, M. (1994) Desiccation tolerance of prokaryotes. *Microbiol. Rev.* **58** 755–804.

(20) McQuain, MK., Seale, K., Peek, J., Levy, S., Haselton, FR. (2003) Effects of relative humidity and buffer additives on the contact printing of microarrays by quill pins. *Anal. Biochem.* **320** 281–291.

SUMMARY

Chapter 1

The emergence of small interfering RNA (siRNA) opened a new opportunity to study gene functions in a genome wide. However, large-scale loss-of-function analyses further require cell-based high-throughput methods that allow simultaneous silencing of the huge number of genes by siRNA. In this chapter, the aim is to fabricate the cell-based siRNA arrays that facilitate parallel introduction of multiple siRNAs into cultured mammalian cells. The siRNA arrays were prepared using surface chemical processes including the micropatterning of a self-assembled monolayer and the layer-by-layer assembly of siRNA and cationic lipid. This chapter examined the feasibility of the siRNA array for the sequence-specific gene silencing in an array format. Furthermore, the effects of siRNA loading and culture period after transfection were studied to optimize cell-based assays on the siRNA arrays. The results obtained in this study demonstrated that our method provides the siRNA arrays with spatial specificity in gene silencing, which will serve to obtain a quantitative data set from the cell-based screens on siRNA arrays.

Chapter 2

Transfection cell arrays provide promising methods for the high-throughput analysis of gene functions. Such analysis is efficiently performed by using small interfering RNA (siRNA). To extend the usefulness of microarrays, this study was devoted to implement siRNA prepared from complementary DNA (cDNA). The preparation of siRNA involves the transcription of cDNA to generate double-stranded RNA followed by digestion with

endoribonuclease, dicer, by which one can obtain the library of siRNAs without target sequence optimization. In this chapter, endoribonuclease digested siRNA (d-siRNA) was prepared using cDNA encoding enhanced green fluorescent protein (EGFP), and loaded to micropatterned substrates through electrostatic interactions of siRNA complex with substrates. Chapter 1 was observed that d-siRNA loading was comparable to the case with siRNA prepared by chemical synthesis. When co-transfected with EGFP plasmid into HEK293 cells on a microarray, d-siRNA suppressed EGFP expression in a loading dependent manner. In addition, d-siRNA triggered gene silencing at a level similar to chemically synthesized siRNA. The similarity between the two types of siRNAs regarding silencing efficiency suggests that heterogeneity in nucleotide sequences of d-siRNA has minor effects. From these results, this chapter concludes that the combination of d-siRNA with the array technology provides much useful tools for high-throughput screening of gene functions.

Chapter 3

This chapter describes the fabrication of microarrays that enable the parallel electroporation of small interfering RNAs (siRNAs) into mammalian cells. To optimize the conditions of microarray preparation and electric pulsing, a self-assembled monolayer was formed on a gold electrode, and a cationic polymer was adsorbed to the entire surface of the monolayer. Then, siRNA was adsorbed by the cationically-modified electrode through electrostatic interactions. Human embryonic kidney cells stably transformed with the expression construct of green fluorescent protein (GFP) were used to examine the electric pulse-triggered transfer of GFP-specific siRNA. A single electric pulse was applied to the

cells cultured on the electrode at a field strength of 240 V/cm. The expression of GFP was significantly suppressed in a sequence-specific manner two days after pulsing. Microscopic observation and flow cytometric analysis revealed that the expression of GFP was attenuated in the majority of cells in a loading-dependent manner. Moreover, the effect of siRNA could be temporally controlled by changing the culture periods before pulsing. When a micropatterned self-assembled monolayer was used as a platform for loading siRNA in an array format, gene silencing was spatially restricted to the regions where specific siRNA was loaded. From these results, this chapter concludes that array-based electroporation provides an excellent means of individual transfer of siRNAs into mammalian cells for high-throughput gene function studies.

Chapter 4

Electroporation microarrays have been developed for the high-throughput transfection of expression constructs and small interfering RNAs (siRNAs) into living mammalian cells. These techniques have potential to provide a platform for the cell-based analysis of gene functions. One of the key issues associated with the microarray technology is an efficiency of transfection. The capability of attaining reasonably-high transfection efficiency is the basis for obtaining functional data without false negative. This chapter aimed at improving the transfection efficiency in the system that siRNA loaded on an electrode is electroporated into cells cultured directly on the electrode. The strategy adapted here is to increase the surface density of siRNA loaded onto electrodes. For this purpose, the layer-by-layer assembly of siRNA and cationic polymers, branched or linear form of poly(ethyleneimine), was performed. The multilayer thus obtained was characterized by

infrared reflection adsorption spectroscopy and surface plasmon resonance analysis. Transfection efficiency was evaluated in a system that siRNA specific for enhanced green fluorescent protein (EGFP) was electroporated on the electrode into human embryonic kidney cells stably transformed with the EGFP gene. The suppression of EGFP expression was assessed by fluorescence microscopy and flow cytometry. These data showed that the layer-by-layer assembly of siRNA with branched poly(ethyleneimine) facilitated to increase the surface density of loaded siRNA. As a result, the expression of EGFP gene in the electroporated cells was suppressed much more on the electrodes with the multilayer of siRNA than that with the monolayer.

Chapter 5

Electroporation microarray is a useful tool for the high-throughput analysis of gene functions. However, transfection efficiency is greatly impaired by the storage of microarrays due to water evaporation from arrayed nucleotides. This chapter aimed at evaluating the effect of saccharides and sugar alcohols added to the solution of plasmid DNA or small interfering RNA (siRNA). Microarrays loaded with plasmids and siRNAs were prepared with various polyols including sugars and sugar alcohols. After storage of these microarrays at different temperatures for various time periods, transfection efficiency was evaluated using human embryonic kidney cells. In the case of plasmid-loaded microarrays, the addition of monosaccharides (glucose, fructose), disaccharides (trehalose, sucrose), and trisaccharide (raffinose) served to retain transfection efficiency at a reasonably high level after storage at –20 °C. The observed effects may be explained from the fact that moisture retention serves to maintain the solubility of DNA. In contrast,

polysaccharide (dextran) and sugar alcohol (glycerol) showed insignificant effects on the retention of transfection efficiency. On the other hand, the addition of saccharides and sugar alcohols had insignificant effects on the transfection of siRNA after storage of a microarray at 25 °C for 7 days, presumably due to the intrinsically-high solubility of siRNA consisting of short nucleotides.

LIST OF PUBLICATIONS

Chapter 1. H. Fujimoto, S. Yosihzako, K. Kato, and H. Iwata

"Fabrication of cell-based arrays using micropatterned aklanethiol monolayers for the parallel silencing of specific genes by small interfering RNA"

Bioconj. Chem., **17**, 1404–1410 (2006).

Chapter 2. H. Fujimoto, K. Kato, and H. Iwata

"Use of microarrays in transfection of mammalian cells with dicer-digested small interfering RNAs"

Anal. Biochem., **374**, 417–422 (2008).

Chapter 3. H. Fujimoto, K. Kato, and H. Iwata

"Electroporation microarray for parallel transfer of small interfering RNA into mammalian cells"

Anal. Bioanal. Chem. In press

Chapter 4. H. Fujimoto, K. Kato, and H. Iwata

"Layer-by-layer assembly of small interfering RNA and poly(ethyleneimine) for substrate-mediated electroporation with high efficiency"

Langmuir Submitted.

Chapter 5. H. Fujimoto, K. Kato, and H. Iwata

"Prolonged durability of electroporation microarrays by saccharide addition to nucleic acid"

Anal. Bioanal. Chem. In press

RELATED PUBLICATION

Y. Inoue, H. Fujimoto, T. Ogino, and H. Iwata

“Site-specific gene transfer with high efficiency onto a carbon nanotube-loaded electrode”

J. R. Soc. Interface., **5**, 909–918. (2008).

ACKNOWLEDGEMENTS

The present research was carried out from 2003 to 2008 under the continuous guidance of Dr. Hiroo Iwata, Professor of the Institute for Frontier Medical Sciences, Kyoto University. The author is deeply indebted to Professor Iwata for his constant guidance, encouragement, valuable discussion, and detailed criticism on the manuscript throughout the present work. The completion of the present research has been an exiting project and one which would not have been possible without his guidance.

The author is very grateful to Dr. Koichi Kato, Associate Professor of the Institute for Frontier Medical Sciences, Kyoto University, for his constant guidance, helpful suggestions, and intimate advice.

General acknowledgments are due to Dr. Yusuke Arima, Dr. Fumio Yamauchi, Dr. Yuuki Inoue, Dr. Yuji Teramura, Satoru Yoshizako and other members of Professor Iwata's laboratory and of the Institute for Frontier Medical Sciences, Kyoto University, for their kind help.

Finally, the author likes to take the opportunity to extend hearty thanks to his wife, Nanae Fujimoto, his parents, Tadashige and Takayo Fujimoto, and his sister, Eri Fujiomoto for their cordial support and continuous encouragement.

October, 2008

Kyoto

Hiroyuki Fujimoto